Neutrino physics at the UNK (accelerator and storage-ring facility at Protvino)

P. S. Isaev

Joint Institute for Nuclear Research, Dubna

V. A. Tsarev

P. N. Lebedev Physics Institute, USSR Academy of Sciences, Moscow

Fiz. Elem. Chastits At. Yadra **20**, 997–1099 (September–October 1989)

Modern problems of neutrino physics at high energies are analyzed. Possibilities for investigating them experimentally with neutrino beams at the large accelerator and storage-ring facility UNK nearing completion at Protvino are discussed.

INTRODUCTION

The possibility of performing neutrino experiments at high-energy accelerators was first discussed by M. A. Markov and his collaborators shortly before the conference on high-energy physics at Kiev (1959). At that time, the idea appeared to many to be beyond the bounds of reality.[1] During the three decades that have since elapsed, investigations with beams of high-energy neutrinos have played an important part in the establishment of modern ideas about the structure of the fundamental particles and the nature of the interactions between them. The specific properties of neutrinos—their pointlike nature, ability to distinguish quarks and antiquarks and "sense" flavor, and the weak dependence [1)] of the neutrino cross sections σ_ν on the square Q^2 of the four-dimensional momentum transfer—make neutrinos a unique probe for the investigation of the structure of hadrons and nuclei and for testing the standard model of the strong and electroweak interactions.[2,3]

Unfortunately, the extremely rich physical information that could, in principle, be obtained in experiments with neutrino beams is to a large degree lost by the poor statistics and the systematic errors traditionally inherent in neutrino experiments and due to the smallness of the neutrino cross sections, the poor knowledge of the energy of the initial neutrino and of the properties of the final particles, and the lack of knowledge in a number of cases of the type of the initial neutrino.

Despite these difficulties, neutrino physics has made great progress in its development during the last 15–20 years, and the neutrino experiments performed at accelerators in the Soviet Union, the United States, and at CERN have made a major contribution to our understanding of the nature of the electroweak and strong interactions and the structure of hadrons (discovery of neutral currents, measurement of structure functions, the parameters $\Lambda_{\overline{\rm MS}}$, $\sin^2\theta_{\rm W}$, ρ, the Kobayashi–Maskawa matrix elements, etc.).

A new step in neutrino investigations will be taken at the large accelerator and storage facility UNK (Uskoritel'no-Nakopitel'nyĭ Kompleks: Accelerator–Storage Ring Facility), which is currently nearing completion at Protvino (Institute of High Energy Physics).[4] Among the multi-TeV accelerators of the new generation, the UNK is unique, because it is intended to produce neutrino beams that will be the most energetic and intense in the world for the foreseeable future. These beams and the planned neutrino detectors will make it possible to overcome a number of traditional difficulties and to achieve for the first time in the practice of neutrino experiments the levels of accuracy obtained in experiments with hadron beams. A high statistical reliability of the neutrino experiments at the UNK will be achieved by the increase in the neutrino energy E_ν and, accordingly, growth of the cross section ($\sigma_\nu \sim E_\nu$, a factor ~ 10 compared with the SpS collider and ~ 3 compared with the Tevatron), and also by the high intensity of the initial protons ($\sim 5\times 10^{12}$ sec^{-1}), which will exceed by an order of magnitude the intensity of the competing accelerator closest in energy—the Tevatron at Fermilab in the United States.

The statistics of experiments at the UNK will be unusually good by the standards of modern neutrino experiments. Thus, one pulse of the accelerator (6×10^{14} protons from the proton beam deflected onto a target[4,5]) will give about 50 νN interactions in one ton of target in the neutrino detectors. The expected statistics[2)] for some of the most important processes are given in Table I.

For the same conditions, Fig. 1 shows the distribution of $\nu_\mu N$-interaction events with respect to the energy, $dN_{\rm int}/dE_\nu$, and $N_{\rm int}$. It can be seen that even at very high neutrino energies $E_\nu \simeq 2$ TeV, good statistics will be possible (about 10^5 events). Even better statistics will be obtained in dichromatic beams: during 100 days in 100 ton, about 2.2×10^7 $\nu_\mu N$ interactions and about 3.4×10^6 $\bar\nu_\mu N$ interactions.[8]

At the UNK it is intended to produce neutrino beams with broad and narrow energy spectra, beams of tagged neutrinos, and direct neutrino beams. The length of the decay base is 3.7 km. The muon background is suppressed by a steel shield of length 500 m and ground of thickness 1000 m. The neutrino detectors are mainly placed at distances 0.5–2.5 km after the shield. The possibility of removing the detectors to distances up to 50 km is also foreseen.

Figures 2 and 3 show spectra of neutrino and antineutrino beams with broad and quasibroad spectra for different

TABLE I. Statistics in a wide-spectrum beam during 100 days (4.32×10^{19} protons) in 100 ton of target.

Process	ν_μ	ν_e
$\nu N \to e^- X$	$3.6\cdot 10^8$	$7.6\cdot 10^6$
$\nu N \to \nu X$	$1.2\cdot 10^8$	$2.5\cdot 10^6$
$\nu N \to l^+ l^- X$	$3.6\cdot 10^6$	$7.6\cdot 10^4$
$\nu N \to \nu e$	$4.7\cdot 10^4$	$7\cdot 10^3$
$\nu_\mu e \to \mu \nu_e$	$5.4\cdot 10^5$	—

 0090-4759/89/050419-47$04.40

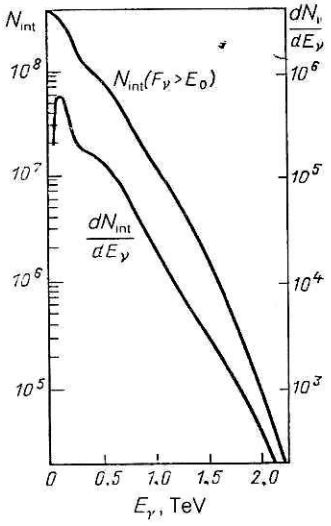

FIG. 1. Energy distribution of the number of $\nu_\mu N \to \mu X$ events, dN_{int}/dE_ν, and N_{int} during 100 days in 100 ton of target.[4]

types of focusing and the chosen geometry of the channel (radius of detector 0.56 m, distance 1.5 km after the shield).[6,9] The neutrino flux at the detector is about 2×10^{-3} $\nu/(m^2\cdot\text{proton})$. The background admixture of antineutrinos in the neutrino beam is $\lesssim 0.3\%$.

The narrow-spectrum neutrino beams are produced on the basis of a high-intensity channel of monochromatized pion and kaon beams with momenta in the interval 500–2250 GeV/c and spread $\pm$ (1.5–14)%. Preliminary estimates[6] lead to the following results. For $\Delta p/p = \pm 2.5\%$ and a detector with radius 1 m at distance 10 km from the shield the neutrino fluxes at the detector will be $(3\times10^{-5}$–$1\times10^{-6})$ $\nu/(m^2\cdot\text{proton})$ and $(1\times10^{-7}$–$8\times10^{-7})\nu/(m^2\cdot\text{proton})$ from the decay of π^+ and K^+ mesons, respectively. The relative width at half-height of the energy peaks will be 7–20% for neutrinos from π^+ decay and 3–6% for neutrinos from K^+ decay. The level of the continuous background will be about 1.5%, and the admixture of $\bar{\nu}$ in the ν beam will be about 0.5%.

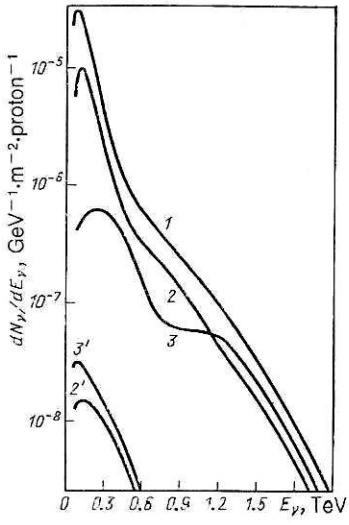

FIG. 2. Energy spectra of ν_μ neutrinos at the UNK in the case of ideal focusing (1) and of a focusing system of three (2) and one (3) lithium lenses; curves 2′ and 3′ give the admixtures of antineutrinos.[3]

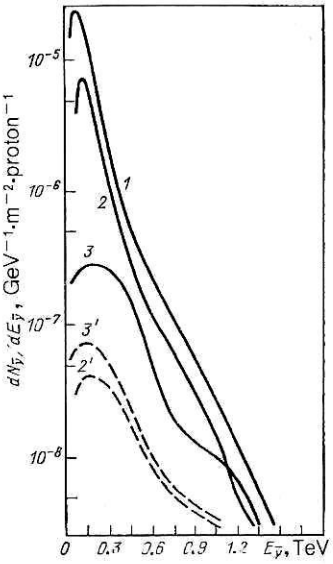

FIG. 3. Energy spectra of $\bar{\nu}_\mu$ antineutrinos at the UNK in the case of ideal focusing (1) and of a focusing system of three (2) and one (3) lithium lenses; curves 2′ and 3′ give the neutrino admixtures.

To ensure high systematic accuracy; the realization of the program of neutrino tagging will be important.[9,10] The tagging method will permit determination of the initial properties of the neutrinos at the level of individual events. The main advantages compared with ordinary beams are the knowledge of the species of the initial neutrino and the high energy ($\sim 3\%$) and angular resolution. Moreover, as can be seen from Table II, a high statistical reliability can be achieved in beams of tagged neutrinos.

The resolution of total-absorption detectors, which are widely used to detect neutrino interactions, increases with increasing energy as $E^{-1/2}$. Therefore, at UNK energies it should be possible to measure the energy with an accuracy of a few percent, a significant advance on existing measurements. The detectors planned for use in the neutrino experiments at the UNK will have high spatial and energy resolution and a fairly large mass.

A further very important advantage of the UNK compared with existing accelerators is the extension of the range of variation of the kinematic variables. The increase of the energy by about an order of magnitude compared with the SpS collider and by more than a factor of three compared with the Tevatron will open up possibilities for the direct production of new particles both in neutrino beams and in proton beams, as well as in beam-dump experiments with the

TABLE II. Statistics in beams of tagged neutrinos[9,10] during 100 days (4.32×10^{19} protons) in 500 ton of target.

Process	ν_μ	ν_e
$\nu N \to e^- X$	$2.2\cdot10^7$	$4.6\cdot10^5$
$\nu N \to \nu X$	$7.5\cdot10^6$	$1.5\cdot10^5$
$\nu N \to l^+ l^- X$	$2.2\cdot10^5$	$4.6\cdot10^3$
$\nu e \to \nu e$	$2.9\cdot10^3$	$4.1\cdot10^2$
$\nu_\mu e \to \nu_\mu e$	$3.2\cdot10^4$	—

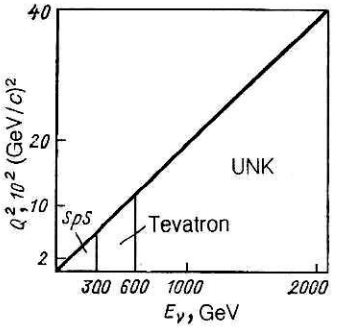

FIG. 4. Kinematic regions (Q^2,E_ν) accessible for the UNK, Tevatron, and SpS.

use of neutrino detectors (massive neutrinos, heavy leptons, and more).

As can be seen from Fig. 4, the kinematic region (the Q^2–E_ν plane) accessible for experiments at the UNK is much wider than for the SpS and the Tevatron. The increase of the Q^2 interval will be important for testing the main propositions of QCD in processes of deep inelastic scattering of neutrinos by nucleons and nuclei (form of the breaking of scaling, separation of the twist corrections from the logarithmic contributions, etc.). For the investigation of the final hadron states important advantages will accrue from the extension of the interval with respect to the rapidity (which will permit better separation of the different fragmentation regions and the identification of jet events) and with respect to W, the invariant mass of the final hadronic system. Figures 5 and 6 show estimates for the expected number of events with definite values of W^2 and Q^2 that can be obtained in a wide-spectrum beam under conditions of a real experiment using a hybrid spectrometer with a bubble chamber and a working target mass 0.4 ton as a vertex part.[6]

Finally, the increase of the Lorentz factor of the produced particles may be important for the investigation of short-lived particles.

Thus, the neutrino complex of the UNK will permit an extensive program of investigations at high energies. The neutrino beams and the detectors will ensure a significant

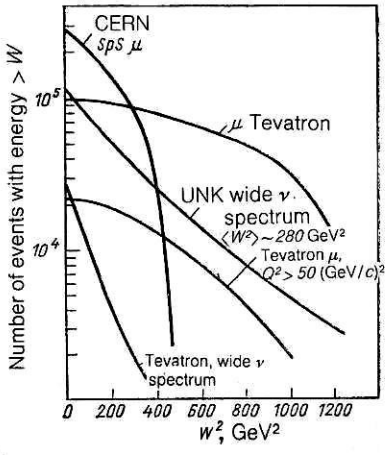

FIG. 5. Expected number of events with square of the hadron mass greater than W^2 for a pulse of 10^{18} protons incident on the target in various experiments.

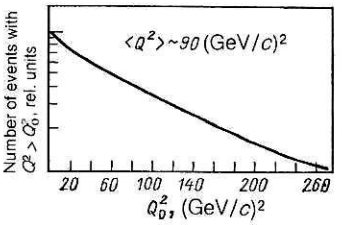

FIG. 6. Integrated Q^2 distribution of neutrino interactions in a UNK wide beam.

advance on the experimental front compared with the existing level and will create prospects for the realization of a new stage of neutrino investigations.

In addition, as a more distant prospect, the UNK program foresees the construction of a linear e^+e^- collider to energy 1 TeV × 1 TeV (with a high rate of acceleration ~1 MeV/cm). This accelerator will in principle permit acceleration of the unstable π and K mesons to energies of about 2 TeV, and this will open up the possibility of obtaining and using intense narrowly directed (at a given angle) beams of monochromatic high-energy neutrinos.[11,12] A discussion of the possibilities of the program of investigations with such beams goes beyond the scope of this review. These questions have been partly considered in Refs. 11 and 12.

This review will also not consider specific, purely experimental questions; in particular, it will not describe the facilities that are currently being built and planned for the UNK neutrino facility. Each of these problems fully warrants a special paper. We are also not in a position to make any reliable analysis of the systematic errors that will arise when some particular physical process is studied under the conditions of a particular experiment. These errors depend on numerous factors relating to the geometry, efficiency, cutoffs, trigger, etc., and they are specific for each individual facility. Where necessary, we shall give only the expected statistical errors. They give an idea of the accuracy of the experiment that can be achieved if the systematic errors can be made smaller than the statistical errors.

We see the main task of the present review as a discussion of the physical problems of investigations with neutrino beams and neutrino detectors at the UNK.

Making an overview of the possible neutrino program of the UNK, we see that a significant part of it must consist of experiments in which a quantitative test of the predictions of the standard model are made. These experiments will be on phenomena already known, but they will be made with accuracies exceeding the accuracy of present experiments, and also in regions of new higher energies and larger momentum transfers. Such measurements can not only give more accurate numerical characteristics of the phenomena and values of the fundamental parameters of the theory but may also lead to qualitatively new results. For example, measurements of the fundamental parameter of the standard model, $\sin^2\theta_W$, on the basis of νe scattering to an accuracy better than 0.002 could, under favorable circumstances, give information about the existence in nature of heavy leptons, heavy quarks, or new intermediate bosons and could be the key to an "extension" of the standard model. However, it must be emphasized that such a step in future experiments will be possible only if theoretical calculations of various phenome-

na have been made at least in the single-loop approximation.

Besides the neutrino investigations already mentioned, the UNK has the potential for the direct detection of new particles (heavy neutrinos, leptons, Z' bosons, and others) and new phenomena (for example, neutrino oscillations).

We make one further remark concerning the relationship of the neutrino program to the possibilities that are opened up with the construction of new e^+e^-, pp, $p\bar{p}$, and ep colliders. There is no doubt that the colliders of the next generation possess a huge potential for a "breakthrough" to a "new physics": the discovery of new particles with masses of hundreds of GeV/c^2, new physical phenomena and behavior due to a possible composite nature of the fundamental particles, new types of symmetry, etc. The UNK accelerator, working with stationary targets, has a much lower collision energy ($\sqrt{s} \lesssim 80$ GeV) and in this respect cannot compete with colliders. However, the UNK beams make possible their own field of investigation, which is entirely or to a large degree outside competition with colliders; in the first place, this applies to the neutrino investigations. The UNK neutrino beams open up possibilities not available for collider investigations, above all on problems associated with the nature of the neutrinos themselves: oscillations, electromagnetic properties of the neutrinos, heavy neutrinos, nondiagonality of the weak neutral current, etc. From the purely experimental point of view, numerous phenomena are more conveniently studied by means of neutrino beams than with colliders. For example, experiments with a fixed target give optimal possibilities for the study of both current and target jets, which are not easily investigated with colliders. Similarly, it is convenient to look for photinos in neutrino experiments but, apparently, very difficult in colliders.

Also restricted to experiments with stationary targets are searches for heavy neutral leptons, axions, and other weakly interacting particles, and also investigations of nuclear effects that can be successfully made in neutrino beams. Finally, one of the remarkable features of the UNK is the real possibility, opened up for the first time, of making fundamental and applied ("neutrino geophysics" [12,13]) investigations with beams of "long-range" neutrinos, i.e., neutrinos detected at large distances (hundreds and thousands of kilometers) from the accelerator.

Further, for numerous phenomena in which the scientific program overlaps with collider physics the specific properties of neutrino probing make its use expedient irrespective of competing possibilities. Even when a particular phenomenon can be studied in two ways, the possibility of its independent investigation in neutrino reactions may have fundamental importance. This is the case, for example, for the verification of the standard model of electroweak interactions, for which the corrections to the Born approximation are different for different processes, and their investigation in all accessible processes will permit the most complete verification of the gauge nature of the theory and the universality of its predictions. Therefore, when we compare collider experiments with neutrino experiments on a fixed target, we should say not that they compete but rather that they complement each other.

The possible program of neutrino investigations with the UNK is exceptionally wide and varied. In this issue of the journal we publish the first part of a survey, which is devoted to a discussion of the problems of the electroweak sector of the standard model and to the investigation of the structure of nucleons in the framework of quantum chromodynamics (QCD) and the possibilities of studying them in experiments with the neutrino beams of the UNK. Above all, we consider all processes in which the parameters $\sin^2\theta_W$ and ρ can be measured with high accuracy. In the following sections, we shall consider problems of the structure of nucleons and nuclei, the final states of the hadronic systems, nuclear effects, exotics, and investigations with beams of "long-range" neutrinos. The complete survey is being published in two issues of the journal. The division is made solely for formal reasons associated with the restriction on the length of reviews accepted for publication.

1. TESTING OF THE STANDARD MODEL

The standard model

The standard $SU(3)_c \otimes SU(2)_L \otimes U(1)$ model of the strong, electromagnetic, and weak interactions of the elementary particles[2,3] gives a good description of practically all the observed facts. It embodies the principles of non-Abelian gauge invariance, spontaneous symmetry breaking, and confinement. The theory is renormalizable and permits calculations of higher orders. The $SU(3)_c$ part—quantum chromodynamics—describes the strong interactions of the elementary particles; the $SU(2)_L \otimes U(1)$ part—the electroweak sector of the standard model— describes the unification of the electromagnetic and weak interactions. The discovery of neutral currents, the proof of the existence of $W^{\pm}$ and Z^0 bosons, the determination of the elements of the Kobayashi–Maskawa matrix, the determination of the parameters of the CP violation in decays of K mesons, the establishment of B^0–$\overline{B}^0$ oscillations, and a number of other important experimental results that confirm the conclusions of the standard model provide convincing evidence that the model describes nature adequately in the investigated region of energies and at the achieved level of accuracy.

The standard model will be subjected to further careful verification at the accelerators SLC (USA), LEP (CERN), HERA (German Federal Republic), and UNK (USSR), which are now or very soon will be commissioned, and also at other planned accelerators (the future pp collider at CERN and the SSC in the United States).

Despite the successes of the standard model, there do exist reasons for dissatisfaction with both quantum chromodynamics and the electroweak sector of the model.

Thus, in the Lagrangian of the standard model, with three generations of leptons, there are 18 free parameters (two coupling constants: e, $\alpha(Q^2)$; 12 masses of fermions and bosons: u, d, s, c, b, t, e, μ, τ, W, Z, χ; and four mixing angles in the Kobayashi–Maskawa matrix), to which, in the case of massive neutrinos, there must be added seven more parameters (the neutrino masses and the mixing angles of the leptons). The reason for the replication of the lepton generations are obscure, there is no reason for their number, the mechanism of generation of the masses of the particles is unknown, and there is no theoretical derivation of their spectrum. The space-time structure of the weak interactions does not follow from any internal requirements of the theory but is introduced phenomenologically, in accordance with experimental facts. The existence of a Higgs boson has not

yet been proved. The t quark has not been found, and there is no direct proof of the existence of the τ neutrino. Some parameters of the standard model are known with insufficient accuracy.

For all these reasons it is necessary to test the standard model more deeply, and also to look for a more general theory that, including the standard model as a part, would eliminate the excessive reliance on phenomenology in the model.

Many different methods have been proposed for the extension of the standard model beyond the existing framework: inclusion of new generations or additional intermediate bosons, technicolor, compositeness, supersymmetry, grand-unification models, and superstrings. In passing to the region of higher energies and larger momentum transfers, we hope to discover signals of a new physics.

The most striking experimental manifestation of such new physics would be the direct discovery of new particles or phenomena that do not fit in the framework of the standard model. However, it is entirely possible that a new physics would not be directly manifested in the considered range of energies but would appear indirectly, through relatively small deviations from the predictions of the standard model. It is this circumstance that stimulates accurate measurements of the parameters of the model. They could indicate the existence of new particles or phenomena and impose restrictions on the structure of a more general theory.

For the neutrino experiments to be discussed in this review, an increase of the accuracy of the measurements is a matter of the first importance. As we have already noted, the UNK neutrino beams and detectors will open up possibilities for a significant improvement in the accuracy of neutrino investigations. They will permit high-precision measurements of the parameters of the electroweak sector of the standard model ($\sin^2\theta_W$, ρ, and the elements of the matrix of the quark mixing), study with high accuracy of the space-time structure of the weak current, verification of the universality of the generations, searches for a flavor-changing neutral current, direct searches for τ neutrinos, etc.

The theoretical discussions in the review will be based on the following Lagrangian of the electroweak sector of the standard minimal $SU(2)_L \otimes U(1)$ theory, written down with allowance for the spontaneous breaking of gauge symmetry in the so-called U (unitary) gauge. In the minimal theory, there is only one doublet of Higgs mesons. In the Lagrangian we give explicitly the relations that arise between the parameters of the theory (of the type $e^2/g^2 \equiv 1 - M_W^2/M_Z^2$), and also the independent constants: the charge e, the masses M_W, M_Z, m_f, etc.

Thus, the explicit expression for the Lagrangian has the form[14]

$$
\begin{aligned}
\mathcal{L}^{EW} = & -\frac{1}{4}(\partial_\mu A_\nu - \partial_\nu A_\mu)^2 \\
& - \sum_f [\bar{f}(\partial_\mu \gamma_\mu + m_f) f + ieQ_f \bar{f}\gamma_\mu f A_\mu] \\
& - \frac{1}{2}|\partial_\mu W_\nu - \partial_\nu W_\mu|^2 - M_W^2 |W_\mu|^2 - \frac{1}{4}(\partial_\mu Z_\nu - \partial_\nu Z_\mu)^2 \\
& - \frac{1}{2} M_Z^2 Z_\mu^2 + \frac{i}{2\sqrt{2}} \frac{e}{(1-R)^{1/2}} \sum_{f_{ij}} [\bar{f}_i^u \gamma_\mu (1+\gamma_5) K_{ij} f_j^d W_\mu^+ \\
& + \bar{f}_i^d \gamma_\mu (1+\gamma_5) K_{ij}^+ f_j W_\mu] + \frac{i}{4} \frac{e}{R^{1/2}(1-R)^{1/2}} \sum_f \bar{f}\{\gamma_\mu s_f [1 \\
& - 4(1-R)|Q_f| + s_f \gamma_\mu \gamma_5\} f Z_\mu + ie\left[\left(\frac{R}{1-R}\right)^{1/2} Z_\nu - A_\nu\right] \\
& \times [W_\mu (\partial_\mu W_\nu^+ - \partial_\nu W_\mu^+) - W_\mu^+ (\partial_\mu W_\nu - \partial_\nu W_\mu) \\
& + \partial_\mu (W_\mu W_\nu^+ - W_\nu W_\mu^+)] \\
& + e\left\{\frac{1}{2(1-R)} W_\mu^+ W_\nu W_\rho^+ W_\sigma + \left[A_\mu - \left(\frac{R}{1-R}\right)^{1/2} Z_\mu\right]\right. \\
& \left. \times \left[A_\nu - \left(\frac{R}{1-R}\right)^{1/2} Z_\nu\right] W_\rho^+ W_\sigma\right\} (\delta_{\mu\rho}\delta_{\nu\sigma} - \delta_{\mu\nu}\delta_{\rho\sigma}) \\
& - \frac{1}{2}(\partial_\mu \chi)^2 \\
& - \frac{1}{2} M_\chi^2 \chi^2 - \frac{e}{2(1-R)^{1/2} M_W} \sum_f m_f \bar{f} f \chi \\
& - \frac{eM_W}{(1-R)^{1/2}} W_\mu^+ W_\mu \chi \\
& - \frac{eM_Z}{2(1-R)^{1/2}} Z_\mu^2 \chi - \frac{e^2}{4(1-R)} W_\mu^+ W_\mu \chi^2 - \frac{e^2}{8R(1-R)} Z_\mu^2 \chi^2 \\
& - \frac{eM_\chi^2}{4M_W(1-R)^{1/2}} \chi^3 - \frac{e^2 M_\chi^2}{32 M_W^2 (1-R)} \chi^4. \qquad (1)
\end{aligned}
$$

In the expression (1), A_μ, Z_μ, W_μ are the operators of the fields of the gauge bosons γ, Z, and W, respectively; f^u and f^d are the "up" and "down" fermion fields:

$$\begin{pmatrix} \nu_e \\ l' \end{pmatrix}, \quad \begin{pmatrix} U \\ D \end{pmatrix} \ldots; \quad U = u,\ c,\ t; \quad D = d,\ s,\ b;$$

$s_{up} = +1$; $s_d = -1$; $Q_f = s_f |Q_f|$, where $|Q_f|$ is the modulus of the charge of the fermion of species f; χ is the scalar field that describes the physical Higgs field; $\langle \chi \rangle = 0$; $\partial_u \equiv \partial/\partial\chi_u$; $R(M_W^2/M_Z^2)$; $f = \binom{f_u}{f_d}$; K in the general case is a nondiagonal matrix and in the quark sector is identical to the Kobayashi–Maskawa matrix; m_f, Q_f, s_f are the corresponding diagonal matrices.

We shall use the definition

$$\sin^2\theta_W \equiv 1 - M_W^2/M_Z^2. \qquad (2)$$

We introduce the quantity

$$\rho \equiv M_W^2/(M_Z^2 \cos^2\theta_W). \qquad (3)$$

It follows from the definition (2) that $\rho \equiv 1$. However, in the general case, as we shall see below, the value of ρ need not be equal to unity.

The reader can find a more detailed discussion of the individual terms of the Lagrangian (1) and of the renormalization procedure together with the explicit form of the counterterms in the theory of the electroweak interactions in the lectures of Ref. 14.

Here, we make just one remark. All the particles of the fields that occur in the Lagrangian (1), except for the t quark, τ neutrino, and Higgs boson, are already known experimentally—they are the fermion fields, the electromagnetic field A_μ, and the gauge fields of the W^+ and Z^0 bosons. The Lagrangian (1) includes a number of terms containing an interaction with the Higgs field or a self-interaction of this field. The experimental investigation of the existence in nature of the t quark and of the Higgs boson is one of the fundamental problems of modern theory. We shall see below which phenomena could permit detection of a contribution of the t quarks and Higgs bosons. In all cases in which our

discussion takes us beyond the framework of the Lagrangian of the standard model we shall specify the corresponding conditions.

The renormalizability of the standard model makes it possible to calculate the contributions of diagrams of higher orders, i.e., the radiative corrections. The radiative corrections of the electroweak sector are usually divided into three types:

1) quantum-electrodynamical vacuum polarization; in the diagrams of this type an intermediate virtual photon is transformed into a pair of fermions (leptons and quarks);

2) diagrams that include weakly interacting particles in loops and at vertices;

3) bremsstrahlung of real photons and virtual photons in loops; these corrections depend on the geometry of the detector and other details of the experiment.

None of the types of diagrams taken separately is gauge-invariant; only the complete set of diagrams of a given order is gauge-invariant. The calculation of the radiative corrections of the first and second types takes into account the contributions of various particles, including ones that have not yet been detected—the t quarks and Higgs particles. Extending the interaction Lagrangian in (1) [going beyond the framework of the minimal $SU(2)_L \otimes U(1)$ sector of the standard model], we can include in the calculations radiative corrections and other particles (for example, Z_0'). In this way one can introduce a dependence of the investigated physical phenomena and theoretical parameters on the masses of the t quarks, Higgs mesons, new fermions, additional Z bosons, and other particles not contained in the minimal standard model.

At the present time, the standard model is being verified at the level of the single-loop approximations. It should be borne in mind that the calculation of the electroweak radiative corrections includes a definite renormalization scheme. The most popular are on-shell schemes and the minimal-subtraction ($\overline{\text{MS}}$) scheme[15]: $(M_0)^2 = M^2 + \delta M^2(\mu)$: on-shell renormalization scheme; $(M_0)^2 = M^2(\mu) + \delta M^2$: minimal-subtraction scheme.

Here, M_0 is the bare value of the mass, M is the physical value of the mass, $M(\mu)$ is the renormalized value of the mass, which depends on the choice of the renormalization point μ, and δM^2 is the radiative (infinitely large) correction. In general, the values of M^2 and $M^2(\mu)$ may differ, and to obtain the physical value of the mass it is necessary to know the connection between M^2 and $M^2(\mu)$ in order to avoid possible confusion. Different values of the masses M^2 and $M^2(\mu)$ lead to different values of the fundamental parameter $\sin^2\theta_W$:

$$\sin^2\theta_W = 1 - M_W^2/M_Z^2 \tag{4a}$$

and

$$\sin^2\theta_W(\mu) = 1 - M_W^2(\mu)/M_Z^2(\mu), \tag{4b}$$

where $M_W(\mu)$ and $M_Z(\mu)$ are the renormalized masses of the W and Z bosons.[15] It is well known that accurate values of $\sin^2\theta_W$ are important for comparisons with the values of $\sin^2\theta_W$ obtained in grand-unification theories and in supersymmetric schemes, to obtain indications of masses of new particles (or determine limits on them), etc. Despite the diversity of the theoretical schemes of the calculations, the theoreticians have achieved unity in the results of the calculations of the radiative corrections in the single-loop approximation.[16] These calculations have already provided the basis of an analysis of experimental data obtained in various reactions (νN, νe, eN, μN scattering, e^+e^- annihilation) and relating to the masses of the intermediate vector bosons and to the weak neutral currents.[17] The results of the analysis indicate that in the investigated region of E and Q^2 there are no deviations from the minimal standard model. In future experiments this conclusion must be subjected to new verification in the region of higher energies and larger momentum transfers, in which the contribution of the t quarks and Higgs bosons or the manifestations of a "new physics" could be more pronounced.

Measurement of the parameters $\sin^2\theta_W$ and ρ

Scattering of neutrinos by electrons

Of very great interest for high-precision verification of the standard model are processes of neutrino scattering by electrons:

$$\nu_e + e \to \nu_e + e; \tag{5a}$$

$$\bar{\nu}_e + e \to \bar{\nu}_e + e; \tag{5b}$$

$$\nu_\mu + e \to \nu_\mu + e; \tag{6a}$$

$$\bar{\nu}_\mu + e \to \bar{\nu}_\mu + e. \tag{6b}$$

Diagrams corresponding to the scattering processes (5a) and (5b) are shown in Fig. 7. They include the contributions of the neutral current [diagram (a)] and the charged current [diagram (b)]. Because of the law of conservation of the lepton number, the processes (6a) and (6b) are described by just a single tree diagram (Fig. 8). Below in the expressions for the differential and total cross sections of the processes (5a), (5b) and (6a), (6b) we shall everywhere omit the factor $M_{W,Z}^2/(q^2 + M_{W,Z}^2)$ (here and in what follows, we take $c = \hbar = 1$), which corresponds to the propagators of the W and Z bosons, since even at very high neutrino energies the momentum transfer q^2 is negligibly small compared with M_Z^2 or M_W^2: $q^2 \approx -2mE_e$, where E_e is the recoil energy of the electron and m is the electron mass. Even when the energy E_e of the scattered electron is equal to the energy of the incident neutrino, the recoil is small. From the theoretical point of view, the processes (5) and (6) are the simplest possible (the electron has no structure). A detailed derivation of the expressions for the differential and total cross sections of these processes for the $V-A$ form of the interaction [in the approximation $M_{W,Z}^2/(q^2 + M_{W,Z}^2) \approx 1$] is given in the book of Ref. 18. We give here all the cross sections corresponding to the tree approximation:

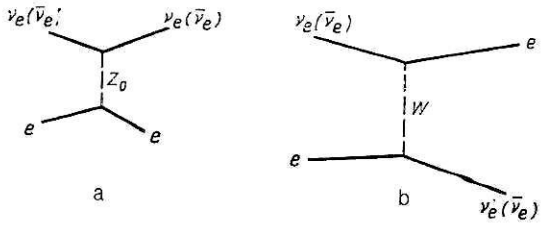

FIG. 7. Diagrams describing the process of $\nu_e(\bar{\nu}_e)$ scattering by electrons in the tree approximation.

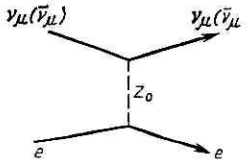

FIG. 8. Diagram describing the scattering of a muon neutrino by an electron in the tree approximation.

$$\frac{d\sigma(\nu_e e+\nu_e e)}{dy}=2\sigma_0\left[\left(\frac{1}{2}+\sin^2\theta_W\right)^2+\sin^4\theta_W(1-y)^2\right]; \tag{7a}$$

$$\frac{d\sigma(\bar{\nu}_e e+\bar{\nu}_e e)}{dy}=2\sigma_0\left[\sin^4\theta_W+\left(\frac{1}{2}+\sin^2\theta_W\right)^2(1-y)^2\right]; \tag{7b}$$

$$\frac{d\sigma(\nu_\mu e+\nu_\mu e)}{dy}=2\sigma_0\left[\left(-\frac{1}{2}+\sin^2\theta_W\right)^2+\sin^4\theta_W(1-y)^2\right]; \tag{7c}$$

$$\frac{d\sigma(\bar{\nu}_\mu e+\bar{\nu}_\mu e)}{dy}=2\sigma_0\left[\sin^4\theta_W+\left(-\frac{1}{2}+\sin^2\theta_W\right)^2(1-y)^2\right], \tag{7d}$$

where $\sigma_0=G_F^2 m_e E_\nu/\pi$, $0\leqslant y=E_e/E_\nu\leqslant 1$, and G_F^μ is the Fermi coupling constant.

Integrating the cross sections (7a)–(7d) with respect to the variable y, we obtain

$$\sigma(\nu_e e)=2\sigma_0\left[\left(\frac{1}{2}+\sin^2\theta_W\right)^2+\frac{1}{3}\sin^4\theta_W\right]; \tag{8a}$$

$$\sigma(\bar{\nu}_e e)=2\sigma_0\left[\sin^4\theta_W+\frac{1}{3}\left(\frac{1}{2}+\sin^2\theta_W\right)^2\right]; \tag{8b}$$

$$\sigma(\nu_\mu e)=2\sigma_0\left[\left(-\frac{1}{2}+\sin^2\theta_W\right)^2+\frac{1}{3}\sin^4\theta_W\right]; \tag{8c}$$

$$\sigma(\bar{\nu}_\mu e)=2\sigma_0\left[\sin^4\theta_W+\frac{1}{3}\left(-\frac{1}{2}+\sin^2\theta_W\right)^2\right]. \tag{8d}$$

The cross sections (7) and (8) are expressed in such a way that the term $\pm\frac{1}{2}+\sin^2\theta_W$ corresponds to the contribution of the electrons with left helicity, and the term $\sin^4\theta_W$ to the contribution of the electrons with right helicity. The restriction

$$\frac{1}{3}\leqslant\frac{\sigma(\bar{\nu}_\mu e)}{\sigma(\nu_\mu e)}\leqslant 3 \tag{9}$$

is obtained from consideration of two limiting cases:

a) $\sin^2\theta_W=0$; b) $\left(-\frac{1}{2}+\sin^2\theta_W\right)^2=0$.

We consider in more detail the processes $\nu_\mu e\to\nu_\mu e$ and $\bar{\nu}_\mu e\to\bar{\nu}_\mu e$, which are due to the neutral currents. In the standard model with $\sin^2\theta_W=0.23$ (and $\rho=1$) we have $\sigma(\nu_\mu e)/E_\nu\approx 1.56\times10^{-42}$ cm^2/GeV and $\sigma(\bar{\nu}_\mu e)/E_\nu\approx 1.33\times10^{-42}$ cm^2/GeV. The experimental values of $\sigma(\nu_\mu e)/E_\nu$ and $\sigma(\bar{\nu}_\mu e)/E_\nu$ are given in Tables III and IV.

The mean value of the branching ratio $R=\sigma(\nu_\mu e\to\nu_\mu e)/\sigma(\bar{\nu}_\mu e\to\bar{\nu}_\mu e)$, measured at the CHARM facility in the second (improved) exposure, is $1.26^{+0.72}_{-0.45}$, and the mean value of $\sin^2\theta_W$ (mean of both exposures) is $0.215\pm0.032\pm0.012$.

The measured branching ratio

$$R=\frac{\sigma(\nu_\mu e\to\nu_\mu e)}{\sigma(\bar{\nu}_\mu e\to\bar{\nu}_\mu e)}=3\,\frac{1-4\sin^2\theta_W+\frac{16}{3}\sin^4\theta_W}{1-4\sin^2\theta_W+16\sin^4\theta_W} \tag{10}$$

[see Eqs. (8c) and (8d)] is a sensitive measure of the weak mixing angle $\sin^2\theta_W$,[3] since

$$\Delta\sin^2\theta_W\sim\Delta R/8R. \tag{11}$$

If we require the error in the determination of the Weinberg angle to be $\lesssim 0.002$, then from (11) we obtain $\Delta R\lesssim 0.025$. It follows from this that the existing error in the measurement of the neutrino–electron cross sections must be reduced by tens of times. From the point of view of the statistics, this means that the number of neutrino–electron elastic scattering events must be tens of thousands.

Such statistics is entirely attainable at the UNK. In the neutrino calorimeter with a 100-ton target 10 000 $\nu_\mu e$ scattering events can be obtained during an exposure of about four months.[8]

The accuracy in the determination of $\sin^2\theta_W$ at the UNK in a beam of tagged neutrinos is expected to be at the level ±0.003 (detector of mass 500 ton). At the same time, the systematic errors will be well monitored. In the broad-spectrum beam the statistical error will be still smaller, by a factor of a few times; in this case the actual accuracy will be determined by the possibilities for overcoming the systematic errors.

In the CHARM-II experiment currently being per-

TABLE III. Values of $\sigma(\nu_\mu e)/E_\nu$.[19]

Experimental facility	Scientific center	Number of events	σ/E_ν, 10^{-42} cm^2/GeV
GGM a)	CERN (pS/SpS)	9	$2.4^{+1.2}_{-0.9}$
AC—PD b)	CERN (pS)	7	1.1 ± 0.6
15 FT c)	FNAL	20.5	$1.60\pm0.29\pm0.26$
UMWOF d)	FNAL	34	1.4 ± 0.5
CHARM e)	CERN (SpS)	83	$1.9\pm0.4\pm0.4$
E 734 f)	BNL	107	$1.60\pm0.29\pm0.27$

a) **Blietschau J., Deden H., Faissner H. e. a.**//Nucl. Phys. 1976. Vol. B114. P. 189-198; **Armenise N., Erriquez O., Fogli-Muciaccia M. T. e. a.**//Phys. Lett. 1979. Vol. 86B. P. 225-228.
b) **Faissner H., Fasold H. G., Frenzel E. e. a.**//Phys. Rev. Lett. 1978. Vol. 41. P. 213-216.
c) **Cnops A. M., Connolly P. L., Kahn S. A. e. a.**//Phys. Rev. Lett. 1978. Vol. 41. P. 357-360; **Murtag M. J.**//Proc. 11th Intern. Conf. on Neutrino Physics and Astrophisics, Dortmund, 1984. P. 290-311.
d) **Heisterberg R. H., Mo L. W., Nunamaker T. A. e. a.**//Phys. Rev. Lett. 1980. Vol. 44. P. 635-639.
e) **Bergsma F., Dorenbosch J., Tonker M. e. a.**//Phys. Lett. 1982. Vol. 117B. P. 272-278; **Bergsma F., Dorenbosch J., Allabi T. V. e. a.**//Phys. Lett. 1984. Vol. 147 B. P. 481-486.
f) **Ahrens L. A., Aronson S. H., Connolly P. L. e. a.**//Phys. Rev. Lett. 1983. Vol. 51. P. 1514-1517; Ibid. 1985. Vol. 54. P. 18-21.

TABLE IV. Values of $\sigma(\bar{\nu}_\mu e)/E_\nu$.[19]

Experimental facility	Scientific center	Number of events	σ/E_ν, 10^{-42} cm^2/GeV
GGM a)	CERN (pS)	3	$1.0^{+1.3}_{-0.6}$
AC—PD b)	CERN (pS)	9.6	2.2 ± 1.0
CHARM e)	CERN (SpS)	112	$1.5\pm0.3\pm0.4$
E 734 f)	BNL	59	$1.16\pm0.20\pm0.14$

*See the list of references in Table III.

formed at CERN with the SpS it is intended to collect 2000 $\nu_\mu e$ and 2000 $\bar{\nu}_\mu e$ events and to measure $\sin^2\theta_W$ with an error $\lesssim 0.005$. There is a proposal to investigate νe scattering at the meson factory in Los Alamos at low energies and to achieve errors $\Delta\sin^2\theta_W \lesssim 0.002$ (the experiment is planned to begin in 1991).

A list of future experiments aimed at determination of $\sin^2\theta_W$ with high accuracy is given in Table V.

The expected high experimental accuracies in the purely leptonic elastic scattering processes (5a), (5b), (6a), and (6b) will permit verification of the theory of the electroweak interactions to a high accuracy. Although the calculations in the Born approximation [see Eqs. (7) and (8)] are free of the theoretical uncertainties associated with allowance for the structure of the hadrons, they are already insufficient for comparison with the experimental data. The radiative corrections must be taken into account. In the single-loop approximation, the radiative corrections include contributions of both light and heavy quarks, and also a contribution of the Higgs bosons.

The expressions for the cross sections with allowance for the radiative corrections have for the scattering processes $\nu_\mu e\to\nu_\mu e$ and $\bar{\nu}_\mu e\to\bar{\nu}_\mu e$ the form (in the approximation $E_\nu \gg m_e$)[20,21]

$$\left.\begin{aligned}\frac{d\sigma(\nu_\mu e)}{dy} &= 2\sigma_0 [\rho_{NC}^{(\nu_\mu e)}]^2\{[g_L^{(\nu_\mu e)}(q^2)]^2+[g_R^{(\nu_\mu e)}(q^2)]^2(1-y)^2\}\\ &\quad+\frac{d\sigma^{\rm QED}(\nu_\mu e)}{dy};\\ \frac{\partial\sigma(\bar{\nu}_\mu e)}{\partial y} &= 2\sigma_0 [\rho_{NC}^{(\nu_\mu e)}]^2\{[g_L^{(\nu_\mu e)}(q^2)]^2(1-y)^2+[g_R^{(\nu_\mu e)}(q^2)]^2\}\\ &\quad+\frac{d\sigma^{\rm QED}(\bar{\nu}_\mu e)}{dy}.\end{aligned}\right\} \quad (12)$$

For brevity, they can be expressed in the form

$$\frac{d\sigma}{dy}=\frac{d\sigma^{\rm EW}}{dy}+\frac{d\sigma^{\rm QED}}{dy},$$

where $d\sigma^{\rm QED}/dy$ includes all the electromagnetic corrections of the third type, and $d\sigma^{\rm EW}dy$ includes all the remaining diagrams. Under the condition $E_\nu \gg m_e$, the expression for $d\sigma^{\rm QED}/dy$ can be written in the form

$$\frac{d\sigma^{\rm QED}}{dy}(\nu_\mu e)=\frac{[G_F^{(\mu)}]^2 s\alpha}{\pi^2}\left[g_L^2\left(\frac{19}{24}-\frac{\pi^2}{6}-\frac{2}{3}\ln\frac{2E_\nu}{m_e}\right)+g_R^2\frac{1}{3}\left(\frac{43}{24}-\frac{\pi^2}{6}-\frac{2}{3}\ln\frac{2E_e}{m_e}\right)\right], \quad (13)$$

where

$$s=(E_\nu+m_e c^2)^2;\quad \alpha=\frac{1}{137};$$

$$g_L=-\frac{1}{2}+\sin^2\theta_W;\quad g_R=\sin^2\theta_W.$$

In (12) we have introduced the notation

$$g_L^{(\nu_\mu e)}(q^2)=-\frac{1}{2}+\sin^2\theta_W(q^2);\quad g_R^{(\nu_\mu e)}(q^2)=\sin^2\theta_W(q^2);$$
$$\sin^2\theta_W(q^2)=\left(1-\frac{M_W^2}{M_Z^2}\right)\varkappa^{(\nu_\mu e)}(q^2). \quad (14)$$

The expression for the Fermi constant $G_F^{(\mu)}$ (without radiative corrections) is determined from muon decay as follows:

$$\frac{1}{\tau}=\frac{[G_F^{(\mu)}]^2 m_\mu^5}{192\pi^3}\left(1-\frac{8m_e^2}{m_\mu^2}\right)\times\left[1+\frac{3}{5}\frac{m_\mu^2}{M_W^2}+\frac{\alpha}{2\pi}\left(\frac{25}{4}-\pi^2\right)\right]. \quad (15)$$

TABLE V. Future experiments to determine $\sin^2\theta_W$ with high accuracy.[19]

Process	Expected error
νN deep inelastic scattering	0.007
$\nu_\mu e$; $\bar{\nu}_\mu e$ (LAMPF)	0.002
$M(Z^0)$(SLC, LEP)	0.0004
Forward–backward asymmetry (200×10^{-3} cm^2) (LEP-I)	0.002
τ polarization (LEP-I)	0.002
$M(W)$ (pp)	0.002
$M(W)$ (LEP-II)	0.002
Left–right asymmetry:	
SLC	0.0018—0.0004
LEP (polarized beams)	0.0003
Forward–backward asymmetry:	
LEP (polarized beams)	0.0006
eN (HERA)	0.002

Allowance for the radiative corrections in the muon-decay process permits expression of the Fermi constant $G_F^{(\mu)}$ in terms of the masses of the heavy bosons and quarks:

$$G_F^{(\mu)} = \frac{\pi}{\sqrt{2}\, M_W^2 \left(1 - \frac{M_W^2}{M_Z^2}\right)} \frac{1}{[1-\Delta r]}. \tag{16}$$

The relation (16) is usually expressed in the different form

$$M_W^2 \left(1 - \frac{M_W^2}{M_Z^2}\right) = \frac{(37.281\ \text{GeV})^2}{1-\Delta r\,(M_W^2,\ M_Z^2,\ M_H^2,\ m_t^2,\ m_f^2)} \equiv \frac{A_0^2}{1-\Delta r} \equiv A^2, \tag{17}$$

where

$$\Delta r = \frac{\alpha}{3\pi} \sum_f Q_f^2 \left(\ln \frac{M_Z^2}{m_f^2} - \frac{5}{3}\right) + \frac{\alpha}{4\pi} \tilde{Y}\,(M_W^2,\ M_Z^2,\ M_H^2,\ m_b^2,\ m^2); \tag{18}$$

$\tilde{Y}$ is a known function of the listed arguments, and $\alpha = 1/137$.

Thus, the expression for $(d\sigma^{\text{EW}}/dy)\ (\nu_\mu e)$ [see Eq. (12)] with allowance for the radiative corrections reduces essentially to the ansatz

$$\frac{d\sigma^{\text{EW}}}{dy}(\nu_\mu e) = \frac{d\sigma^{\text{EW}}}{dy}(\text{BORN})\,[G_F \to \rho_{NC}^{(\nu_\mu e)} G_F^{(\mu)};\ \sin^2\theta_W \to \varkappa_{NC}^{(\nu_\mu e)}(q^2)\sin^2\theta_W]. \tag{19}$$

The functions $\rho_{NC}^{(\nu_\mu e)}$ and $\varkappa_{NC}^{(\nu_\mu e)}$ have the form

$$\rho_{NC}^{(\nu_\mu e)}(q^2) = 1 + \frac{3\alpha}{16\pi(1-R)}\left\{\frac{\ln R}{1-R} + \xi\left[\frac{\ln\xi}{R(1-\xi)} + \frac{\ln(R/\xi)}{R-\xi}\right] + \frac{5}{8} + 8R - 9 + \frac{m_t^2}{M_W^2}\right\}, \tag{20}$$

where $R = M_W^2/M_Z^2$ and $\xi = M_H^2/M_Z^2$, and

$$\varkappa_{NC}^{(\nu_\mu e)}(q^2) = 1 + \frac{3\alpha}{4\pi(1-R)} \times \left\{\frac{R}{1-R}[Z(-1) - W(-1)] - \frac{9}{4R} + \frac{5}{2} - \frac{20}{3}R + 4I_3(q^2,\ m_l^2,\ m_l^2) + \sum_f c_f [8(1-R)Q_f^2 - 2|Q_f|]\, I_3(q^2,\ m_f^2,\ m_f^2)\right\}. \tag{21}$$

The integral I_3 has the form

$$I_3(q^2,\ m_1^2,\ m_2^2) = \int_0^1 x(1-x)\,dx \ln \frac{q^2 x(1-x) + m_1^2 x + m_2^2(1-x)}{M_W^2}. \tag{22}$$

Note that the expression for $\varkappa_{NC}^{(\nu_\mu e)}(q^2)$ contains the term $I_3(q_l^2, m_l^2, m_l^2)$, which arises from the diagrams that contribute to the neutrino charge radius (Fig. 9). The determination of the neutrino mean-square electroweak radius

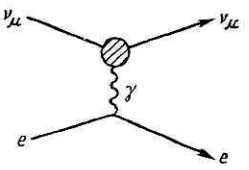

FIG. 9. Diagram describing the contribution to the electromagnetic radius of the neutrino.

$\langle r^2 \rangle$ is discussed below [see Eq. (34)]. [The second term $I_3(q^2, m_f^2, m_f^2)$ corresponds to the contribution of Z–γ mixing (Fig. 10).]

The expressions (20)–(22) are obtained in the approximation $q^2 \ll M_{W,Z}^2$. (This approximation is valid for the considered range of energies $E_\nu \leqslant 3$ TeV.) The self-energy functions $Z(-1)$ and $W(-1)$ are also known. Their difference in the leading term in m_t^2 in the expression (21) has the form

$$Z(-1) - W(-1) \simeq \frac{3m_t^2}{4M_W^2}.$$

The quantum-electrodynamical neutrino scattering cross section (12) is related to the antineutrino scattering cross section by the simple equation

$$\frac{d\sigma^{\text{QED}}}{dy}(\nu_\mu e) = \frac{d\sigma^{\text{QED}}}{dy}(\bar{\nu}_\mu e)\,(g_L \leftrightarrow g_R). \tag{23}$$

Omitting a discussion of the details of the calculations, we note the following two circumstances.

1. The cross section (12) contains fully the corrections taken into account in the single-loop approximation (except for unimportant terms that give a small correction to the radiative correction itself).

2. In the single-loop approximation there is an explicit dependence of the $\nu_\mu e \to \nu_\mu e$ and $\bar{\nu}_\mu e \to \bar{\nu}_\mu e$ cross sections on the masses of the t quarks and the Higgs bosons. This dependence occurs in the functions $\varkappa_{NC}^{(\nu e)}(q^2)$ and $\rho_{NC}^{(\nu e)}(q^2)$ and is expressed in analytic form. For masses $10 \leqslant m_t \leqslant 200$ GeV and $100 \leqslant M_H \leqslant 1000$ GeV the contributions from m_t and M_H will be detectable if the functions $\varkappa_{NC}^{(\nu e)}(q^2)$ and $\rho_{NC}^{(\nu e)}(q^2)$ are measured with an error 1–3% (Tables VI and VII).

The single-loop radiative corrections to the cross sections $\sigma(\nu_e e \to \nu_e e)$ and $\sigma(\bar{\nu}_e e \to \bar{\nu}_e e)$ have also been calculated. The actual cross sections and corrections can be obtained from the expressions (12)–(22) by the substitutions[20,21]

$$\left.\begin{aligned} &g_L^{(\nu_\mu e)}(q^2) \to g_L^{(\nu_e e)}(q^2) = -\frac{1}{2} + \sin^2\theta_W(q^2) + \frac{1}{\rho_{NC}^{(\nu_\mu e)}(q^2)};\\ &g_R^{(\nu_\mu e)}(q^2) \to g_R^{(\nu_e e)}(q^2) = \sin^2\theta_W(q^2);\\ &g_L^{(\nu_e e)} = g_L^{(\nu_\mu e)} + 1;\\ &g_R^{(\nu_e e)} = g_R^{(\nu_\mu e)}. \end{aligned}\right| \tag{24}$$

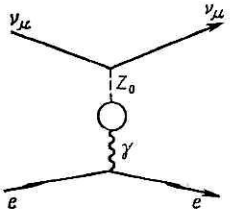

FIG. 10. Diagram corresponding to Z–γ mixing.

TABLE VI. Dependence of $[\varkappa_{NC}^{(\nu_\mu e)} - 1]$ on m_t and M_H, GeV, at the point $|q^2| = 0.05$ (Ref. 14).

m_t	M_H		
	10	100	1000
30	−0.41	−0.71	−1.53
60	−0.75	−1.05	−1.85
90	0.71	0.39	−0.47
130	2.37	2.02	1.10
180	4.89	4.49	3.46
230	8.44	7.95	6.77
300	16.65	15.94	14.30

TABLE VII. Dependence of $[\rho_{NC}^{(\nu_\mu e)} - 1]$ on m_t and M_H, GeV (Ref. 14).

m_t	M_H		
	10	100	1000
30	0.51	0.47	0.27
60	0.59	0.55	0.35
90	0.73	0.69	0.49
130	1.01	0.97	0.77
180	1.52	1.47	1.27
230	2.23	2.18	1.96
300	3.68	3.61	3.37

With allowance for the radiative corrections, the relation (10) can be rewritten in the form

$$R = \frac{\sigma(\nu_\mu e)}{\sigma(\bar{\nu}_\mu e)} = \frac{g_L^2(q^2) + \frac{1}{3} g_R^2(q^2) + \sigma^{\mathrm{QED}}(\nu_\mu e)}{\frac{1}{3} g_L^2(q^2) + g_R^2(q^2) + \sigma^{\mathrm{QED}}(\bar{\nu}_\mu e)}. \quad (25)$$

Substituting the notation (14) in (25), we obtain

$$R = 3\frac{\left[1 - 4\sin^2\theta_W(q^2) + \frac{16}{3}\sin^4\theta_W(q^2)\right] + 4\sigma^{\mathrm{QED}}_{(\nu_\mu e)}}{[1 - 4\sin^2\theta_W(q^2) + 16\sin^4\theta_W(q^2)] + 12\sigma^{\mathrm{QED}}_{(\bar{\nu}_\mu e)}}, \quad (26)$$

where $\sin^2\theta_W(q^2)$ is given by the expression (14). Estimates show that even at neutrino energy $E_\nu \sim 1$ TeV, σ^{QED} gives a correction in the numerator (26) to the bracket containing the $\sin^2\theta_W(q^2)$ combination that does not exceed 3% and, in addition, the correction σ^{QED} has the same sign in the numerator and the denominator. It hardly changes the branching ratio R. If it is ignored, then from the relation (14) we can determine directly $\varkappa_{NC}^{(\nu_\mu e)}(q^2)$, which can be compared with theoretical calculations if M_W^2 and M_Z^2 are known with good accuracy.

The existing results of measurements of the masses of the intermediate bosons are presented in Table VIII (Ref. 22). The main source of errors is the uncertainty in the energy determined by calorimetric measurements. In principle, they should cancel in the measurement of the ratio M_W^2/M_Z^2. However, in reality the different selection criteria and different detected decay modes for the W and Z still lead to errors in the ratio M_W/M_Z. Measurement of both masses M_W and M_Z makes it possible to find $\sin^2\theta_W$ and ρ [see (2) and (3)] or Δr [see (17)], whereas knowledge of only one of the masses (M_W or M_Z) gives a measurement of $\sin^2\theta_W$ that depends on Δr. Making definite assumptions about m_t and M_H in the framework of the standard model, one can calculate the correction Δr.

If we combine the existing results of measurements of M_W, M_Z, and νN scattering and assume that $\rho = 1$, then we can find[22]

$$\sin^2\theta_W = 0.230 \pm 0.005. \quad (27)$$

Significant progress in measurements of $\sin^2\theta_W$ and ρ will be achieved in experiments at the e^+e^- colliders SLC and LEP,

TABLE VIII. Masses of the W and Z bosons and parameters of the standard model deduced from $p\bar{p}$ experiments (Ref. 22).*

Quantity	Experiment		Average	Notes
	UA-1 (a)	UA-2 (b)		
M_W	$83.5^{+1.0}_{+1.1}+2.7$	$80.2+0.6+0.5+1.3$	80.9 ± 1.3	—
M_Z	$93.0+1.4+3.0$	$91.5+1.2+1.7$	91.9 ± 1.8	—
$\sin^2\theta_W - 1 - \frac{M_W^2}{M_Z^2}$	$0.194+0.031$	$0.232+0.025+0.010$	0.216 ± 0.020	$\rho=1$, no assumptions o Δr
$\sin^2\theta_W = \frac{A^2}{M_W^2(1-\Delta r)}$	$0.214+^{0.005}_{0.006}+0.015$	$0.232+0.003+0.008$	0.228 ± 0.008	$m_t = 36$ GeV, $M_H = 100$ GeV, $\rho = 1$
$\sin^2\theta_W = \frac{A^2}{M_Z^2(1-\Delta r)\cos^2\theta_W}$				
$\sin^2\hat{\theta}_W$ (from A_{FB}, $Z \to e^+e^-$)	$0.18+0.04$	—	—	$\sin^2\hat{\theta}_W(M_Z)$, no assumptions o ρ, Δr

*If two errors are given, the first is the statistical error and the second is the systematic error, which is mainly due to the calibration. In the UA-2 results a specific error associated with the assumptions about p_T is identified. If a single error is given, this means that the statistical and the systematic errors have been taken into account. a) D. Denegri (UA-1 Collaboration), Saclay Preprint, Dph PE 86-26 (1986); Sixth Topical Workshop on $p\bar{p}$ Collider Physics (Aachen, 1986); b) R. Ausari *et al.* (UA-2 Collaboration), Phys. Lett. **186B**, 440 (1987).

and also by using the antiproton accumulator ACOL. A measurement of the mass of the Z boson is expected with accuracy $\Delta M_Z = \pm 45$ MeV at SLC and ± 20 MeV at LEP; these results will be achieved by means of special techniques (beam spectrometer at SLC and the technique of spin resonance depolarization at LEP), without which the error in the value of M_Z would be at least twice as large.[22]

At the $p\bar{p}$ collider with an antiproton accumulator the experimental statistics will be improved by about 20 times, and, according to estimates, this should lead to an improvement in the accuracy of the determination of M_Z to the level $\pm$ (150–300) MeV. Subsequently, experiments at LEP-II may reduce this value to $\Delta M_Z = \pm 100$ MeV, and this would lead to accuracies $\Delta \sin^2\theta_W \sim \pm 0.002$ (the statistical and systematic errors are here of the same order). Even greater accuracy can be achieved using polarization of the e^+ and e^- beams (possibly) at LEP: $\Delta \sin^2\theta_W \approx \pm 0.0004$ (Ref. 22). We recall once more that these measurements are not in competition. Rather, the widest possible comparison of results obtained in different processes will permit the fullest verification of the predictions of the standard model.

We return to the expression (26). In principle, the contribution σ^{QED} can be readily taken into account, although in this case the dependence of R on $\sin^2\theta_W$ will be more cumbersome, since $\sin^2\theta_W$ also occurs in σ^{QED}.

With regard to $\rho_{NC}^{(\nu_\mu e)}$, it occurs both in the definition of $g_L^{(\nu_e e)}$ [see (24)] and in the ratio

$$R = \frac{\sigma(\nu_\mu e \to \nu_\mu e)}{\sigma(\nu_\mu e \to \mu^- e)}, \tag{28}$$

from which it can be deduced experimentally and compared with theoretical calculations.[20]

In the single-loop approximation, $\sigma(\nu_\mu e \to \mu^- \nu_e)$ has the form[23]

$$\sigma = \sigma^{Born}\left[1 + \frac{\alpha}{\pi} F(m_e, m_\mu, E_\nu)\right], \tag{29}$$

where

$$\sigma^{Born} = \frac{(G_F^\mu)^2}{\pi} \frac{(s - m_\mu^2)}{s}; \quad s \approx 2E_\nu m_e.$$

In the approximation $s \gg m_\mu^2$ and for the inclusive arrangement of the experiment (only the muon is detected—a condition that is satisfied at the UNK), the function F has the form

$$F(m_e, m_\mu, E_\nu) = \frac{19}{24} - \frac{\pi^2}{6} - \frac{2}{3} \ln \frac{2E_\nu}{m_e}.$$

Thus, experiments on ν_μ and ν_e scattering by electrons at the UNK will ensure a high-precision verification of the electroweak sector of the standard model in the single-loop approximation.

We now make some general remarks about the estimate of the background. The main sources of the background in, for example, the processes $\nu_\mu e \to \nu_\mu e$ and $\bar{\nu}_\mu e \to \bar{\nu}_\mu e$ are the following processes:

a) elastic and quasielastic $\nu_e e$ and $\bar{\nu}_e e$ scattering—from the admixture of ν_e and $\bar{\nu}_e$ neutrinos in the beams of ν_μ and $\bar{\nu}_\mu$ neutrinos (i.e., there is a background from the charged current);

b) coherent production of π^0 mesons and bremsstrahlung of photons in processes of ν_μ ($\bar{\nu}_\mu$) interaction with electrons;

c) interactions of neutrinos (and antineutrinos) with protons (of the type $\bar{\nu}_e p \to e^+ n$) (see, for example, the selection criteria and background estimates in Ref. 23).

The event selection criterion based on the $E_\nu \theta^2$ kinematic criterion is good in that, since each of the listed backgrounds is a fairly slowly varying function of θ^2, the background can be simply extrapolated with respect to θ^2 into the region of the observed signal from the neighborhood of the signal. The background from the coherent production of π^0 mesons must be reduced at the UNK by 2–3 times on the transition from the energy $\langle E_\nu \rangle \sim 6$ GeV to $\langle E_\nu \rangle \sim 180$ GeV because the π^0 production cross section increases slower than the neutrino scattering cross section (despite the relativistic contraction of the forward cone, which leads to an increase of the background by several times). In the experiment of the CHARM collaboration,[24] the background was calculated using the results of Ref. 25. In particular, we note that the background associated with coherent production of the π^0 meson may have independent scientific interest in connection with the study of the space-time structure of the neutral currents (verification of the "confusion theorem"[25]; see below).

The background-elimination procedure is intimately related to the geometry of the experiment, to its physical parameters, and to the particular parameters of the beam. For each experiment there is a corresponding procedure for separation of the signal from the background.

Let us now say a few words about the parameter ρ (3). In the Salam–Weinberg model, it is equal to unity. This corresponds to the so-called minimal $SU(2)_L \times U(1)$ model, in which there is one doublet of Higgs bosons. If we allow the existence of higher representations of the Higgs bosons with respect to the isotopic spin (besides $I = \frac{1}{2}$), then all the cross sections in the standard model that owe their existence to the neutral current must be multiplied by the factor ρ^2, which, in general, need not be equal to unity. Therefore, in the cross sections that owe their origin to the neutral current one measures not only $\sin^2\theta_W$, which, as a rule, is sought from the branching ratio $R = \sigma(\nu_\mu e)/\sigma(\bar{\nu}_\mu e)$ (in which the factor ρ^2 cancels), but also ρ^2, which occurs in the definition of the cross sections:

$$\sigma(\nu_\mu e) = \rho^2 2\sigma_0\left[\left(-\frac{1}{2} + \sin^2\theta_W\right)^2 + \frac{1}{3}\sin^4\theta_W\right] \tag{30}$$

[cf. the expression (8c)]. Then to determine ρ^2 and $\sin^2\theta_W$ it is necessary to measure not only the ratio $R = \sigma(\nu_\mu e)/\sigma(\bar{\nu}_\mu e)$, in which ρ^2 cancels, but also one of the cross sections (8c) or (8d), in which it is necessary to substitute the value of $\sin^2\theta_W$ determined from the ratio R and then make a comparison with the theoretically calculated value. A deviation of ρ^2 from unity will indicate a deviation from the minimal version of the standard model. The value of ρ^2 can also be measured from the branching ratio

$$\tilde{R} = \frac{\sigma(\nu_\mu e \to \nu_\mu e)}{\sigma(\nu_\mu e \to \mu \nu_\mu)}, \tag{31}$$

since ρ^2 does not occur in the cross section due to the charged current, $\sigma(\nu_\mu e \to \mu \nu_\mu)$.

The method of tagged neutrinos[9] permits measurement of the values of ρ^2 and $\sin^2\theta_W$ from the y distribution. We

multiply all the expressions (7) by ρ^2. Under the assumption $\rho^2 = \text{const}$, the coefficient of $(1-y)^2$ can be separated from the "constant" term, which depends only on $\sin^2\theta_W$. For example, in the cross section $d\sigma(\bar{\nu}_\mu e)/dy$ the $\sin^2\theta_W$ and $(-\frac{1}{2}\sin^2\theta_W)^2$ coefficients can be separated. The ratio

$$A = \frac{\sin^4\theta_W}{(-1/2+\sin^2\theta_W)^2} \tag{32}$$

will depend only on $\sin^2\theta_W$. At the same time $\Delta\sin^2\theta_W = \Delta A/16A$. But if in the analysis of the experimental data we include the value of ρ^2, then, as before, it is necessary to substitute the value of $\sin^2\theta_W$ [see (32)] in one of the differential cross sections and compare it with the theoretically calculated value. Of course, one can also use the branching ratio R and a measurement, additionally, of one of the cross sections.

Experiments at the UNK on $\nu_\mu e$ scattering could improve the existing limits on the magnetic moment and other electromagnetic characteristics of the neutrino. The most general expression for the matrix element that describes the electromagnetic interaction of the neutrino can be expressed in the form

$$\langle \nu_f | J_\mu^{em}(0) | \nu_i \rangle = \bar{u}_f [F_1(q^2)\gamma_\mu + F_2(q^2)\sigma_{\mu\nu}q^\nu + F_3(q^2)(q^2\gamma_\mu - (q\gamma)q_\mu)\gamma_5 + F_4(q^2)\sigma_{\mu\nu}q^\nu\gamma_5] u_i, \tag{33}$$

where ν_f and ν_i are the initial and final neutrino states, u_f and u_i are the corresponding spinors describing the neutrino states, q^2 is the 4-dimensional momentum transfer, γ_μ, $\sigma_{\mu\nu}$, and γ_5 are Dirac matrices, and F_1, F_2, F_3, and F_4 are the neutrino form factors. Here, $F_1(q^2)$ is the neutrino charge form factor; $F_1(0)$ is the electric charge of the neutrino. At small momentum transfers

$$F_1(q^2) \approx F_1(0) - \frac{1}{6}\mathbf{q}^2\langle r^2\rangle, \tag{34}$$

where $\mathbf{q}^2$ is the square of the 3-dimensional momentum transfer, and $\langle r^2\rangle$ is the mean-square radius of the electric-charge distribution of the neutrino.[26] If the electric charge of the neutrino is zero, then the expression (34) must be started with the second term:

$$F_1(q^2) \approx -\frac{1}{6}\mathbf{q}^2\langle r^2\rangle. \tag{35}$$

It does not appear to be possible to give a gauge-invariant definition of the neutrino electric-charge radius in the framework of the standard model (it should now be called the neutrino electroweak radius). The set of diagrams that contribute to the neutrino electroweak radius is given in Fig. 11. However, in order to obtain a finite and gauge-invariant expression for $\langle r_\nu^2\rangle$ it is necessary to include in the calculation, besides the diagrams shown in Fig. 11, the diagrams of vertex type for the charged leptons (Figs. 12a and 12b) and of "box" type (Figs. 12c–12f). We shall denote the contribution of all the diagrams shown in Figs. 11 and 12 by $k(q^2)$. Then for the neutrino electroweak radius we can give the definition[20]

$$\langle r_{\nu_e}^2\rangle_{EW} = \frac{3}{2M_W^2}[1-k(0)].$$

Experimental restrictions on the values of $F_1(0)$ and $\langle r^2\rangle$ are given in Table IX. The strongest restriction, $F_1(0) \lesssim 10^{-21}$–10^{-22}, follows from the neutrality of atoms under the assumption of charge conservation in β decay.[27] The function $F_2(q^2)$ is the form-factor function normalized to the anomalous magnetic moment of the neutrino, $F_2(0) = \mu_\nu$, and is usually expressed in electron Bohr magnetons. In the $SU(2)_L \otimes U(1)$ scheme, the analogous magnetic moment is expressed by

$$\mu_\nu = \frac{3G_F e m_\nu}{8\sqrt{2}\pi} \sim 3.2\cdot 10^{-19}\mu_B\left(\frac{m_\nu}{1\text{ eV}}\right). \tag{36}$$

It is proportional to m_ν and is equal to zero if $m_\nu = 0$. In connection with the problem of solar neutrinos,[28] models have been considered[27,29] in recent years that go beyond the framework of the standard model; in them, μ_ν could take a much larger value (up to $\sim 10^{-10}\mu_B$).

If the neutrino has a magnetic moment $\mu_\nu/2m_e$, it must lead to an increase of the differential cross section of $\nu_\mu e$ and $\bar{\nu}_\mu e$ scattering by the amount[30,31]

$$\Delta\frac{d\sigma(\bar{\nu}_\mu e)}{dy} = \frac{\pi\alpha^2\mu_\nu^2}{m_e^2}\left(\frac{1}{y}-1\right);\quad y = \frac{E_e - m_e}{E_\nu}. \tag{37}$$

Data on $\bar{\nu}_\mu e$ scattering lead to the restriction $\mu_{\nu_\mu} < 0.9\times 10^{-9}$, and data on $\bar{\nu}_e e$ scattering lead to $\mu_{\nu_e} < 2\times 10^{-10}$ (see Table IX). With regard to the form-factor functions $F_3(q^2)$ and $F_4(q^2)$, we shall not discuss them here. We merely mention that $F_3(0)$ is the anomalous magnetic moment of the neutrino introduced by Zel'dovich,[32] while $F_4(0)$ is the dipole electric moment of the neutrino. It is usually assumed that $F_4(0) = 0$.

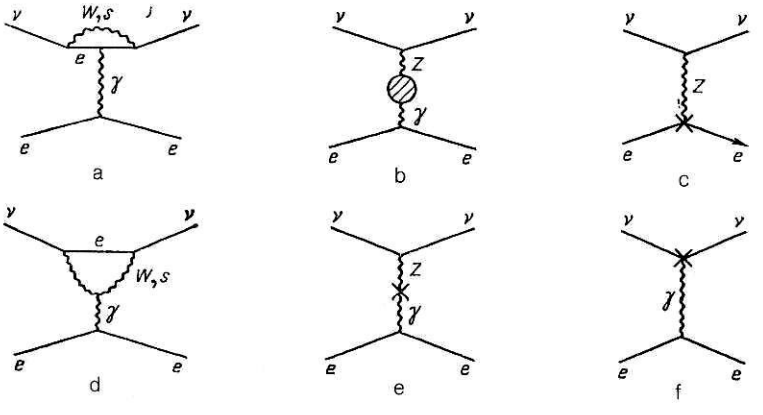

FIG. 11. The set of diagrams corresponding to the contribution to the charge radius of the neutrino (a, d) and to Z–γ mixing (b), and the diagrams of the counterterms (c,e,f).

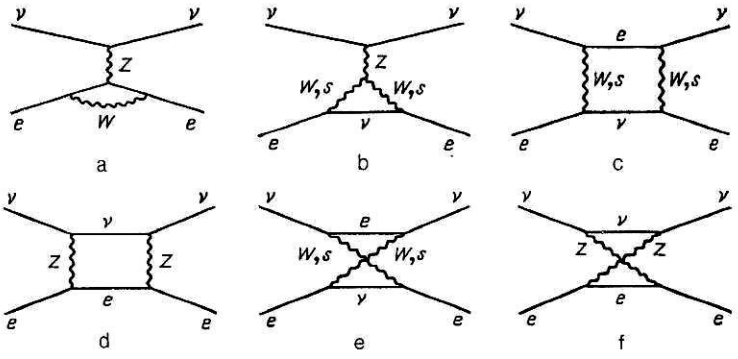

FIG. 12. Diagrams corresponding to the vertex corrections (a,b) and diagrams of "box" type (c–f).

Elastic scattering of neutrinos by nucleons

In the $SU(2)_L \otimes U(1)$ model in the lowest order of perturbation theory, the processes

$$\nu\,(\bar{\nu})\,p,\ n \to \nu\,(\bar{\nu})\,p,\ n$$

are due to exchange of a neutral Z^0 boson (see the diagram in Fig. 13).

We consider the scattering process $\nu_\mu p \to \nu_\mu p$. The corresponding matrix element has the form

$$\langle f|S-1|i\rangle \sim \bar{\nu}\gamma_\alpha(1+\gamma_5)\,\nu\,\langle p'|J^Z_\alpha|p\rangle,$$

where p' and p are the final and initial states of the proton, respectively. The proton vertex can be written in the form

$$\langle p'|J^Z_\mu|p\rangle \sim \gamma_\mu F_1(q^2) + i\sigma_{\mu\nu}\frac{q^\nu}{2M}F_2(q^2) + \gamma_\mu\gamma_5 F_A(q^2),$$

where the 4-dimensional momentum transfer q^2 can be expressed in terms of the difference of the 4-momenta of the final and initial protons: $q^2 = (p'-p)^2$; M is the proton mass, and F_1, F_2, and F_A are the proton form factors. In the standard model, they are related to the electromagnetic form factors of the protons and neutrons by the equations

$$\left.\begin{aligned} F_1(q^2) &= \tfrac{1}{2}[F_1^p(q^2) - F_1^n(q^2)] - 2\sin^2\theta_W F_1^p(q^2);\\ F_2(q^2) &= \tfrac{1}{2}[F_2^p(q^2) - F_2^n(q^2)] - 2\sin^2\theta_W F_2^p(q^2);\\ F_A(q^2) &= \tfrac{1}{2}G_A(q^2). \end{aligned}\right\} \quad (38)$$

The electromagnetic form factors of the nucleons are normalized as follows: $F_1^p(0)=1$, $F_1^n(0)=0$, $F_2^p(0)=\mu_p$, $F_2^n(0)=\mu_n$, where $\mu_p = -1.79$ and $\mu_n = 1.91$ are the anomalous magnetic moments of the proton and neutron, respectively; $G_A(q^2)$ is the axial form factor of the proton, measured in the processes $\nu_\mu n \to \mu^- p$ or $\bar{\nu}_\mu p \to \mu^+ n$. For the axial form factor, the dipole form is usually chosen:

$$G_A(q^2) = \frac{1.26}{\left(1-\frac{q^2}{M_A^2}\right)^2} f(s,\ c,\ b,\ t), \quad (39)$$

where $M_A \approx 1.03$ GeV is a parameter, and $f(s, c, b, t)$ is a function, nearly equal to unity, that describes the contribution of the heavy s, c, b, and t quarks.[33] The number 1.26 in the numerator of the expression (39) is also a parameter of the fit to the experimental data.

The differential cross section for the process $\nu_\mu p \to \nu_\mu p$ ($\bar{\nu}_\mu p \to \bar{\nu}_\mu p$) has the form[34]

$$\begin{aligned} \frac{d\sigma}{dq^2} = \frac{G^2}{2\pi}\cos^2\theta_C \Big\{ &\frac{1}{2}(F_1 \pm F_A)^2 + \frac{1}{2}(1-y)(F_1 \mp F_A)^2 \\ &+ \frac{My}{2E}(F_A^2 - F_1^2) + yF_2\Big[(1-y)\frac{E}{2M}F_2 \\ &+ y\left(F_1 + \frac{F_2}{4} \mp F_A\right) \pm 2F_A\Big]\Big\}, \end{aligned} \quad (40)$$

where θ_C is the Cabibbo angle, $y = q^2/(2ME_\nu)$, and M is the nucleon mass. The upper sign is for the $\nu_\mu p \to \nu_\mu p$ cross section, and the lower sign for antineutrino scattering.

The expression (40) does not include radiative correc-

TABLE IX. Limits on the charge, charge radius, and magnetic moment of the neutrino.[19,27]

Method	$F_1^{(0)}$	$\langle r^2\rangle^{1/2}$	μ, $10^{-9}\,\mu_B$
$\nu_\mu e$ scattering	10^{-6}	$0.9\cdot10^{-16}$	0.95
Astrophysics	10^{-13}	—	0.0085
Supernova SN 1987A	10^{-17}	—	—
$\nu_e e$ scattering	—	—	0.2
Neutron decay	$4\cdot10^{-17}$	—	—
μ decay	$3\cdot10^{-5}$	—	—

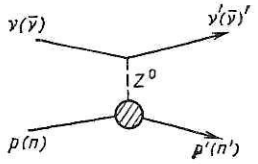

FIG. 13. Diagram describing the process of elastic $\nu(\bar{\nu})N$ scattering (with allowance for the nucleon form factor).

tions. In the region of energies $\leqslant 10$ GeV they are negligibly small.[33,35] In the region of UNK energies, they must be included in the analysis, as in the extraction of the parameters of the axial form factor F_A from the reactions $\nu_\mu p \to \mu^+ n$ and $\nu_\mu n \to \mu^- p$.

Thus, in the framework of the standard model we can determine from the expressions (38) and (40) (after determination of the form factor F_A) the single remaining unknown parameter $\sin^2\theta_W$. The problem of the background is discussed in detail in Refs. 33 and 35.

Deep inelastic scattering of neutrinos by nucleons

Whereas leptons have not hitherto revealed structure and can be regarded as point particles, nucleons are composite systems consisting of quarks of various species and gluons, which the quarks within the nucleons can exchange. The presence of couplings of quarks within nucleons (hadrons) leads to appreciable uncertainties in the interpretation of the results of measurements and the extraction of information about the electroweak interaction of the quarks and the parameters of the theory. However, in the region of deep inelastic interactions the existence of asymptotic freedom (at short distances the quarks interact weakly) offers hope that the corrections for the coupling of the quarks will be small.

The cross section for the inelastic νN interaction is approximately four orders of magnitude greater than for elastic νe scattering, and this ensures a higher statistical accuracy in the measurement of the parameters of the standard model (such as $\sin^2\theta_W$ or ρ).

Indeed, at the present time it is precisely in deep inelastic scattering of neutrinos by nucleons (and nuclei) that the most accurate values of the parameter $\sin^2\theta_W$ are obtained.

The value of $\sin^2\theta_W$ is generally obtained, not from the Paschos–Wolfenstein relation[36]

$$R_- \equiv \frac{\sigma_{NC}(\nu N) - \sigma_{NC}(\bar{\nu}N)}{\sigma_{CC}(\nu N) - \sigma_{CC}(\bar{\nu}N)} = \rho^2\left[\frac{1}{2} - \sin^2\theta_W\right], \quad (41)$$

but from the ratio of the cross sections for deep inelastic scattering of neutrinos by an isoscalar target for the neutral and charged currents:

$$R_\nu \equiv \frac{\sigma_{NC}(\nu N)}{\sigma_{CC}(\nu N)} = g_L^2 + \frac{1}{3}g_R^2 = \frac{1}{2}\rho^2\left[1 - 2\sin^2\theta_W + \frac{40}{27}\sin^4\theta_W\right], \quad (42)$$

where

$$g_L^2 = \rho^2\left(\frac{1}{2} - \sin^2\theta_W + \frac{5}{9}\sin^4\theta_W\right); \quad g_R^2 = \rho^2\frac{5}{9}\sin^4\theta_W \quad (43)$$

[or $g_L^2 = \varepsilon_L^2(u) + \varepsilon_L^2(d)$, $g_R^2 = \varepsilon_R^2(u) + \varepsilon_R^2(d)$].[4)]

The analogous ratio for the antineutrino cross section is

$$R_{\bar{\nu}} \equiv \frac{\sigma_{NC}(\bar{\nu}N)}{\sigma_{CC}(\bar{\nu}N)} = g_L^2 + 3g_R^2 = \frac{1}{2}\rho^2\left[1 - 2\sin^2\theta_W + \frac{40}{9}\sin^4\theta_W\right]. \quad (44)$$

However, it is practically not used, since its sensitivity to variation of $\sin^2\theta_W$ is approximately 30 times poorer [ratio of derivatives $(dR_\nu/d\sin^2\theta_W) : (Rd_{\bar{\nu}}/d\sin^2\theta_W) \approx 30.6$ for a value $\sin^2\theta_W = 0.22$].

The ratios (41)–(44) are obtained in the framework of the simplest parton model with allowance for the contributions of only the valence quarks and without radiative corrections. We mention here that the theoretical corrections associated with the contribution of the sea quarks, the contribution of higher twists, etc., in the region of energies accessible to present-day accelerators have a small influence on the value of $\sin^2\theta_W$ (Table X, Ref. 37). With increasing energy, the influence of the first three corrections increases.

The Paschos–Wolfenstein ratio (41) is attractive because from the theoretical point of view, if one assumes that in the neutrino and antineutrino interactions the structure functions and breaking of scaling are the same, it will not depend on the form of the structure functions and the breaking of the scaling. However, as we have already noted, the ratio (41) does not take into account the contributions of the s, c, t, and b quarks, the importance of which will increase with increasing energy of the incident neutrinos. And whereas at present-day energies the contribution of these quarks to the ratio R_- is unimportant ($\sim$1–2%; see Table X), the problem of the contribution of the heavy s, t, b, and c quarks in the R_- region of TeV energies must be given a theoretically more rigorous treatment. In addition, large systematic errors arise because of the possible errors in the normalization of the neutrino and antineutrino fluxes [the cross sections $\sigma_{NC}(\nu N)$ and $\sigma_{NC}(\bar{\nu}N)$ are subtracted in the numerator of the ratio (41)]. As regards the ratios R_ν and $R_{\bar{\nu}}$, in them the systematic errors due to the uncertainty in the knowledge of the absolute fluxes is less important. In this case the errors arise from the lack of knowledge of the exact

TABLE X. Influence of theoretical corrections on the values of $\sin^2\theta_W$.

Theoretical correction	Change in $\sin^2\theta_W$	Theoretical correction	Change in $\sin^2\theta_W$
From antiquark sea	±0.001	From charmed quarks	±0.001
From strange quarks	±0.001	Higher twist corrections	±0.002

shape of the spectra and the need to take into account corrections in the determination of the minimal values (cutoffs) of the momenta and energies of the hadrons and muons in order to distinguish events due to neutral currents from events due to charged currents. The uncertainties associated with the knowledge of the hadron structure tend to cancel each other in the branching ratios (42) and (44).[38]

The upshot is that the ratio (42) is most often used to determine the value of $\sin^2\theta_W$. In this connection, we draw attention to the following two circumstances. First, in the framework of the quark–parton model for isoscalar targets and in the limit of isospin symmetry ($u \rightleftarrows d$) the contributions of the u, d, $\bar{u}$, and $\bar{d}$ quarks are proportional to the combinations $\varepsilon_L^2(u) + \varepsilon_L^2(d)$ and $\varepsilon_R^2(u) + \varepsilon_R^2(d)$. Second, allowance for the radiative corrections does not introduce significant changes in the structure of the ratio (42)—it leads to a "renormalization" of the constants $\varepsilon_L(f)$ and $\varepsilon_R(f)$, where f denotes any quark flavor[20] [for the notation ε_L and ε_R, see the note on Eq. (43)]:

$$
\begin{aligned}
\varepsilon_L(u) &= \rho_{NC}^{(\nu h)}\left[\frac{1}{2} - \frac{2}{3}\varkappa_{NC}^{(\nu h)}(q^2)\, s^2\right] + \frac{\alpha}{2\pi^2 c^2 s^2} a_{bL}\left(c^2 + \frac{s^2}{3}\right);\\
\varepsilon_L(d) &= \rho_{NC}^{(\nu h)}\left[-\frac{1}{2} + \frac{1}{3}\varkappa_{NC}^{(\nu h)}(q^2)\, s^2\right]\\
&\quad + \frac{\alpha}{2\pi^2 c^2 s^2} a_{bR}\left(c^2 - \frac{s^2}{3}\right);\\
\varepsilon_R(u) &= -\rho_{NC}^{(\nu h)}(q^2)\,\varkappa_{NC}^{(\nu l)}(q^2)\,\frac{2}{3}s^2 + \frac{\alpha}{\pi c^2}\frac{s^2}{20};\\
\varepsilon_R(d) &= \rho_{NC}^{(\nu h)}(q^2)\,\varkappa_{NC}^{(\nu h)}(q^2)\,\frac{1}{3}s^2 + \frac{\alpha}{\pi c^2}\frac{s^2}{10};\\
a_{bL} &= -\left(\frac{9}{16} - \frac{3}{4}s^2 + \frac{4}{15}s^4\right)\frac{1}{c^2};\\
a_{\beta R} &= -\frac{3}{10}s^4;\\
s^2 &= \sin^2\theta_W;\quad c^2 = \cos^2\theta_W.
\end{aligned}
\tag{45}
$$

The functions $\rho_{NC}^{(\nu h)}(q^2)$ and $\varkappa_{NC}^{(\nu h)}(q^2)$ differ slightly from the corresponding functions for the leptons [see Eqs. (20) and (21)]. However, this difference is very small, and we shall assume that $\rho_{NC}^{(\nu h)}(q^2) \approx \rho_{NC}^{(\nu l)}(q^2)$ and $\varkappa_{NC}^{(\nu h)}(q^2) \approx \varkappa_{NC}^{(\nu l)}(q^2)$. The "tree approximation" is obtained by making the substitution $\rho_{NC}^{(\nu h)} = \varkappa_{NC}^{(\nu h)} = 1$, and also by ignoring the terms $\sim\alpha$. It is convenient to rewrite the expression (42) in a form in which the terms responsible for the contributions of the t quarks or the Higgs bosons are explicitly separated[14]:

$$
\begin{aligned}
\widetilde{R}_\nu &= (1 + 2\rho_{NC}^{(t)})\left[\frac{1}{2} - \sin^2\theta_W(1 + \varkappa_{NC}^{(t)})\right.\\
&\quad \left. + \frac{20}{27}\sin^4\theta_W(1 + 2\varkappa_{NC}^{(t)})\right]\\
&\approx R_\nu + 2\rho_{NC}^{(t)} R_\nu + \left[-1 + \frac{40}{27}\sin^2\theta_W\right]\sin^2\theta_W \varkappa_{NC}^{(t)},
\end{aligned}
$$

where $\rho_{NC}^{(t)}$ and $\varkappa_{NC}^{(t)}$ are given by the expressions (20) and (21), respectively.

If in (42) we substitute the expression

$$
\sin^2\theta_W^{\exp} = \sin^2\theta_W + \Delta\sin^2\theta_W,
$$

then

$$
\Delta\sin^2\theta_W = \varkappa_{NC}^{(t)} - \frac{2R_\nu}{1 - \frac{40}{27}\sin^2\theta_W}\rho_{NC}^{(t)}. \tag{46}
$$

Substituting in (46) the expressions (20) and (21) and retaining only the terms quadratic in m_t, we can obtain the explicit dependence of $\Delta\sin^2\theta_W$ on the mass m_t:

$$
\Delta\sin^2\theta_W = -\frac{3\alpha m_t^2}{4\pi M_W^2}\left[\frac{R_\nu}{\sin^2\theta_W} - \frac{2R_\nu}{\sin^2\theta_W\left(1 - \frac{40}{27}\sin^2\theta_W\right)}\right]. \tag{47}
$$

For $\sin^2\theta_W = 0.23$, the term in the square brackets is very close to zero, and the correction to $\Delta\sin^2\theta_W$ associated with the mass m_t^2 is strongly suppressed. We reproduce from the preprint of Ref. 39 Table XI, which characterizes the dependence of $\Delta\sin^2\theta_W$ on m_t (this dependence is not restricted to just the term quadratic in the mass of the t quark).

In contrast, the values of $\varkappa_{NC}$ and Δr [see Eq. (18)] depend strongly on m_t.

Analysis of the experimental data of Ref. 17 shows that the radiative corrections were small, as expected. The smallness of the radiative corrections is intimately related to the choice of the renormalization scheme, namely, the masses of the W and Z bosons are determined by the relations

$$
M_W = \frac{A_0}{\sin^2\theta_W(1 - \Delta r)^{1/2}};\qquad M_Z = \frac{M_W}{\cos\theta_W}
$$

[see the relations (17)]. Here $A_0 = \left(\pi\alpha/\sqrt{2}G_F\right)^{1/2} = 37.281$ GeV. The predicted value $\Delta r = 0.0713 \pm 0.0013$ for $m_t = 45$ GeV and $M_H = 100$ GeV is in excellent agreement with the experimental value $\Delta r_{\exp} = 0.077 \pm 0.037$. The values for $\sin^2\theta_W$ and ρ are

$$
\sin^2\theta_W = 0.229 \pm 0.0064;\quad \rho = 0.998 \pm 0.0086.
$$

[For the other definition $\sin^2\theta_W(0) = e^2\hat{g}^2$, where e is the proton charge, $\hat{g}^2/8M_W^2 \equiv G^2/\sqrt{2}$, and $\cos\theta_W = M_W/M_Z$, the weak mixing angle will differ by 6.7%, and then the values of the radiative correction will be significantly larger.] Despite the smallness of the radiative corrections, they cannot be ignored, since there is then a disagreement with the experimental data (if $\sin^2\theta_W^0 = \sin^2\theta - \Delta s^2$, where $\sin^2\theta_W^0$ is the value of the weak mixing angle without allowance for the radiative corrections, then $\sin^2\theta_W^0 = 0.242 \pm 0.0006$ and $\Delta s^2 = -0.009 \pm 0.001$).

From analysis of experimental data Amaldi *et al.*[17] obtained bounds on the mass of the t quark (Fig. 14), on the mass difference of the quarks of the fourth generation, $|m_{t'} - m_{b'}| < 180$ GeV, $|m_L - m_{\nu_L}| < 310$ GeV (for $M_H = 100$ GeV), and on the masses of the additional Z' bosons

TABLE XI. Dependence of $\Delta\sin^2\theta_W$ on m_t.

m_t, GeV	30	45	60	90 120 180 240
$\Delta\sin^2\theta_W$	−0.010	−0.009	−0.008	−0.010

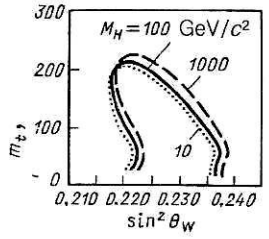

FIG. 14. Allowed region of values of the mass of the t quark and of $\sin^2\theta_W$ for different values of the mass of the Higgs meson (90% C.L.).

which arise in different schemes of extension of the standard model.

In grand-unification theories, a running value of $\sin^2\hat{\theta}_W(\mu)$ is introduced. The variable mass μ for the electroweak processes is usually taken as $\mu = M_W$. Such a choice is very insensitive to the masses of the Higgs boson and the t quark. The relationship between $\sin^2\hat{\theta}_W(\mu)$ and $\sin^2\theta_W = 1 - M_W^2/M_Z^2$ for $M_H = 100$ GeV has the form[17]

$$\sin^2\hat{\theta}_W(M_W) = \left[0.9945 - F\left(\frac{m_t^2}{M_W^2}\right)\right]\sin^2\theta_W,$$

where $F(m_t^2/M_W^2)$ is some complicated function satisfying $F(0) = 0$. For m_t45 GeV, $F(0.31) = 0.0038$. Thus, $\sin^2\theta_W(M_W) = 0.9907\sin^2\theta_W \to 0.228 \pm 0.0044$.

For other values of the masses of the t quark and the Higgs boson the connection between $\sin^2\theta_W$ and $\sin^2\hat{\theta}_W$ is given in Table XII. The $SU(5)$ model predicts the value $\sin^2\theta_W = 0.214^{+0.003}_{-0.004}$, which does not agree well with the experimental data. The values of $\sin^2\hat{\theta}_W(M_W)$ can be interpreted as being in agreement with SUSY GUT.

Thus, measurement of $\sin^2\theta_W$ in processes of deep inelastic scattering of neutrinos by nucleons and nuclei is important for high-precision tests of the standard model. There is hope that in the process of theoretical and experimental analysis of the relation (42) it will be possible to determine more accurately the part played by a number of approximations used in its derivation and to understand better the dependence of $\Delta\sin^2\theta_W$ on: a) the masses of the quarks; b) the distribution functions of the quarks within the nucleons; c) the degree of breaking of scaling; d) the contribution of higher twists; e) the inclusion of the quarks s, c, b, and t in the distribution functions; f) allowance for the effect of nuclear structure (distribution of nucleons in the nuclei), etc.

All these corrections are implicitly contained in $\Delta\sin^2\theta_W$, and this has the consequence that the theoretical error becomes large compared with the experimental error.

We have already noted that at the UNK the statistical accuracy of the measurements will be improved and reduced to the level $\Delta\sin^2\theta_W \simeq \pm 10^{-3}$ in beams of tagged neutrinos and by a further order of magnitude in a wide-spectrum beam. It is to be expected that some of the theoretical uncertainties in the interpretation of the data will be decreased. For example, detailed measurements of the νN reaction (charged currents; see below) will permit more accurate determination of the quark distributions. There is hope[40] that with increasing energy and Q^2 interval at the UNK it will be possible to separate reliably the contribution of the twist corrections to the structure functions, and this will also reduce the theoretical uncertainty in the distribution functions of the quarks with respect to the momenta within the nucleons and permit more accurate determination of the contribution of the twist corrections in the region of TeV energies. Future measurements will give more accurate values of the elements of the quark mixing matrix. If the error in the normalization of the neutrino and antineutrino fluxes at the UNK is reduced, then for the determination of $\sin^2\theta_W$ it may become expedient to use the Paschos–Wolfenstein ratio (41).

Search for the τ neutrino

The category of "unknown" particles currently includes one of the fundamental fermions in the standard model—the τ neutrino—though few doubt its existence. Nevertheless, it is important to prove it experimentally by detecting ν_τ interactions, since the absence of this neutrino would lead to radical changes in the standard model. The most convenient method for looking for the ν_τ neutrino is provided by beam-dump experiments with a vertex detector. The main source of ν_τ must be decays of D_S mesons: $p + A \to D_S + \bar{D}_S + X$, $D_S \to \tau + \nu_\tau$, $\tau \to \nu_\tau + X$. Figures 15a and 15b show the expected energy distribution of the number of events due to ν_τ ($\nu_\tau + N \to \tau + X$) and to all direct neutrinos ($\Sigma\bar{\nu}_e$) in a detector of mass 5 ton situated at 100 m from the shield during 100 days of exposure.[5)] Although $\Sigma\nu_\tau/\Sigma\nu_e \sim 10^{-2}$, the expected statistics of ν_τ events is fairly high[6)]: $\Sigma\nu_\tau \simeq 5.2\times10^4$. The produced τ lepton decays over a distance of a few millimeters from the primary vertex ($l_{\text{dec}} \simeq 0.06\,\text{mm}\cdot E/\text{GeV}$). Thus, the signature of ν_τ is the presence of two showers with vertices positioned along the direction of the neutrino. The semileptonic modes [$\tau^+ \to \pi^+\nu_\tau$ (11%), $\rho^\pm\nu_\tau$ ($\sim$23%), $\pi^\pm\pi^0\pi^0\nu_\tau$ (11%), $\pi^+3\pi^0\nu_\tau$, $\pi^\pm\pi^+\pi^-\nu_\tau$, $\pi^\pm\pi^-\pi^+\pi^0\nu_\tau$] look like neutral-current events; however, they can be selected by means of a kinematic criterion that takes into account the fact that the hadrons from τ decay must on the average have a larger transverse momentum than normal hadronic (quark) jets.

TABLE XII. Relationships between $\sin^2\theta_W$ and $\sin^2\hat{\theta}_W$ for different values of m_t and M_H.

m_t, GeV	M_H, GeV	$\sin^2\theta_W$	$\sin^2\hat{\theta}_W$
25	100	0.229±0.004	0.227±0.004
45	100	0.230	0.228
100	100	0.227	0.229
200	100	0.222	0.233
400	100	0.209	0.248±0.005
45	10	0.229	0.228
45	1000	0.231	0.227

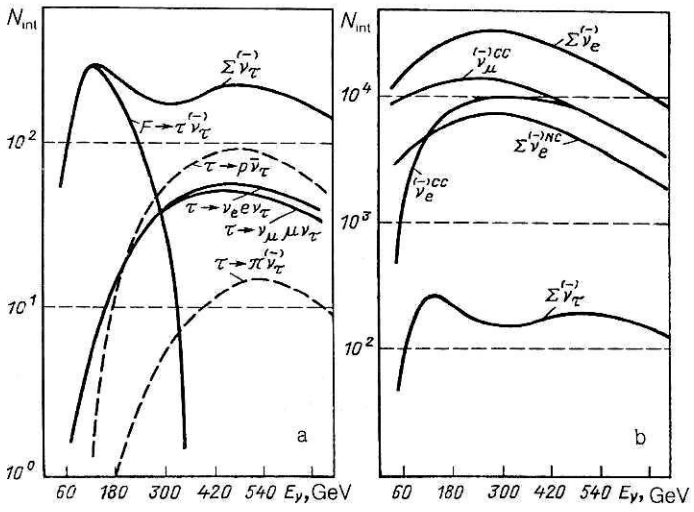

FIG. 15. Expected distribution of the number of events due to ν_τ interactions and to all direct neutrinos, $\Sigma\, \nu_e$, and antineutrinos, $\Sigma\, \bar{\nu}_e$.

Space-time structure of weak currents

This subsection departs from our basic approach, in which we base the treatment entirely on the Lagrangian (1).

General principles permit the following types of interaction: scalar (S), vector (V), axial (A), tensor (T), and pseudoscalar (P). These types correspond to the currents that can be constructed from the spinors ψ_ν ($\bar{\psi}_\nu$) and ψ_e ($\bar{\psi}_e$) which describe the neutrino (antineutrino) and electron–positron fields, respectively. We have: scalar current (S): $\bar{\psi}_\nu \psi_\nu$ or $\bar{\psi}_e \psi_e$, $\bar{\psi}_\nu \psi_e$; vector current (V): $\bar{\psi}_\nu \gamma_\alpha \psi_\nu$ or $\bar{\psi}_e \gamma_\alpha \psi_e$, $\bar{\psi}_\nu \gamma_\alpha \psi_e$; antisymmetric tensor current (T): $\bar{\psi}_\nu \sigma_{\alpha\beta} \psi_\nu$ or $\bar{\psi}_e \sigma_{\alpha\beta} \psi_e$, $\bar{\psi}_\nu \sigma_{\alpha\beta} \psi_e$; axial current ($A$): $\bar{\psi}_\nu \gamma_\alpha \gamma_5 \psi_\nu$ or $\bar{\psi}_e \gamma_\alpha \gamma_5 \psi_e$, $\bar{\psi}_\nu \gamma_\alpha \gamma_5 \psi_e$; pseudoscalar current ($P$): $\bar{\psi}_\nu \gamma_5 \psi_\nu$ or $\bar{\psi}_e \gamma_5 \psi_e$, $\bar{\psi}_\nu \gamma_5 \psi_e$, where γ_α are 4-row Dirac matrices, $\gamma_5 = \gamma_1 \gamma_2 \gamma_3 \gamma_4$, and $\sigma_{\alpha\beta} = \gamma_\alpha \gamma_\beta - \gamma_\beta \gamma_\alpha$.

There are currently a good number of indications that the space-time structure of the weak charged currents is described by the V and A types of interaction, with the $V-A$ type for charged currents. However, a really accurate test of this structure is difficult (particularly for neutral currents) because of the so-called confusion theorem, in which it is established that the $V-A$ interaction type can be mimicked by a suitable mixture of S, P, and T interaction types.[41]

It is well known that the matrix γ_5 anticommutes with V and A couplings and commutes with S, T, and P couplings (by Γ_i we denote any of the sets of γ matrices):

$$\bar{\psi}_e \Gamma_i (1+\gamma_5)\, \psi_\nu = \begin{cases} \psi_e (1-\gamma_5)\, \Gamma_i \psi, & i = V, A; \\ \bar{\psi}_e (1+\gamma_5)\, \Gamma_i \psi, & i = S,\ T,\ P. \end{cases}$$

Thus, in weak interactions the electron is a particle with left helicity for the $V-A$ form of the theory and a particle with right helicity for the S, P, and T versions. The $V-A$ version always couples a neutrino with left helicity to a neutrino with left helicity, while the S, P, and T variants couple "left" neutrinos with "right" neutrinos.

The cleanest test of the predictions of the model relating to helicity can be made by investigating elastic scattering of neutrinos by electrons [see (5a), (5b) and (6a), (6b)]. We shall here give explicit expressions for the cross sections of the processes (5a), (5b) and (6a), (6b) with allowance for the scalar (S), vector (V), axial (A), tensor (T), and pseudotensor (P) couplings[30,38] (in the approximation $m_e/E_\nu \ll 1$):

$$\frac{d\sigma}{dy}(\nu e \to \nu e) = \sigma_0 [A + 2B(1-y) + C(1-y)^2], \qquad (48)$$

where $y = E_e/E_\nu$, $\sigma_0 = G^2 m_e E_\nu / 2\pi$,

$$A = (g_S + g_T)^2 + (g_P + g_T)^2 + 2(g_V + g_A)^2;$$
$$B = 2g_T^2 - g_S^2 - g_P^2;$$
$$C = (g_S - g_T)^2 + (g_P - g_T)^2 + 2(g_V - g_A)^2.$$

For the muon neutrino,

$$\left.\begin{aligned} g_V^\mu &= -\tfrac{1}{2} + 2\sin^2\theta_W; \\ g_A^\mu &= -\tfrac{1}{2}. \end{aligned}\right\} \qquad (49)$$

For the electron neutrino,

$$\left.\begin{aligned} g_V^e &= g_V^\mu + 1; \\ g_A^e &= g_A^\mu + 1. \end{aligned}\right\} \qquad (50)$$

For the antineutrino scattering cross section it is necessary to make the substitution $A \rightleftarrows C$ of the coefficients in Eq. (48).

If we take pure S and P couplings ($g_S \neq 0$, $g_P \neq 0$) and set the remaining coupling constants equal to zero, then

$$A^\nu = A^{\bar{\nu}} = C^\nu = C^{\bar{\nu}};\quad B^\nu = B^{\bar{\nu}}$$

In this case, the difference of the cross sections is zero:

$$\frac{d\sigma(\nu e)}{dy} - \frac{d\sigma(\bar{\nu} e)}{dy} = 0.$$

We obtain the same result for the purely tensor variant.

Irrespective of the choice of the coupling, the difference of the cross sections is

$$\frac{1}{2\sigma_0}\left(\frac{d\sigma(\nu e)}{dy} - \frac{d\sigma(\bar{\nu} e)}{dy}\right) = (A-C)\, y \left(1 - \frac{y}{2}\right). \qquad (51)$$

If the relation (51) is found not to hold, a revision of the theory of weak interactions will be necessary.[42]

The presence of the coefficient B in the expression (48) would be a direct proof of the presence of the S, P, and T

couplings in the neutral currents. If $B = 0$, this would not yet be a proof of the $V - A$ version, since V and A couplings can be mimicked by the S, P, and T couplings, whose contributions are contained in the coefficients A and C.

Using the expressions (49) and (50) for the connection of g_V^e and g_A^e with g_V^μ and g_A^μ, we find that

$$\left.\begin{aligned} A^e &= A^\mu + 4(g_V + g_A) + 4; \\ B^e &= B^\mu; \\ C^e &= C^\mu. \end{aligned}\right\} \qquad (52)$$

If these relations are substituted in the cross section (48), then for the difference of the differential cross sections for scattering of the electron and muon neutrinos (and antineutrinos) we obtain

$$\frac{d\sigma(\nu_e e)}{dy} - \frac{d\sigma(\nu_\mu e)}{dy} = 4\sigma_0(g_V + g_A + 1);$$

$$\frac{d\sigma(\bar{\nu}_e e)}{dy} - \frac{d\sigma(\bar{\nu}_\mu e)}{dy} = 4\sigma_0(g_V + g_A + 1)(1-y)^2,$$

and, after integration over y,

$$\frac{\sigma(\nu_e e) - \sigma(\nu_\mu e)}{\sigma(\bar{\nu}_e e) - \sigma(\bar{\nu}_\mu e)} = 3.$$

These relations are valid for any interaction set, provided that μ–e universality holds.[43]

We make a remark concerning the $V - A$ version of the weak interaction. It follows from (52) that the cross section for $\nu_e e$ scattering contains a term corresponding to interference of the neutral and charged currents; this term is $\sim 4(g_V + g_A)$. In the standard model, $4(g_V + g_A) < 0$ (for $\sin^2\theta_W < 0.5$ and for $\sin^2\theta_W = 0.23$). A negative value of the interference term agrees with experimental reactor data.[44] However, the statistics and accuracy of the measurements are very poor ($49 \pm 15 \nu_e e$ events, subtraction of the background, monitoring of the beam). As a result, there are appreciable errors in the determination of $\sin^2\theta_W$:

$$\frac{\sigma(\nu_e e \to \nu_e e)}{E_\nu} = (9.8^{+2.7+1.5}_{-2.6-1.6}) \cdot 10^{-42}\ \text{cm}^2/\text{GeV};$$

$$\sin^2\theta_W = 0.24^{+0.09+0.05}_{-0.10-0.05}.$$

The $\nu_e e \to \nu_e e$ reaction was studied at Los Alamos (by the IRVIN–Los Alamos–Maryland group).[45] The authors found 250 ± 50 events of elastic scattering. Analysis of the data led to the conclusion that the interference I is destructive, i.e., negative, and its value is

$$I = -0.85 \pm 0.3\ (\text{st}) \pm 0.1\ (\text{syst})$$

($I < 0$ at the 2.7 level). Thus, the experimental data confirm the $V - A$ coupling. These conclusions need further verification with higher statistics and at higher energies. Experiments at the UNK can significantly improve the statistics (see Tables I and II).

Another possibility for measurement of interference of the neutral and charged currents is associated with the production of lepton pairs in the Coulomb field of the proton (or a nucleus):

$$\bar{\nu}_\mu N(A) \to \bar{\nu}_\mu + e^+e^- + N(A); \qquad (53a)$$

$$\bar{\nu}_\mu N(A) \to \bar{\nu}_\mu + \mu^+\mu^- + N(A) \qquad (53b)$$

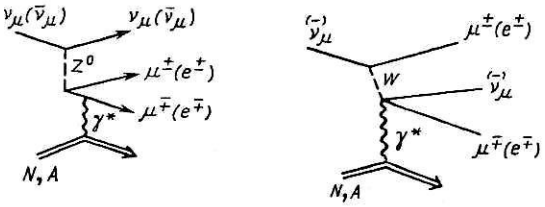

FIG. 16. Diagrams describing the production of $\mu^+\mu^-$ and e^+e^- lepton pairs in interactions of neutrinos with a nucleon (N) or a nucleus (A).

(Fig. 16). In the leading logarithmic approximation, the cross section of the processes (53a) and (53b) has the form[46]

$$\sigma \simeq \frac{2Z^2\alpha^2G^2}{9\pi^3} s_{\max} \ln\left(\frac{s_{\max}}{4m_e^2}\right), \qquad (54)$$

where Z is the charge of the nucleus and $s_{\max} = 2E_\nu Q_{\max} \approx 2E_\nu/R_{\text{nuc}} \sim 2E_\nu m_\pi/A^{1/3}$, in which $Q_{\max}$ is the maximal momentum that can be transferred to the nucleus without its disintegration.

The value of $s_{\max}$ increases faster than E_ν, and, thus, it is advantageous to study the reactions (53a) and (53b) at high energies. However, even at the maximal UNK energies the absolute value of this cross section is two to three orders of magnitude less than the value of the cross section $\sigma(\nu_e e \to \nu_e e)$.

As yet there has been only one relevant experiment.[47] For 1.5×10^6 events involving neutrino charged currents and 1.8×10^6 events involving antineutrino charged currents, this experiment found only 1.7 ± 1.7 events corresponding to "recoilless" production of $\mu^+\mu^-$ pairs in the Coulomb field, whereas estimates led to the expectation of 10 ± 2.6 events. The reason for the discrepancy is not clear.

Polarization experiments play an important part in the determination of the space-time structure of the neutral currents. We shall consider $\nu_\mu p$ and $\bar{\nu}_\mu p$ elastic scattering processes in which the transverse polarization of the scattered proton is measured.[34]

We define the directions of polarization in the laboratory coordinate system in the manner shown in Fig. 17. We denote the transverse, orthogonal, and longitudinal polarizations of the scattered proton by p_T, p_0, and p_L, respectively. The values of p_T and p_0 can be measured by an observation of the angular asymmetry which arises as a result of rescattering of the final proton in the material of the target. It is difficult to measure the coefficient p_L—it does not contribute to the rescattering. The results of the analysis are given in Table XIII. Since the value $Q^2 = 0$ is unattainable, the measurements must be made for the smallest attainable values of Q^2, at which one can hope that p_T will tend to reproduce its limiting values given in Table XIII.

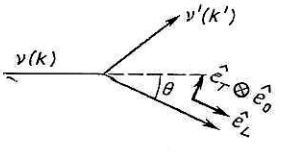

FIG. 17. Directions of polarization in the laboratory system.

TABLE XIII. Values of the transverse polarization p_T for $Q^2 = 0$ (p_L and p_0 are equal to zero at $Q^2 = 0$).

Variant of theory	p_T (for $\nu_\mu p$)	p_T (for $\bar{\nu}_\mu p$)	Variant of theory	p_T (for $\nu_\mu p$)	p_T (for $\bar{\nu}_\mu p$)
$V-A$	+1	+1	V or A	0	0
$V+A$	−1	−1	S, P, T	−1	+1

Neutrino–quark interaction

We now consider the interaction of neutrinos with the fundamental fermions belonging to the quark sector. In contrast to the leptons, the quarks are in a strongly bound state in hadrons, and this leads to theoretical uncertainties in the extraction of information about the electroweak interaction of the quarks and in the determination of the parameters that describe this interaction. However, in events in which there is a large energy transfer ν and large momentum transfer Q^2 the interacting quark can in a first approximation be regarded as free.

Moreover, the cross section of the νN interaction creates conditions much more favorable than does the νe interaction for experimental study of the various phenomena which arise in neutrino–nucleon interactions. Here we shall consider only the aspects that are associated with the electroweak interaction of the quarks. The use of neutrinos to investigate hadron structure and to test the basic propositions of QCD will be discussed in the following subsections.

The Kobayashi–Maskawa mixing matrix

One of the fundamental problems associated with the verification of the theory of the electroweak interactions at the level of the radiative corrections is the problem of the unitarity of the Kobayashi–Maskawa (KM) matrix.[48] In connection with this, we recall that a neutrino interacts with the quarks of nucleons through the exchange of $W^\pm$ and Z^0 bosons. For the charged currents the eigenstates of the quarks that participate in the weak interactions are not identical to their mass states. The interaction of the W bosons with the quarks is described by the Lagrangian $\mathscr{L}_{\text{int}} = -\frac{1}{2}G\,(J_\alpha^+ W_\alpha + \text{h.c.})$, in which the weak eigenstates d', s', b' are related to the mass eigenstates d, s, b by the KM matrix:

$$\begin{pmatrix} d' \\ s' \\ b' \end{pmatrix} = \begin{pmatrix} V_{ud}V_{us}V_{ub} \\ V_{cd}V_{cs}V_{cb} \\ V_{td}V_{ts}V_{tb} \end{pmatrix} \begin{pmatrix} d \\ s \\ b \end{pmatrix}. \tag{55}$$

At the same time, the weak hadronic current J_α is expressed in the form [see (1)]

$$J_\alpha = (\bar{u}\bar{c}\bar{t})\,\gamma_\alpha\,(1-\gamma_5)\begin{pmatrix} d' \\ s' \\ b' \end{pmatrix}.$$

The theory requires that the matrix (55) be unitary. Any deviation from unitarity makes it necessary to introduce new physics or a fourth generation of quarks. This is why it is so important to test the KM matrix as accurately as possible.

Experimental tests of the unitarity property have made it necessary to take into account radiative corrections in the determination of the values of the matrix elements.

For example, the sum of the square of the matrix element V_{ud} deduced from data on β and μ decays (without radiative corrections) and the square of the matrix element V_{us} deduced from semileptonic decays ($\Delta Q = \Delta S = \pm 1$) (also without allowance for radiative corrections) was found to be greater than unity:

$$|V_{ud}|^2 + |V_{us}|^2 > 1$$

(by about 4%), and this immediately violated the unitarity of the KM matrix. The radiative corrections calculated for the β and μ decays were found to have the necessary sign and eliminated the discrepancy.[49]

The KM matrix (55) can be parametrized by means of three mixing angles θ_{ik} (three "rotation" angles) and a complex phase δ, giving four parameters in all. We mention in passing that an accurate determination of the phase can establish whether CP violation is due to the parameters of the KM matrix or has a different nature. There are many choices of the parametrization. (The physics does not depend on the choice of the parametrization.) We shall consider the "standard" parametrization, introduced in the papers of Ref. 50:

$$V = \begin{pmatrix} c_{12}c_{13} & s_{12}c_{13} & s_{13}e^{-i\delta} \\ -s_{12}s_{23} - s_{23}s_{13}c_{12}e^{i\delta} & c_{12}c_{23} - s_{12}s_{23}s_{13}e^{i\delta} & s_{23}c_{13} \\ s_{12}s_{23} - s_{13}c_{12}c_{23}e^{i\delta} & -s_{23}c_{12} - s_{12}s_{13}c_{23}e^{i\delta} & c_{23}c_{13} \end{pmatrix} \begin{matrix} u \\ c \\ t \end{matrix}$$
$$\begin{matrix} d & s & b \end{matrix} \tag{56}$$

Here, c is the cosine of the mixing angle, and s is the sine of the mixing angle.

In an approximate form, in which we ignore the terms $s_{13}^2 \ll s_{23}^2 \ll 1$, i.e., $c_{13} \approx 1$ and $c_{23} \approx 1$, it can be expressed as

$$V = \begin{pmatrix} c_{12} & s_{12} & s_{13}e^{-i\delta} \\ -s_{12} & c_{12} & s_{23} \\ s_{12}s_{23} - s_{13}c_{12}e^{i\delta} & -s_{23}c_{12} & 1 \end{pmatrix}.$$

Experimental determination of the elements of the KM matrix

The word "experimental" used here may not have an entirely precise meaning, since without a calculation of, for example, the two-loop radiative corrections to β decay it would be impossible to determine accurately enough the matrix element $|V_{ud}|$. For V_{ud} the following values are currently given[51]:

$$|V_{ud}| = 0.9744 \pm 0.0010;\ |V_{ud}| = 0.9748 \pm 0.0010;$$
$$|V_{ud}| = 0.9747 \pm 0.0011.$$

We shall follow the exposition given in Ref. 51. The matrix element V_{us} is determined from decays of kaons ($K \to \pi e \nu$):

$$| V_{us} | = 0.2196 \pm 0.0023$$

and leptonic decays of hyperons (WA-2 experiment):

$$\Sigma^- \to n, \ \Lambda^0; \ \Xi^- \to \Lambda, \ \Sigma^0; \ \Lambda \to p;$$
$$| V_{us} | = 0.220 \pm 0.001 \text{ (st)} \pm 0.003 \text{ (theor.)}.$$

The mean value $|V_{us}|$ of these data is

$$| V_{us} | = 0.2197 \pm 0.0019.$$

The matrix element V_{cd} is measured in the process of production of the charmed c quark on the d quark in ν and $\bar{\nu}$ interactions. It is much more difficult to investigate decays of charmed particles and extract from these decays values of V_{cd} (by analogy with V_{us}) than it is to investigate decays of strange particles, because of the short lifetime, the small production cross section, and the large number of particles produced by the decay. It is therefore more expedient to use the production of charmed particles in neutrino interactions. The cross sections for production of the c quark have the form

$$\nu: \ \frac{d^2\sigma}{dx\,dy} = \frac{G^2 M E_\nu x}{\pi} [|V_{cd}|^2 (u(x) + d(x)) + 2s(x) |V_{cs}|^2]; \tag{57a}$$

$$\bar{\nu}: \ \frac{d^2\sigma}{dx\,dy} = \frac{G^2 M E_{\bar{\nu}} x}{\pi} [|V_{cd}|^2 (\bar{u}(x) + \bar{d}(x)) + 2\bar{s}(x) |V_{cs}|^2]. \tag{57b}$$

By measuring both cross sections and making model assumptions about the distributions $u(x)$, $d(x)$, and $s(x)$ (see Sec. 4 for more details about this), we can determine $|V_{cd}|^2$ and $|V_{cs}|^2$ from these cross sections. The detection of dimuons of opposite signs can serve as the experimental signature of such processes. In the dimuons, the second muon arises from semileptonic decay of an excited c quark:

$$\nu_\mu + d \to \mu^- + c \ (c \to s\mu^+\nu_\mu) \sim (u(x) + d(x)) |V_{cd}|^2;$$
$$\nu_\mu + s \to \mu^- + c \sim 2s(x) |V_{cs}|^2;$$
$$\bar{\nu}_\mu + \bar{d} \to \mu^+ + \bar{c} \ (\bar{c} \to \bar{s}\mu^-\bar{\nu}_\mu) \sim (\bar{u}(x) + \bar{d}(x)) |V_{cd}|^2 \text{ (small)};$$
$$\bar{\nu}_\mu + \bar{s} \to \mu^+ + \bar{c} \sim 2\bar{s}(x) |V_{cs}|^2.$$

From a linear combination of the dimuon production cross sections, the CDHS group obtained the value

$$\beta | V_{cd} |^2 = (0.41 \pm 0.07) \cdot 10^{-2}, \tag{58}$$

where β is the effective semileptonic decay ratio of a mixture of charmed particles (D^0, D^+, Λ_c) produced under definite experimental conditions. The value of β was found to be $9.3 \pm 1.0\%$. Thus, from (58) we have

$$| V_{cd} | = 0.21 \pm 0.03.$$

The matrix element V_{cs} can be determined from the cross sections (57) if the quark distributions $u(x)$, $d(x)$, and $s(x)$ are known. Since these distributions are themselves an important subject of investigation (see Sec. 4 below), only a more or less reliable assumption can be made about them: $2s/(\bar{u} + \bar{d}) \leqslant 1$ (we shall call it the "conservative" assumption). Under this assumption $|V_{cs}| > 0.59$ (90% C.L.). From the semileptonic decay of the D mesons, $D \to \bar{K} e^+ \nu_e$, the matrix element $|V_{cs}|^2$ can be determined:

$$\Gamma (D \to \bar{K} e^+ \nu_e) = | F(0) |^2 | V_{cs} |^2 \, 1.54 \cdot 10^{11} \text{ sec}^{-1}, \tag{59}$$

where $F(0)$ is the form-factor function of the D meson.

From the lifetimes of the D^+ and D^0 mesons the MARK II and MARK III groups found the value

$$| F(0) |^2 | V_{cs} | = 0.51 \pm 0.07. \tag{60}$$

Unfortunately, the value of $|F(0)|$ calculated by different authors has a considerable spread: $0.6 \leqslant F(0) \leqslant 0.76$. Thus, if we make the conservative assumption that $|F(0)| < 1$, then from data on the decay of the D mesons we obtain $|V_{cs}| > 0.66$, and if we substitute the mean theoretical value $|F(0)|$, then $|V_{cs}| = 0.96 \pm 0.12$.

The determination of the matrix elements V_{ub} and V_{cb} involves both measurement of the B-meson lifetime and the transition $b \to u$. The B-meson lifetime is related to the matrix elements V_{ub} and V_{cb} by the equation[52]

$$|V_{ub}|^2 + 0.48 |V_{cb}|^2 = \frac{BR(B \to l\nu X)}{\Gamma (B \to l\nu X)} \frac{1}{\tau_B}. \tag{61}$$

The semileptonic decay $B \to l\nu X$ was measured by the decay of the $\Upsilon(4s)$ state. The mean value of the branching ratio was found to be $\text{BR}(B \to l\nu X) = 0.114 \pm 0.005$, and $\text{BR}(B \to \mu\nu X) = 0.113 \pm 0.08$. The transition $b \to u$ can be directly related to muon decay:

$$\frac{\Gamma (B \to l\nu X)}{\Gamma (\mu \to l\nu\nu)} = \frac{m_b^5}{m_\mu^5}. \tag{62}$$

The value $m_b = 5.00 \pm 0.25$ GeV of the mass in the b quark leads to a significantly larger error in the determination of the matrix element $|V_{cb}|$, since the ratio (62) contains the mass to the fifth power. From the unitarity condition $|V_{ud}|^2 + |V_{us}|^2 + |V_{ub}|^2 = 1$ there follows the restriction $|V_{ub}| < 0.01$. Then from (61) we can conclude that $0.034 < |V_{cb}| < 0.051$ and $|V_{cb}| = 0.043 \pm 0.009$. By investigating the decay $b \to u$, we can obtain information about the value of V_{bu}. Figure 18 shows the scheme of the decay $b \to u$.

Because of the difference of the masses of the c and u quarks, the limiting value of the momentum of the spectrum of the leptons l will be different for different decays (transitions), namely, for $b \to c$ it is 2.32 GeV/c and for $b \to u$ it is 2.64 GeV/c. Unfortunately, it is not a simple matter to separate the one decay from the other, and additional theoretical models, which include a number of parameters, are necessary. The new data for the decay-width ratio

$$\frac{\Gamma (b \to u)}{\Gamma (b \to c)} f = \left| \frac{V_{ub}}{V_{cb}} \right|^2,$$

where $f \leqslant 1$, lead to values $|V_{ub}/V_{bc}| < 0.20$, and under weaker restrictions on $f (f = 0.47)$ to the value $|V_{ub}/V_{cb}| < 0.14$ (Ref. 51) (90% C.L.).

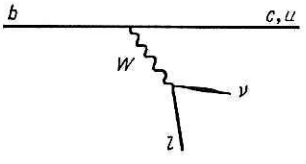

FIG. 18. Scheme of the decays $b \to cW$ and $b \to uW$.

The matrix elements V_{td}, V_{tb}, and V_{ts} can be estimated from the unitarity condition for the KM matrix: $|V_{tb}| \geqslant 0.9982$, $|V_{ts}| \leqslant 0.060$, $|V_{td}| \leqslant 0.026$. Thus, $|V_{ts}|*|V_{td}| \leqslant 0.0016$.

As a consequence of this relation, the contribution of the t quark to the delay $K^+ \to \pi^+ \nu\bar{\nu}$ is strongly suppressed and BR $(K^+ \to \pi^+ \nu\bar{\nu})$ is expected to be at the level of a few units of 10^{-10}. If experiments give a value $\sim 10^{-9}$, this will be a strong argument for the existence of a fourth generation.

We give without comments the values of the mixing angles:

$$\sin^2 \theta_{12} = 0.2197 \pm 0.0019; \ \sin^2 \theta_{23} = 0.044 \pm 0.010;$$
$$0.003 < \sin^2 \theta_{13} < 0.008 \ (90\ \%\ \text{C.L.})$$

Neutral-current interactions

One of the main problems in the analysis of the relation (42) is the determination of the constants $\varepsilon_L(u)$, $\varepsilon_R(u)$, $\varepsilon_L(d)$, and $\varepsilon_R(d)$ [see the note on Eq. (43)]. Such an analysis was made in the studies of Refs. 17 and 53 under the assumption of equality of the constants:

$$\varepsilon_{L,R}(u) = \varepsilon_{L,R}(c) = \varepsilon_{L,R}(t);$$
$$\varepsilon_{L,R}(d) = \varepsilon_{L,R}(s) = \varepsilon_{L,R}(b). \qquad (63)$$

Ultimately, everything reduced to an accurate determination of $\sin^2\theta_W$, in terms of which the constants (63) are expressed.

The ratio R_ν [see (42)] can be expressed in a "model-independent" manner in the form

$$R_\nu = \sum_i [a_i \varepsilon_L^2(i) + b_i \varepsilon_R^2(i)]$$

with a similar expression for $R_{\bar{\nu}}$.

Measurement of the neutral-current–charged-current cross-section ratios on isoscalar targets provides a possibility for determination of the combinations $g_L^2 = \varepsilon_L^2(u) + \varepsilon_L^2(d)$ and $g_R^2 = \varepsilon_R^2(u) + \varepsilon_R^2(d)$. To separate the couplings of the u and d quarks, additional data on nonisoscalar targets (such as hydrogen) are needed. The problem of extracting the coupling constants of the heavy quarks is much more complicated. The CHARM group[54] attempted to determine $\varepsilon_L^2(s) + \varepsilon_R^2(s)$ from the expression

$$\frac{\varepsilon_L^2(s) + \varepsilon_R^2(s)}{\varepsilon_L^2(d) + \varepsilon_R^2(d)}, \qquad (64)$$

using the y distributions of events obtained in charged and neutral currents. For the ratio (64) they obtained the value 1.39 ± 0.43, which agrees with the prediction of the standard model; however, the error was very large.

For the charmed quarks the chiral constants of the neutral current can be obtained from the mass spectra of dimuons of opposite signs:

$$\bar{\nu}_\mu N \to \mu^+\mu^- X.$$

Separating the peak at $M_{\mu^+\mu^-} \sim 3.26$ GeV, corresponding to production of J/ψ particles, and using in the theoretical interpretation of the results the model of photon–gluon fusion, the CDHS collaboration obtained

$$\sigma(\nu N \to \nu\psi N) = (4.2 \pm 1.5) \cdot 10^{-41} \text{cm}^2/\text{nucleon}$$
$$(E_p = 350 \text{ GeV})$$
$$\text{and} \quad [\varepsilon_L^2(c) + \varepsilon_R^2(c)]/[\varepsilon_L^2(u) + \varepsilon_R^2(u)] = 2.1 \pm 0.8.$$

To within the error, this result also agrees with universality of the quarks with the same charge.

This study shows that a program of high-precision measurements of the parameters of the weak hadronic current can be realized with the neutrino beams of the UNK. In all the problems that we have just discussed, the experimental accuracy can be made much higher than the accuracy of the current data and brought to a level $\sim$1–3%. This may lead to important physical results.

Beams of tagged neutrinos permit reduction of the systematic error in the determination of $R = \sigma_{NC}(\nu N)/\sigma_{CC}(\nu N)$ to the level $\leqslant 0.5\%$,[2] and this will permit experimental determination of $\sin^2\theta_W$ with an error of 1%.

However, the following remark must be made. As we have already noted, the theoretical analysis of the semileptonic processes is seriously complicated by the uncertainties associated with the QCD dynamics of the quarks. At the UNK energies, some of these uncertainties (for example, the contributions of the higher twists) become small. However, a sufficiently complete analysis of the various QCD effects in the region of high energies has not yet been made. Therefore, full exploitation of the potential of νN experiments at the UNK is to a large degree dependent on progress in the theoretical analysis or quark dynamics and on the possibilities for reduction of the theoretical uncertainties.

Restrictions on flavor-nonconserving neutral currents

In the standard model, the neutral current conserves flavor. Hitherto decays of the type $s \to dZ^0$, $c \to uZ^0$, $b \to s(d)Z^0$ have not been observed. Neutrino processes permit a test of flavor conservation through a search for events with muons of the "incorrect" signs. Such muons arise from the $\nu_\mu u \to \nu_\mu c$ reaction and the subsequent decay of the c quark. The CDHS group give the result

$$\frac{\nu_\mu u \to \nu_\mu c}{\nu_\mu N \to \nu_\mu X} < 0.026 \ (90\%\ \text{C.L.})$$

In Ref. 55, various experimental possibilities for testing flavor-nonconserving neutral currents are discussed.

It is assumed that the Lagrangian of the interaction of the Z bosons with the neutrinos has the form

$$\mathcal{L}_{\text{int}} = \frac{\bar{g}}{4} [f_{ee}\bar{\nu}_e Z\nu_e + f_{\mu\mu}\bar{\nu}_\mu Z\nu_\mu + f_{\tau\tau}\bar{\nu}_\tau Z\nu_\tau + f_{e\mu}(\bar{\nu}_e Z\nu_\mu + \bar{\nu}_\mu Z\nu_e)$$
$$+ f_{\mu\tau}(\bar{\nu}_\tau Z\nu_\mu + \bar{\nu}_\mu Z\nu_\tau) + f_{\tau e}(\bar{\nu}_\tau Z\nu_e + \bar{\nu}_e Z\nu_\tau)].$$

Here, $Z = Z_\alpha \gamma_\alpha (1 + \gamma_5)$ and $g = e/\sin\theta_W \cdot \cos\theta_W$, $e^2 = 4\pi\alpha$. The standard model corresponds to the case when

$$f_{ee} = f_{\mu\mu} = f_{\tau\tau} = 1, \ f_{e\mu} = f_{\mu\tau} = f_{\tau e} = 0.$$

The cross sections of the $\nu_e e$ and $\bar{\nu}_e e$ elastic scattering processes (the cases of interest for the UNK physics program) have, with allowance for the interaction Lagrangian $\mathcal{L}_{\text{int}}$, the form

$$\sigma_{\nu_e e} = \frac{G_F^2 s}{\pi} \left[\left(\frac{1}{2} + \sin^2\theta_W \right)^2 + \frac{1}{3} \sin^4\theta_W \right.$$
$$\left. + (1 - f_{ee})(1 - 2\sin^2\theta_W) \right];$$

$$\sigma_{\bar{\nu}_e e}=\frac{G_F^2 s}{\pi}\left[\frac{1}{3}\left(\frac{1}{2}+\sin^2\theta_W\right)^2+\sin^4\theta_W+\frac{1}{3}(1-f_{ee})(1-2\sin^2\theta_W)\right],$$

where G_F is the Fermi constant [see the definition (15)], and s is the square of the total c.m.s. energy. A deviation of the value of $1-f_{ee}$ from zero would indicate nonvanishing flavor-nonconserving neutral currents. In the region of UNK energies it is necessary to take into account radiative corrections. The processes of $\mu^+\mu^-$ pair creation in the Coulomb field of a nucleus, $\nu_\mu \to \mu^+\mu^-\nu_\mu$ and $\bar{\nu}_\mu \to \mu^+\mu^-\bar{\nu}_\mu$, are similar to the elastic scattering process. In them, nondiagonal currents would make the cross section of pair production larger than its value in the standard model.

There are many other theoretical models that permit processes with neutral currents that change the flavor: extended models with technicolor, composite models, models with a large number of Higgs doublets with a mixture of flavors in the Higgs sector, models with heavy neutral leptons and mixing in the lepton sector, superstring models, etc. We shall not consider any of them here. As an example, we give the present experimental bounds obtained in the E-691 experiment on the decays of D mesons that are forbidden in the standard model[56]:

$$D^0 \to \mu^+ e < 8\cdot 10^{-5};\ D^+ \to \pi^+\mu^+ e < 2\cdot 10^{-4}.$$

Verification of universality of the generations

The standard model predicts universality of the electroweak properties of the fundamental fermions belonging to different generations. The most accurate comparison of the coupling constants of the charged currents of the e and μ leptons in the region of low energies was obtained from the $\pi \to e\nu_e$ and $\pi \to \mu\nu_\mu$ decays[57]: $g_{e\nu_e}/g_{\mu\nu_\mu} = 0.9939 \pm 0.057$.

For neutral currents measurements of the $\nu_\mu e$ scattering cross section[58] and of the forward–backward asymmetry in the $e^+e^- \to \mu^+\mu^-$ reaction give for the relative strength of the axial-vector couplings of e and μ the following values[17]: $g_A^e g_A^\mu = 0.272 \pm 0.015$ and $g_A^e g_A^\tau = 0.232 \pm 0.026$, in good agreement with the prediction of the standard model and universality.

The ratio of the coupling constants of the leptons of different generations can also be obtained from a measurement of the total cross sections for neutrino semileptonic reactions:

$$\frac{g_{e\nu_e}}{g_{\mu\nu_\mu}}=\left[\frac{\sigma_{\nu_e}}{\sigma_{\nu_\mu}}\right]^{1/2}.$$

With approximately 10% accuracy the existing data confirm universality in both the charged and the neutral currents.

Finally, in the recent experiment of the UA1 group a first verification of universality was achieved for the $\tau\nu_\tau$ coupling constant (for $Q^2 = M_W^2$. The experimental results were[58]

$$g_{\tau\nu_\tau}/g_{e\nu_e} = 1.01 \pm 0.09 \pm 0.05;$$
$$g_{\mu\nu_\mu}/g_{e\nu_e} = 1.05 \pm 0.07 \pm 0.08.$$

A review of the ν_μ–ν_e universality problem is given in Ref. 19.

In experiments at the UNK the universality of the generations can be verified with much higher accuracy and in a new range of energies. As was emphasized in Ref. 2, in beams of tagged ν_e and ν_μ neutrinos universality can be verified directly in the charged and neutral currents, in contrast to the traditional method based on separate measurement of the total (or differential) cross sections of $\nu_\mu N$ and $\nu_e N$ scattering. In beams of tagged neutrinos the cross-section ratios will not contain errors associated with the absolute normalization, and the ratios of the cross sections of the $\nu_e N$ and $\nu_\mu N$ interactions in the charged and neutral currents can be measured with an error $\sim$0.5–1%. Moreover, to measure the ratio of the total probability of interaction through the charged current and the neutral current it is sufficient merely to detect the fact of interaction of a neutrino in the detector. On the other hand, a good determination of the neutrino energy by the tagging system will permit reliable separation (with a systematic error not greater than 1%) of the contributions of the charged and neutral currents. A fundamentally important advantage of the tagging system is the possibility of measuring the ratio of the total (and differential) cross sections of the $\nu_e N$ and $\nu_\mu N$ interaction processes in the neutral-current channel and the neutral–charged-current channel, which is not possible by the traditional methods.

2. STRUCTURE OF NUCLEONS AND VERIFICATION OF QCD

Investigations with beams of high-energy leptons, including neutrinos, played an important part in the investigation of nucleon structure. In processes of deep inelastic scattering of neutrinos by nucleons (Figs. 19a and 19b, in which x and Q^2 are defined) one can measure the structure functions $F_i(x,Q^2)$ averaged over the spin [see Eq. (65) below]. This makes it possible to verify numerous predictions of the quark–parton model (QPM) such as the Gross–Llewellyn-Smith[59] and Adler[60] sum rules and the Callan–Gross relations,[61] to compare the x dependences of the structure functions $F_i(x,Q^2)$ measured in electromagnetic processes and weak charged currents, to obtain information about the quark charges, and to compare the fundamental parameters of the standard model obtained from deep inelastic scattering of neutrinos by nucleons ($\Lambda_{\overline{\rm MS}}$, $\sin^2\theta_W$) with their val-

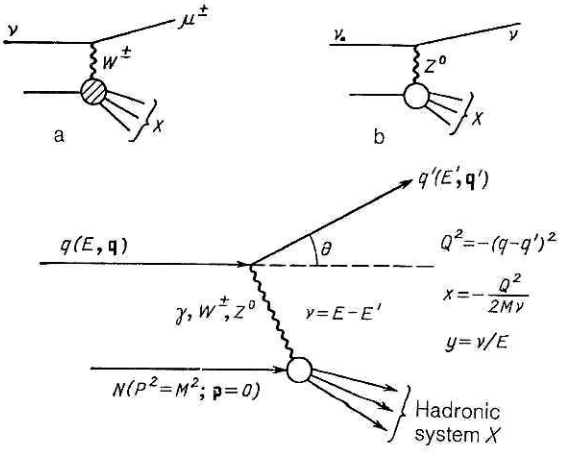

FIG. 19. Diagrams of deep inelastic lepton scattering by nucleons: a) charged current; b) neutral current.

ues found from other measurements). Finally, determination of the structure functions $F_i(x,Q^2)$ opens up the possibility for the most direct investigation of the momentum distributions of the quarks and gluons within nucleons, and also verification of the Q^2 evolution predicted by QCD. These last problems require very careful determinations of the structure functions $F_i(x,Q^2)$ in terms of the distribution functions of the quarks of species j, $q_j(x,Q^2)$, and of the gluons, $G(x,Q^2)$, in the higher orders of QCD perturbation theory, particularly when the determination of the higher twist corrections is under consideration (we shall discuss this question in more detail below).

We consider the inclusive processes

$$\nu + N \to (e^{\pm},\ \mu^{\pm}) + X \text{ (charged currents)};$$
$$\nu + N \to \nu + X \text{ (neutral currents)},$$

where X is an arbitrary hadronic final state (Fig. 19). Let q and q' be the 4-momenta of the initial and final leptons, and p and p' be the 4-momenta of the initial nucleon and the hadronic final state X ($p'^2 = M_X^2$, where M_X is the invariant mass of the final state). In the laboratory coordinate system $p = M$ (M is the mass of the nucleon at rest), $q = (E, \mathbf{q})$, $q' = (E'_\nu, \mathbf{q})$ or $(E'_e, \mathbf{q}')$, $(E'_\mu, \mathbf{q}')$, $Q^2 = -(q-q')^2 = +4EE'\sin^2(\theta/2)$, where θ is the scattering angle of the lepton, and

$$\nu = pQ/M = E - E';\ x = Q^2/(2M\nu);$$
$$y = \nu/E = (E - E')/E.$$

For the charged currents, the inclusive cross section for scattering of a neutrino (antineutrino) by a proton (or a neutron) in the Bjorken limit ($Q^2/\nu \to \text{const}$, $Q^2 \to \infty$, $\nu \to \infty$) can be expressed in the variables x and y in the form

$$\frac{d^2\sigma^{\nu N;\ \bar\nu N}}{dx\,dy} = \frac{G^2ME}{\pi}\left[\left(1 - y - xy\frac{M}{2E}\right)F_2^{(\nu,\bar\nu)}(x) + \frac{y^2}{2}2xF_1^{(\nu,\bar\nu)}(x) \pm \left(y - \frac{y^2}{2}\right)xF_3^{(\nu,\bar\nu)}(x)\right], \quad (65)$$

where the signs $\pm$ in front of the last term correspond to the neutrino or antineutrino scattering processes, respectively, and F_{ip}^{ν} are the structure functions of the process $\nu_\mu + p \to \mu^- + X$:

$$F_{ip}^{\bar\nu} \to \bar\nu_\mu + p \to \mu^+ + X;$$
$$F_{in}^{\nu} \to \nu_\mu + n \to \mu^- + X;$$
$$F_{in}^{\bar\nu} \to \bar\nu_\mu + n \to \mu^+ + X.$$

Under the assumption of charge symmetry,

$$F_{ip}^{\nu} = F_{in}^{\bar\nu};\quad F_{in}^{\nu} = F_{ip}^{\bar\nu}. \quad (66)$$

For isoscalar targets (nuclei with equal numbers of protons and neutrons) the expression (65) is unchanged if $F_i^{\pm}$ is replaced by F_i, where for neutrino scattering

$$F_i(x) = \frac{1}{2}[F_{ip}^{\nu} + F_{in}^{\nu}],$$

and for antineutrino scattering

$$F_i(x) = \frac{1}{2}[F_{ip}^{\bar\nu} + F_{in}^{\bar\nu}].$$

The expression (65) takes a simpler form if the validity of the Callan–Gross relation is assumed:

$$2xF_1(x) = F_2(x). \quad (67)$$

In this case (and under the condition $E_\nu \gg M$)

$$\frac{d^2\sigma^{\nu N;\ \bar\nu N}}{dx\,dy} = \frac{G^2ME}{\pi}\left\{\frac{1}{2}[(1-y)^2+1]F_2(x) \pm \frac{1}{2}[1-(1-y)^2]xF_3(x)\right\}. \quad (68)$$

Thus, for isoscalar targets [see (66)] we have

$$F_2(x)[1+(1-y)^2]\frac{G^2ME}{\pi} = \frac{d^2\sigma^{\nu}}{dx\,dy} + \frac{d^2\sigma^{\bar\nu}}{dx\,dy}; \quad (69)$$

$$xF_3(x)[1-(1-y)^2]\frac{G^2ME}{\pi} = \frac{d^2\sigma^{\nu}}{dx\,dy} - \frac{d^2\sigma^{\bar\nu}}{dx\,dy}, \quad (70)$$

i.e., the structure functions can be expressed in terms of the sum and the difference of the neutrino and antineutrino cross sections.

If we introduce the notation[7]

$$q(x) = u(x) + d(x) + s(x) + c(x);$$
$$\bar q(x) = \bar u(x) + \bar d(x) + \bar s(x) + \bar c(x), \quad (71)$$

where $u(x)$, $\bar u(x)$, $d(x)$, ... are distributions of the u, $\bar u$, d, ... quarks with respect to the momentum within the nucleon, then for the proton

$$F_{2p}^{\nu}(x) = 2x[d(x) + s(x) + \bar u(x) + \bar c(x)];$$
$$F_{3p}^{\nu}(x) = 2[d(x) + s(x) - \bar u(x) - \bar c(x)];$$
$$F_{2p}^{\bar\nu}(x) = 2x[u(x) + c(x) + \bar d(x) + \bar s(x)];$$
$$F_{3p}^{\bar\nu}(x) = 2[u(x) + c(x) - \bar d(x) - \bar s(x)].$$

For the neutron the corresponding functions are obtained from the proton functions by the substitutions $u \rightleftarrows d$ and $\bar u \rightleftarrows \bar d$ (condition of isotopic invariance). Note that $q(x) - \bar q(x) = q_v(x)$, where $q_v(x)$ is the distribution of all the valence quarks (for the proton $q_v = 2u + d$, and for the neutron $q_v = 2d + u$).

The isoscalar structure functions $F_i(x)$ can be expressed in terms of the quark distributions as follows:

$$F_2^{\nu}(x) = x[q(x) + \bar q(x)] + x[s(x) - \bar s(x)] - x[c(x) - \bar c(x)];$$
$$F_2^{\bar\nu}(x) = x[q(x) + \bar q(x)] - x[s(x) - \bar s(x)] + x[c(x) - \bar c(x)];$$
$$F_3^{\nu}(x) = q(x) - \bar q(x) + [s(x) + \bar s(x) - [c(x) + \bar c(x)];$$
$$F_3^{\bar\nu}(x) = q(x) - \bar q(x) - [s(x) + \bar s(x)] + [c(x) + \bar c(x)]. \quad (72)$$

If it is assumed that the distribution of the sea quarks is symmetric, i.e., $s(x) = \bar s(x)$, $c(x) = \bar c(x)$, ..., then the last two terms in $F_2^{\nu,\bar\nu}(x)$ can be ignored, and $F_3^{\nu,\bar\nu}(x)$ can be written in the form $F_3^{\nu,\bar\nu}(x) = q(x) - \bar q(x) \pm 2[s(x) - c(x)]$. The last term in the square brackets is often ignored.

Substituting the relations (67) and (72) in (65), we obtain

$$\left.\begin{aligned}
&\frac{d^2\sigma^{\nu N}}{dx\,dy} = \sigma_0 x[q(x) + s(x) - c(x) + (1-y)^2(\bar q(x) - \bar s(x) + \bar c(x))];\\
&\frac{d^2\sigma^{\bar\nu N}}{dx\,dy} = \sigma_0 x[\bar q(x) + \bar s(x) - \bar c(x) + (1-y)^2(q(x) - s(x) + c(x))];\\
&\sigma_0 = G^2ME/\pi.
\end{aligned}\right\} \quad (73)$$

If (73) is integrated over x (from 0 to 1), we obtain

$$\frac{d\sigma^{\nu N}}{dy} = \sigma_0 [Q + S - C + (1-y)^2 (\bar{Q} - \bar{S} + \bar{C})]; \quad (74)$$

$$\frac{d\bar{\sigma}^{\bar{\nu} N}}{dy} = \sigma_0 [\bar{Q} + \bar{S} - \bar{C} + (1-y)^2 (Q - S + C)], \quad (75)$$

where we have introduced the notation

$$Q = \int_0^1 xq(x)\,dx \text{ etc.}$$

As follows from the definition, the quantities $Q, \bar{Q}, S, \bar{S}, C, \bar{C}$ are the fractions of the nucleon momentum divided among the quarks of the corresponding flavors.

Integrating (74) and (75) over y, we obtain

$$\sigma^{\nu N} = \sigma_0 \left[Q + S - C + \frac{1}{3} (\bar{Q} - \bar{S} + \bar{C}) \right]; \quad (74a)$$

$$\sigma^{\bar{\nu} N} = \sigma_0 \left[\bar{Q} + \bar{S} - \bar{C} + \frac{1}{3} (Q - S + C) \right]. \quad (75a)$$

In QCD, all the QPM expressions given above have the same form in the leading order of perturbation theory. However, in all the quark distributions and QPM structure functions it is necessary to introduce a dependence on Q^2, i.e., it is necessary to write $F_i(x,Q^2), \bar{q}(x,Q^2), c(x,Q^2)$, etc., instead of $F_i(x), \bar{q}(x), c(x)$, etc. In the framework of QCD, the Q^2 dependence of the quark distributions is determined by the Altarelli–Parisi–Lipatov equations[62] [see Eqs. (112) below]. We shall merely mention some consequences of QCD. For example, the mean value of the momentum fraction $\langle q_V(x,Q^2) \rangle$ distributed to all the valence quarks and the mean value of the momentum of a valence quark of a definite species, $\langle x_v \rangle$, decrease with increasing Q^2:

$$\langle q_v(x, Q^2) \rangle = \langle q_v(Q_0^2) \rangle \exp \left[-\frac{64}{3(33-2f)} \left(\frac{\ln(Q^2/\Lambda^2)}{\ln(Q_0^2/\Lambda^2)} \right) \right];$$

$$\langle x_v(x, Q^2) \rangle = \langle x_v(Q_0^2) \rangle \exp \left[-\frac{12}{(33-2f)} \left(\frac{\ln(Q^2/\Lambda^2)}{\ln(Q_0^2/\Lambda^2)} \right) \right]. \quad (76)$$

Calculations made in the framework of QCD give the following asymptotic relations:

$$\langle q(Q^2) \rangle \xrightarrow[Q^2 \to \infty]{} \frac{3f}{16+3f}; \quad (77)$$

$$\langle G(Q^2) \rangle \xrightarrow[Q^2 \to \infty]{} \frac{16}{16+3f}. \quad (78)$$

Since $\lim \langle q_v(Q^2) \rangle \to_{Q^2 \to \infty} 0$, it follows that $\langle q(Q^2) \rangle \to \langle O(q^2) \rangle$, where $O(Q^2)$ is the contribution of all the remaining sea quarks. In particular, for $f=4$, $\langle q(\infty) \rangle \to 43\%$, and $G(\infty) \to 57\%$. The fraction of the momentum corresponding to the sea quarks and gluons increases with increasing Q^2, since they acquire the fraction of the momentum lost by the valence quarks.

Transition of some of the momentum from the valence quarks to the sea and to the gluons with increasing Q^2 has the consequence that the mean values $\langle x \rangle$ for the sea quarks and gluons will be shifted to lower values, i.e., they must become softer. Naturally, this behavior must be reflected in the Q^2 behavior of the structure functions of deep inelastic scattering.

As we have already noted, allowance for the corrections in the coupling constant of the strong interaction, $\alpha_S(Q^2)$, to the leading logarithmic approximation introduces an ambiguity in the method of determining the distribution functions of the quarks and gluons within a nucleon.[63,64] Already in the second approximation in the effective coupling constant $\alpha_S(Q^2)$ there is a violation of the relations of the quark–parton model for the structure functions (72) of deep inelastic scattering. This circumstance makes a parton interpretation of the corresponding QCD expressions difficult and leads to the uncertainty which we have mentioned. It is important to have this uncertainty in mind when processes of deep inelastic scattering are analyzed with allowance for the higher orders of perturbation theory.

In particular, the relation (67), which is valid in the QPM approximation (as $Q^2 \to \infty$), is only approximate in the region of actually measurable Q^2:

$$2xF_1(x) \approx F_2(x). \quad (79)$$

The difference

$$F_2(x, Q^2) - 2xF_1(x, Q^2) = F_L(x, Q^2) \quad (79a)$$

is called the longitudinal function. It reflects the presence in the structure of the nucleon of components with spin $\neq \frac{1}{2}$ (for example, the presence of diquarks, scalar components, etc.). In the region of TeV energies the verification of the relation (79) is of independent interest.

The currently existing lepton beams have permitted measurement of $F_2(x,Q^2)$ in eN, μN, and νN interactions and of $xF_3(x,Q^2)$ in νN interactions up to $Q^2 \simeq 280$ (GeV/c)^2. The behavior of the structure functions $F_i(x,Q^2)$ in their dependence on x and Q^2 was investigated, the problems of the breaking of scaling and the evolution of the structure functions with respect to Q^2 were studied, and approximate quark–gluon distributions in nucleons and nuclei were determined.

The neutrino beams at the UNK will permit a significant extension and deepening of the investigation of deep inelastic scattering processes on nucleons and nuclei. This will be guaranteed by the higher event statistics and by the wider range of variation of the variables x and Q^2 available for the experiments. If the limit with respect to Q^2 is extended by about an order of magnitude, one can, for example, hope to separate with high accuracy the logarithmic dependence with respect to Q^2 in the structure functions $F_i(x,Q^2)$ from the power-law dependence on Q^2, i.e., one can hope to separate the twist corrections. As was already noted in the Introduction, the possibilities presented by the UNK are unique in that for a fairly long time the UNK neutrino beams will have the highest energies and intensities in the world. There is no plan to produce neutrino beams at the SSC accelerator. However, even if that is done, preliminary studies[65] show that the energy resolution needed to investigate the structure functions will hardly be achieved there.

Of particular interest are investigations of the distribution functions of the heavy b and t quarks. Their influence on the analysis of the process of deep inelastic scattering becomes important at values $Q^2 \sim 2m_{b,t}^2$. At the UNK energies it will be possible to follow the appearance of the contributions of the heavy quarks to the structure functions $F_i(x,Q^2)$.[66] The identification of these contributions and the determination of the limits of their appearance with respect to Q^2 are, in turn, important in connection with determina-

tion of a fundamental QCD parameter: $\Lambda_{\overline{MS}}$. It is well known that in the theoretical analysis of deep inelastic scattering it is usually assumed that for a number $f=3$ of the quarks (u, d, s) the region most reliable for the determination of $\Lambda_{\overline{MS}}$ is the region $Q^2 < M_c^2$, while for $f=4$ quarks it is the region $M_c^2 < Q^2 < M_b^2$, etc. (the value of f is sometimes determined by means of the Georgi–Politzer formula[67]

$$f(Q^2) = \sum_f \left[1 - \frac{sM_f^2}{Q^2}\right]^{-1},$$

where M_f is the threshold for production of the fth quark pair). The studies of Ref. 68 established a quantitative law of variation of the parameter $\Lambda_{\overline{MS}}$ on the transition from the three-quark region of Q^2 to the six-quark region. The renormalization-group differential equation in the two-loop approximation for the invariant charge $\alpha_S(Q^2)$ was solved with allowance for the finite masses of the particles, and an explicit expression for the dependence of $\Lambda_{\overline{MS}}$ on Q^2 was obtained.

The considerations mentioned above stimulate interest in the study of nucleon structure in the neutrino beams at the UNK. All the phenomena listed above occur together in the theoretical QCD analysis of deep inelastic scattering processes, and at the UNK energies none of these phenomena can be ignored without a distortion of the QCD picture of the phenomenon.

Total cross sections of the νN interaction

The simplest demonstration of the pointlike nature of the nucleon constituents is the linear growth with the energy of the total cross section for the νN interaction. Such a dependence, which is a reflection of the growth of the phase space for the s-wave scattering of point particles, must occur at relatively low E_ν: $E_\nu \ll M_W^2/2M$. In the region of energies so far investigated, $E_\nu \lesssim 250$ GeV, the influence of the mass of the W boson is unimportant, and the linear growth of the neutrino scattering cross section is confirmed by the experimental data (Fig. 20, Ref. 69). For isoscalar targets (measurements made during the period from 1979 through 1986) the mean value $\sigma/E_\nu \approx 0.67 \times 10^{-38}$ cm^2/GeV was obtained for νN scattering and approximately 0.34×10^{-38} cm^2/GeV for $\bar{\nu}N$ scattering.

Experiments at the UNK will make it possible to extend by almost an order of magnitude the region of energies accessible for measurements of total cross sections and will greatly increase their accuracy. Knowledge of the total cross sections will make it possible to measure the fractions of the momentum of a nucleon (or nucleus) carried by the various species of quarks and gluons [see (74a) and (75a)] and to make a comparison with the structure functions obtained in experiments on deep inelastic scattering of electrons and muons.

It is possible to test some effects predicted by the QPM and the standard model with allowance for QCD corrections.[70] For example, at low energies the influence of M_W is unimportant, the quark distributions do not depend on Q^2, and $\sigma_{\nu N} \sim E_\nu$. Up to energies $E \simeq 100$ GeV a well-known manifestation of the QCD evolution of the parton distributions is the decrease of the valence component [see Eq. (76)] and, therefore, a decrease of the cross section. At higher energies, the propagator of the W boson restricts the momentum transfer $Q^2 = 2M_W xy$ to values $\leqslant M_W^2$ and, thus, restricts the effective interval with respect to $x \lesssim M_W^2/2M_N E_\nu$, and this also makes the cross section smaller than the QPM prediction. However, as we have already noted above, with increasing Q^2 there is a shift of the distribution of the quarks in the nucleons in the region of small x in the direction of an increasing number of soft quarks, and this leads to a growth of the cross section. The combined influence of these effects has been calculated in a number of studies and is shown in Fig. 21, which also gives the contributions of the main components. It can be seen that as E_ν is increased from 10 to 1000 GeV the ratio $\sigma_{\nu N}/E$ varies by 15–20%, a difference that could be detected in UNK experiments. It should also be emphasized that the standard methods for measuring cross sections encounter a number of serious problems related to the nonmonochromaticity of the beams and the monitoring of the neutrino fluxes. These difficulties can be overcome in beams of tagged neutrinos.

Proton and neutron structure functions

Measurement of the doubly differential cross sections (68) for neutrinos and antineutrinos permits information to

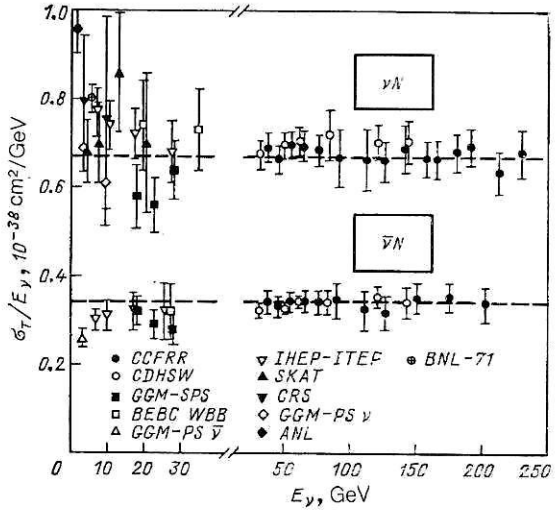

FIG. 20. Total cross sections of νN and $\bar{\nu}N$ interactions.

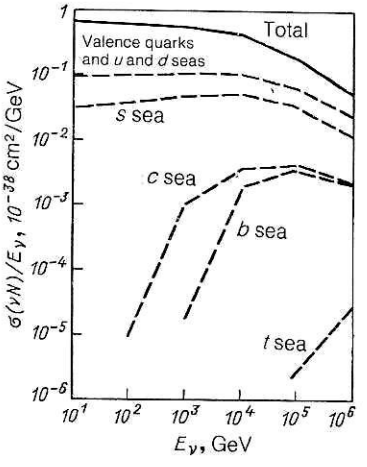

FIG. 21. Expected behavior of $\sigma_{\nu N}$ at high energies. The contributions of the various quarks are shown.

be drawn from the expressions (69) and (70) about the functions $F_2(x,Q^1)$ and $F_3(x,Q^2)$.

The relations (69) and (70) can be integrated with respect to y, and they then take the simpler form

$$\frac{4}{3}\sigma_0 F_2(x,\ Q^2)=\frac{d\sigma^\nu}{dx}+\frac{d\bar{\sigma}^{\bar{\nu}}}{dx}\ ; \tag{69a}$$

$$\frac{2}{3}\sigma_0 x F_3(x,\ Q^2)=\frac{d\sigma^\nu}{dx}-\frac{d\bar{\sigma}^{\bar{\nu}}}{dx}\ . \tag{70a}$$

These relations can also be used to analyze experimental data. Note that the expressions (69), (70) and (69a), (70a) have been obtained under the assumption of validity of the Callan–Gross relation (67), which itself needs to be verified [see (79)]. Quantum chromodynamics does not predict the x dependence of the structure functions $F_i(x,Q^2)$, and it must be extracted as accurately as possible from experimental data.

By means of various combinations of the relations (72) and (73) and sensible approximations (smallness of the contributions of the strange and charmed quarks, etc.) some distributions have been extracted from the experimental data on νN and μN scattering.

In Fig. 22 (Ref. 71) we give the distributions $xu_v(x)$, $xd_v(x)$, and $x\bar{q}(x)$.

Wide use is made in the literature of simple expressions for the quark and gluon distributions with respect to x. They are based on arguments about the behavior of the Regge amplitudes of the processes of deep inelastic neutrino scattering by nucleons in the region of small $x(x\to 0)$ and on quark counting rules in the region $x\to 1$:

$$\left.\begin{array}{ll} q(x)\sim C_1 x^{C_2}(1-x)^{C_3} & \text{for quarks,}\\ G(x)\sim A(1-x)^m & \text{for gluons,}\end{array}\right\} \tag{80}$$

where C_1, C_2, C_3, A, and m are arbitrary parameters whose values are determined by comparison of the theoretically calculated functions $F_i(\bar{x},Q^2)$ with the experimentally measured functions. For the different quark flavors the coefficients C_i must, in principle, be different. Such a parametrization, which is well established but somewhat dated, has a number of shortcomings. First, it leads to a large number of free parameters ($\gtrsim 10$). Second, the choice of the distribution functions (70) may lead to a value of the fundamental parameter $\Lambda_{\overline{MS}}$ that is unjustified from the point of view of QCD. It is well known that the structure functions $F_i(x,Q^2)$ are divided into a nonsingular part $F_i^{NS}(x,\ Q^2)$ and a singular part $F_i^S(x,Q^2)$ (see Sec. 3), which evolve differently with variation of Q^2. The initial functions for the QCD evolution of these parts with respect to Q^2 are, naturally, chosen in the same form (80) (Ref. 72):

$$\left.\begin{array}{l} F_i^{NS}(x,\ Q^2)=C_1 x^{C_2}(1-x)^{C_3};\\ F_i^S(x,\ Q^2)=C_4 x^{C_5}(1-x)^{C_6},\end{array}\right\} \tag{81}$$

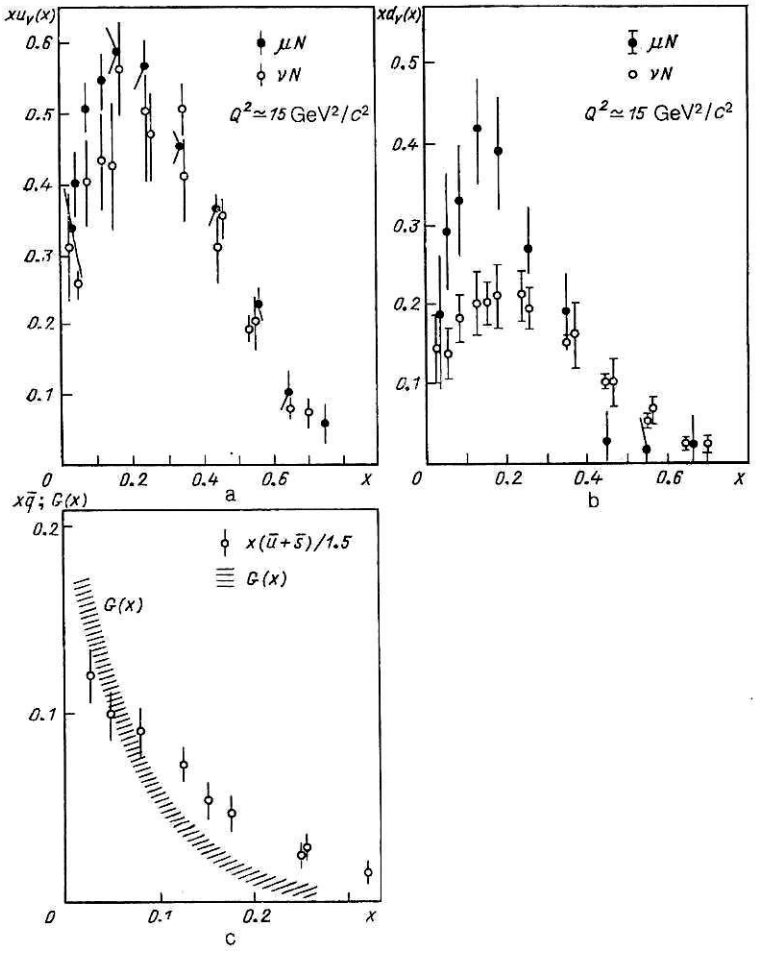

FIG. 22. Quark distributions in the nucleon xu_v (a), xd_v (b), and $x\bar{q}$ (c); the hatched region shows the estimates of the gluon distribution.

where $Q_0^2 \approx 5$ (GeV/c)^2 is the point of reference from which the evolution begins, and C_i are fitting parameters. However, the behavior of the higher moments of functions of the type (81) [for the definition, see (105) and (103)] with respect to Q^2 is very different from the QCD prediction. Only the first moments of the functions F_i^S and F_i^{NS} can satisfy the requirements of QCD to within a given accuracy. The range of validity of QCD with respect to Q^2 is significantly reduced (it is bounded by the values of Q^2 above which deviations from the QCD evolution appear in the higher moments). To improve the agreement with QCD, it is necessary to introduce a dependence of the coefficients C_i on Q^2, and this further increases the number of fitting parameters.[53] But in this case, to achieve better agreement with the experimental data in the region of small Q^2, the authors were forced to give up the requirement of QCD evolution with respect to Q^2 for the distribution function of the valence quarks.

Third, it is well known that the parameter C_2 in the expressions (81), which ought to be equal to $\frac{1}{2}$ according to the Regge asymptotic behavior of the amplitudes of deep inelastic scattering, is found by analysis of experimental data to be equal to 0.6–0.8. For example, in the just quoted study of Ref. 53 the parameter C_2 is a function of Q^2 and does not have a constant value. Fourth, in the gluon distribution function (80) the choice of the values $m = 3, 4, 5, 6, 7, 8$ hardly affects the degree of reliability of the analysis. Fifth, the large number of free parameters leads to great expenditure of computer time in the analysis of experimental data.

This is the list of the main shortcomings of distributions of the type (80) and (81).

It is known from QCD that the functions $F_i(x,Q^2)$ have not only logarithmic behavior with respect to Q^2 (leading logarithmic approximation) but also power-law behavior (twist corrections):

$$F_i(x,\ Q^2) = F_i^{\tau=2}(x,\ Q^2) + \sum_{\tau>2} \left(\frac{h}{Q^2}\right)^{\tau-2} F_i^{\tau}(x,\ Q^2). \qquad (82)$$

In this expression, τ denotes the value of the twist, the term $F_i^{\tau=2}(x, Q^2)$ contains only the logarithmic dependence on Q^2, and $\Sigma_{\tau>2}$ contains terms with a power-law dependence ($\sim 1/Q^{2n}$, where n is an integer), which are called the twist corrections. On the basis of (82) it can be expected that with increasing Q^2 the contribution of the twist terms must decrease.

Besides the above-mentioned shortcomings in the choice of the distribution functions in the form (80) [or of the structure functions in the form (81)], the theoretical analysis of deep inelastic scattering of neutrinos by nuclei and nucleons is made under the assumption that the contributions of the twist terms are negligibly small and that the contribution of the singlet part $F_i^S(x,Q^2)$ can also be ignored (as a rule, it is $\lesssim 20\%$). For example, in the recently published analysis of Ref. 17 the same assumptions are made with regard to the choice of the shape of the distribution functions in the form (80), with regard to the smallness of the contribution of the twist corrections, and with regard to the fact that only the first two moments of the structure functions evolve correctly with respect to Q^2 (we have already noted the inadequacy of this condition).

At the present time it can be said with confidence that in the determination of the parameter $\Lambda_{\overline{\rm MS}}$ from processes of deep inelastic scattering of leptons by nucleons and nuclei the theoretical analysis of the experimental data must be made with allowance for all the contributions (large and small) and with a careful justification of the choice of the dependence of the structure functions on the variable x. In the study of Ref. 66 a quantitative analysis was made of the influence on the value of the fundamental QCD parameter $\Lambda_{\overline{\rm MS}}$ extracted from analysis of deep inelastic lepton–nucleon scattering of the following factors:

a) the choice of the form of the structure functions $F_i(x,Q^2)$ and, therefore, of the quark and gluon distributions;

b) the requirement that not only the first few but also the higher moments of the structure functions $F_i(x,Q^2)$ satisfy the evolution equations of QCD [this extends to the interval of applicability of the functions $F_i(x,Q^2)$ with respect to Q^2];

c) allowance for the singlet part $F_i^S(x,Q^2)$;

d) allowance for the twist corrections;

e) allowance for the post-logarithmic term in the coupling constant $a_S(Q^2)$ in the evolution equations of QCD.

It was shown that allowance for all these listed factors can change the value of $\Lambda_{\overline{\rm MS}}$ by at least a factor 2.

In a number of studies,[73] theoreticians at Dubna have proposed and justified other model momentum distribution functions of the quarks and gluons that satisfy the requirements of QCD to high accuracy. They contain significantly fewer arbitrary parameters (only four were used in the studies of Refs. 66 and 73) and ensure: a) agreement with all the requirements of QCD; b) Regge behavior of the structure functions at the point $x = 0$ and a zero value at $x = 1$; c) good statistical description of the complete set of experimental data on the deep inelastic scattering of leptons by nucleons and nuclei (with a small number of parameters); d) a large gain in computer time in the analysis of experimental data.

A more detailed discussion of the problems of the QCD analysis of deep inelastic scattering can be found in Refs. 66 and 73.

Thus, the determination of structure functions $F_i(x,Q^2)$ and of momentum distributions of the quarks and gluons within nucleons that adequately meet the requirements of QCD must be regarded as important and not yet fully solved problems that could be solved at a new level of statistical reliability and accuracy by neutrino experiments at the UNK.

As yet there is no understanding of the origins and mechanisms of the breaking of the isotopic symmetry of the distribution functions of the light quarks. We are referring here to the different behavior of the distribution functions of the u and d quarks in the proton. Figure 23 shows the ratio $d_v(x)/u_v(x)$. At $x \approx 0$ it agrees with the behavior expected in the framework of the naive quark–parton model. However, in the limit $x \to 1$ it is appreciably less than the QPM predictions. As $x \to 1$, QCD predicts the ratio $d_v(x)/u_v(x) \approx 0.2$ (Ref. 74), whereas arguments based on broken $SU(6)$ symmetry lead to values $d_v(x)/u_v(x) = 0$ (Ref. 75). Advance into the region $x \to 1$ will permit verification of these theoretical predictions.

More accurate data on the structure functions will permit verification of the Adler sum rule with greater accuracy:

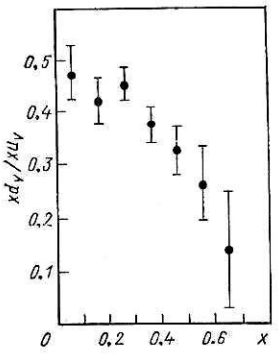

FIG. 23. Ratio xd_v/xu_v as a function of x.

$$\left.\begin{aligned}
&\frac{3\pi}{2G^2M_NE_\nu}\left(\int\limits_{x_{\min}}^{1}\frac{d\sigma(\bar\nu p)}{dx}\frac{dx}{x}-\int\limits_{x_{\min}}^{1}\frac{d\sigma(\nu p)}{dx}\frac{dx}{x}\right)\\
&=\frac{1}{2}(2+3R)(U_v-D_v)+2(\bar D-\bar U);\\
&\frac{\pi}{2G^2M_NE_\nu}\left(\int\limits_{x_{\min}}^{1}\frac{d\sigma(\nu n)}{dx}\frac{dx}{x}-\int\limits_{x_{\min}}^{1}\frac{d\sigma(\nu p)}{dx}\frac{dx}{x}\right)\\
&=\frac{1}{2}(2+R)(U_v-D_v)-\frac{2}{3}(\bar D-\bar U).
\end{aligned}\right\}\quad(83)$$

Here, U_v and D_v are the numbers of the corresponding quarks. In the integrals (82), the limit $x_{\min}\to 0$ is understood. Calculating the left-hand sides of these relations using existing data on νp, $\bar\nu p$, νn, and $\bar\nu n$ scattering and assuming $R=0$, one finds[76]

$$U_v - D_v = 1.01 \pm 0.08 \pm 0.08;$$
$$\bar D - U = 0.05 \pm 0.05 + 0.11.$$

It is also of interest to test the Gross–Llewellyn-Smith sum rule

$$\int\limits_0^1 F_3(\nu N)\,dx=\int\limits_0^1 \Sigma q_v(x)\,dx\left(1-\frac{\alpha_S}{\pi}\right),\quad(84)$$

which is obtained under the assumption of symmetry of the sea. Allowance for the QCD correction improves the agreement with the expected value for the number of valence quarks (equal to three) in the nucleon.[77]

It is important to investigate the influence of the excitation thresholds of the heavy quarks and the differences between them in νN and $\bar\nu N$ reactions. In the investigation of Ref. 78, the distribution functions of the heavy quarks were obtained by solving the QCD evolution equations with allowance for the quark masses. The initial conditions for the evolution equations, i.e., the quark and gluon distribution functions at certain values Q_0^2, are chosen at sufficiently small Q_0^2. This makes it possible in the specification of the initial conditions to make a restriction to the distributions of the light (valence) quarks and gluons. On the basis of numerical solution of the evolution equations the authors of Ref. 78 obtained distribution functions of the heavy c, b, and t quarks possessing the correct threshold behavior, namely, in the region $Q^2 \ll m_q^2$ (m_q is the mass of the corresponding quark) the distribution is suppressed, while at $Q^2 \sim 2m_q^2$ it effectively comes into play. The x dependence of the distribution functions was considered. It was shown that for the heavy quarks the widely used parametrization of the form $x^\alpha(1-x)^\beta$ [see the expression (80)] can lead to appreciable (10–15%) deviations from the correct values. Moreover, the calculations show that the distributions of the sea quarks (including the c, b, and t quarks) arise immediately in a form that cannot be represented by (80). Figure 24, from Ref. 78, shows the Q^2 dependence of the momentum fractions of the quark and gluon distributions, i.e., the second moments of the distribution functions $\langle q(x)\rangle_2$ and $\langle G(x)\rangle_2$. A decrease of the contribution of the gluons and of the u and d quarks and a growth of the contributions of the c, b, and t quarks with increasing Q^2 are clearly demonstrated.

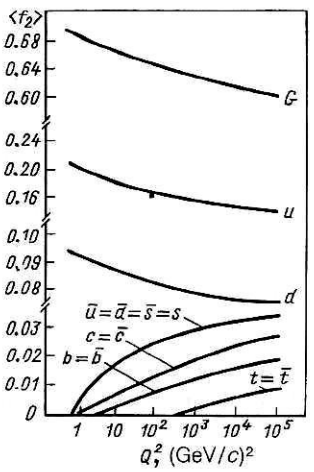

FIG. 24. Dependence of the momentum fractions of the gluon and quark distributions, $\langle f_2\rangle$, on Q^2.

Overall, neutrino investigations at the UNK, in conjunction with the results of experiments on eN and μN scattering, will make it possible to obtain more complete and accurate information about the "flavor" content of the nucleon.

Comparison of the structure functions obtained from neutrino and muon experiments

It is of interest to compare the structure functions obtained from νN, eN, and μN deep inelastic scattering. In contrast to the νN case, the eN and μN scattering cross sections do not contain a contribution from the structure function $F_3(x,Q^2)$, and the connection of the structure functions with the quark distributions includes the square of the quark charge:

$$\left.\begin{aligned}
&(F_2^{\rm EM}(x))_p=x\left[\frac{4}{9}(u+\bar u)+\frac{1}{9}(d+\bar d)\right.\\
&\left.+\frac{4}{9}(c+\bar c)+\frac{1}{9}(s+\bar s)+\frac{4}{9}(t+\bar t)+\frac{1}{9}(b+\bar b)\right];\\
&(F_2^{\rm EM}(x))_n=x\left[\frac{4}{9}(d+\bar d)+\frac{1}{9}(u+\bar u)\right.\\
&\left.+\frac{4}{9}(c+\bar c)+\frac{1}{9}(s+\bar s)+\frac{4}{9}(t+\bar t)+\frac{1}{9}(b+\bar b)\right].
\end{aligned}\right\}\quad(85)$$

(On the transition from the proton to the neutron EM function, the substitution $d\rightleftarrows u$ is made.) For isoscalar targets, $F_2^{\rm EM}=(F_{2p}^{\rm EM}+F_{2n}^{\rm EM})/2$, from which we deduce

$$F_2^{\rm EM}(x)=\frac{5}{18}x[q(x)+\bar q(x)]+\frac{1}{6}x[c+\bar c]+\frac{1}{6}x[t+\bar t]-\frac{1}{6}x[b+\bar b],\quad(86)$$

where $q = u + d + s + c + t + b$ and $\bar{q} = \bar{u} + \bar{d} + \bar{s} + \bar{c} + \bar{t} + \bar{b}$.

In the distributions (72) and (86), all terms apart from the first are usually ignored as small. The discrimination between the quark flavors in deep inelastic μN scattering is not so direct as it is in νN scattering. To extract $u_v(x)$ and $d_v(x)$ from the structure functions $[F_2^{\mathrm{EM}}(x)]_{p,n}$ found in μN scattering several assumptions must be made. Thus, in the study of Ref. 71 it is assumed that $s/d = 0.5$, $q_s(x) = \bar{q}_s(x)$, and $\bar{c}(x)$ is taken from other experiments. Additional restrictions imposed by the Adler and Gross–Llewellyn-Smith sum rules are also imposed. The quark distributions found from νN and μN scattering are compared in Fig. 22. Whereas $x\bar{q}$ and xu_v are in reasonable agreement, the xd_v distributions from the μ and ν experiments differ significantly. Systematic errors could be responsible for the discrepancy. Experiments at the UNK, at which a high accuracy can be ensured, may cast light on this problem.

Comparison of the structure functions found from νN and μN deep inelastic scattering permits determination of the quark charges. For an isoscalar target in the QPM [omitting in (86) the contribution of the b and t quarks] we obtain

$$\frac{F_2^{\mathrm{EM}}(\mu N)}{F_2(\nu N)} = \frac{5}{18}(1+\delta), \tag{87}$$

where

$$\delta = \frac{3}{5}\frac{(c+\bar{c})-(s+\bar{s})}{F_2(\nu N)}$$

[see Eqs. (72) and (86)]. The number 5/18 arises from the quark charges for the $SU(4)$ flavor-symmetric nucleon.

The predictions of the QPM are compared with experimental data in Fig. 25. To within the errors, the data do not reveal a strong dependence of the ratio $f_2(\mu N)/F_2(\nu N)$ on x, although the structure functions themselves vary by more than an order of magnitude. The experimental mean value

$$\left\langle \frac{F_2(\mu N)}{F_2(\nu N)} \right\rangle = 0.29 \pm 0.02 \; (5/18 \approx 0.28)$$

indicates smallness of the contribution of the strange and charmed sea quarks, which is characterized by the term δ in (87) (it is $\approx 6\%$ for $x = 0.03$ and decreases with increasing x). For μN scattering, assuming that the quark seas in the proton and neutron are the same [see (85)], we obtain

$$\int_0^1 [F_2(\mu p) - F_2(\mu n)]\frac{dx}{x} = \frac{e_u^2 - e_d^2}{2}. \tag{88}$$

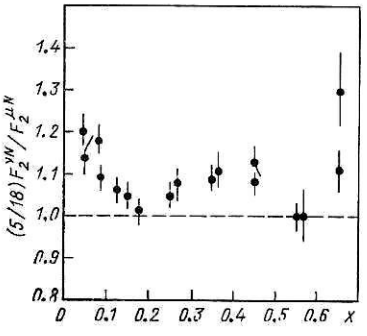

FIG. 25. Ratio of the structure functions measured in experiments on neutrino and muon scattering by iron nuclei.

The integral on the left is equal to 0.25 ± 0.12 (Ref. 79). In conjunction with $\langle F_2(\mu F)/F_2(\nu N)\rangle$, this gives the following values for the charges of the u and d quarks:

$$|e_u| = 0.64 \pm 0.05; \quad |e_d| = 0.41 \pm 0.08.$$

However, it must be emphasized that the poor knowledge of the energy of the initial neutrinos in present-day experiments renders them rather insensitive to small effects, for example, the contributions of the heavy quarks. In Fig. 26 we compare the structure functions $F_2(\mu N)$ and $F_2(\nu N)$ obtained in experiments on hydrogen and deuterium targets; these indicate an x-dependent deviation from the predictions of the quark–parton model. However, the same effect can arise simply as a result of a small ($\sim 1\%$) possible shift in the determination of E_ν (broken curve).[77] Experiments with tagged neutrinos will establish whether the effect shown in Fig. 26 has a physical origin (for example, opening of the thresholds of the heavy quarks) or is due to systematic errors.

Longitudinal structure function

An important problem in the investigation of nucleon structure is accurate measurement of the "longitudinal" structure function

$$F_L(x) = \left(1 + \frac{4M^2x^2}{Q^2}\right)F_2(x) - 2xF_1(x), \tag{89}$$

which takes into account the absorption by nucleons of longitudinally polarized virtual vector bosons, or, equivalently, the ratio

$$R = \sigma_L/\sigma_T, \tag{90}$$

where M is the nucleon mass, and

$$\left.\begin{aligned} \sigma_L &= \sqrt{2}\frac{G\pi}{K}\left[\left(\frac{2Mx}{Q^2} + \frac{1}{2Mx}\right)F_2(x) - \frac{1}{M}F_1(x)\right]; \\ \sigma_T &= \sigma_+ + \sigma_-; \\ \sigma_\pm &= \sqrt{2}\frac{G\pi}{K}\left[F_1(x) \pm \frac{1}{2}\left(1 + \frac{Q^2}{2(\Delta E)^2}\right)F_3(x)\right]. \end{aligned}\right\} \tag{91}$$

In (91), $\sigma_\pm$ are the cross sections for absorption of W bosons with helicities 0, ± 1 and σ_T is the cross section for the

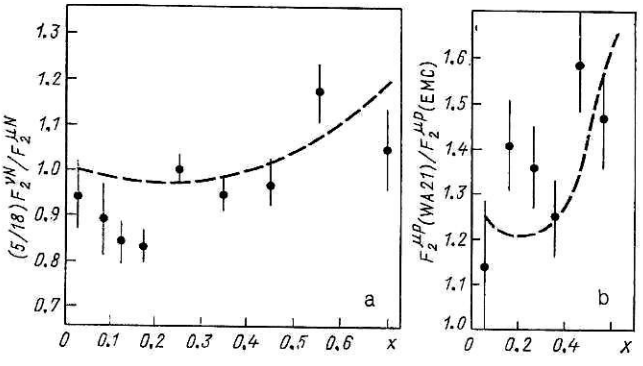

FIG. 26. Comparison of structure functions F_2 measured on deuterium (a) and hydrogen (b): $F_2^{\mu p}$ (WA21) are the values calculated by means of the quark distributions measured in the neutrino experiment of the WA21 collaborations. The broken curves show the effect of a systematic decrease (of about 1%) in the measured energy of the incident neutrinos together with a shift of $\sim 25\%$ in the normalization in (b).

absorption of transverse W bosons; K is the flux factor of the W bosons.

The requirement for measurements of the function $F_L(x)$ is dictated by the need to extract from deep inelastic scattering information about the structure functions $F_2(x)$ and $F_3(x)$ (and about the quark distributions related to them). We note that observation of the EMC effect has the consequence that the extraction of information about the structure of protons and neutrons from data obtained for different nuclei must be made with allowance for the nuclear structure, and the data obtained for different nuclei must probably be considered separately.

From the theoretical point of view, the interest in the function $F_L(x)$ (or the ratio R) is due to the possibility of study of the deviations from the naive QPM, in which allowance is made only for constituents with spin $\frac{1}{2}$ and QCD effects are absent.

Inclusion of the quark mass (r), of the finite transverse momenta (p_T), and of the corrections for the binding energy (Δ) leads in the framework of the QPM to the expression[80]

$$R = 4\frac{M^2x^2r^2 + \langle p_T\rangle^2 + \Delta}{Q^2}. \tag{92}$$

In QCD in the logarithmic approximation, $R = 0$. However, bremsstrahlung of gluons leads to the appearance of a transverse momentum of the quarks. In addition, an effective interaction of gluons with $q\bar{q}$ pairs and the production of $q\bar{q}$ pairs are possible.

In the first order in the QCD coupling constant $\alpha_S(Q^2)$ the expression for R takes the form[81]

$$R_{\rm QCD}(Q^2) = \frac{\alpha_S(Q^2)}{\pi}\frac{x\int_x^1 \frac{2y}{y^3}\left[\frac{8}{3}F_2(y, Q^2) + 4a\left(1-\frac{x}{y}\right)yG(y, Q^2)\right]}{2xF_1(x, Q^2)}. \tag{93}$$

For ν interactions $a = 4$, while for charged leptons $a = 10/9$. At large Q^2 transition to the QCD regime is expected:

$$R_{\rm QCD}(Q^2) \sim \frac{1}{\ln(Q^2/\Lambda^2)}. \tag{94}$$

These perturbation-theoretical estimates can be used at smaller Q^2 if the experimental data are analyzed by means of the Nachtmann variable[82]

$$\xi = \frac{2x}{1+\sqrt{1+\frac{4M^2x^2}{Q^2}}}. \tag{95}$$

The function $F_L(x)$ is usually found by measurement of the y dependence of the difference of the cross sections:

$$\frac{\pi}{G^2mE_\nu}\left[\frac{d^2\sigma^{\bar\nu}}{dx\,dy} - (1-y)^2\frac{d^2\sigma^{\nu}}{dx\,dy}\right] \simeq \bar q^{\bar\nu}[1-(1-y)^4 + F_L[(1-y)-(1-y)^3]]$$

(in this expression the contribution of the heavy quarks is ignored).

In Fig. 27 we give data on deep inelastic scattering of electrons[83] that demonstrate rather clearly the expected decrease of R with increasing Q^2.

The investigation of nucleon structure in neutral currents

This is an important problem for testing the universality of the nucleon structure functions.

We write down here expressions for the differential cross sections of neutrinos and antineutrinos on isoscalar targets, calculated in the QPM[84]:

$$\begin{aligned}\frac{d^2\sigma^{\nu N}}{dx\,dy} = \sigma_0 x\{&(q-\bar q)[\varepsilon_L^2(u) + \varepsilon_L^2(d) + (\varepsilon_R^2(u) \\ &+ \varepsilon_R^2(d))(1-y)^2] \\ &+ [u_s(x) + d_s(x) + \bar u(x) + \bar d(x)](\varepsilon_L^2(u) + \varepsilon_L^2(d) + \varepsilon_R^2(u) \\ &+ \varepsilon_R^2(d))[1 + (1-y)^2] + [s(x) + \bar s(x)][\varepsilon_L^2(d) \\ &+ \varepsilon_R^2(d)][1 + (1-y)^2] \\ &+ [c(x) + \bar c(x)][\varepsilon_L^2(u) + \varepsilon_R^2(d)][1 + (1-y)^2]\}.\end{aligned} \tag{96}$$

In (96), we have introduced the notation $q = u + d + s + c$, $\bar q = \bar u + \bar d + \bar s + \bar c$, $q - \bar q = q_v$; u_s and d_s are the u and d quark distributions of the sea quarks:

$$\left.\begin{aligned}&\varepsilon_L(u) = \varepsilon_L(c) = \frac{1}{2} - \frac{2}{3}\sin^2\theta_W; \\ &\varepsilon_L(d) = \varepsilon_L(s) = -\frac{1}{2} + \frac{1}{3}\sin^2\theta_W; \\ &\varepsilon_R(u) = \varepsilon_R(c) = -\frac{2}{3}\sin^2\theta_W; \\ &\varepsilon_R(d) = \varepsilon_R(s) = \frac{1}{3}\sin^2\theta_W.\end{aligned}\right\} \tag{97}$$

The antineutrino cross section is obtained from the cross section (96) by replacement of the factor in the square brackets multiplying the term $(q - \bar q)$ by the expression

$$[(\varepsilon_L^2(u) + \varepsilon_L^2(d))(1-y)^2 + \varepsilon_R^2(u) + \varepsilon_R^2(d)].$$

The quark content of the structure functions for the neutral currents has the form [cf. (72)]

$$\begin{aligned}F_2(x) = {}& x[\varepsilon_L^2(u) + \varepsilon_L^2(d) + \varepsilon_R^2(u) + \varepsilon_R^2(d)](q + \bar q) \\ &+ x[\varepsilon_L^2(u) + \varepsilon_R^2(u) - \varepsilon_L^2(d) - \varepsilon_R^2(d)] \\ &\times (c(x) - s(x) + \bar c(x) - \bar s(x)); \\ F_3(x) = {}& [\varepsilon_L^2(u) + \varepsilon_L^2(d) - \varepsilon_R^2(u) - \varepsilon_R^2(d)](q - \bar q).\end{aligned} \tag{98}$$

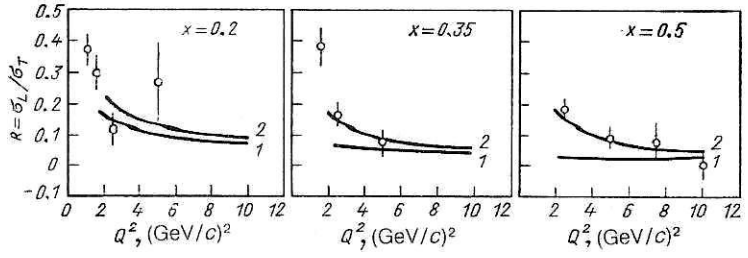

FIG. 27. The ratio $R = \sigma_L/\sigma_T$ from the experiment on deep inelastic scattering of electrons by a deuterium target as a function of Q^2: 1) results of calculations in perturbative QCD; 2) with allowance for the effects of the finite mass of the target.

After integration of the expressions (73) and (96) with respect to x and y it is possible to obtain the ratio (42), which is used to determine $\sin^2\theta_W$.

In Sec. 1 we considered the problem of accurate determination of the value of $\sin^2\theta_W$ from deep inelastic scattering of neutrinos by nucleons. We mentioned the smallness of the influence of the theoretical corrections on the values of $\sin^2\theta_W$ (see Table X), in particular, the weak influence of the shape of the distributions of the heavy c, b, and t quarks on the deduced values of the weak mixing angle. As a rule, the quark and gluon distribution functions occur in an integrated form in the determination of $\sin^2\theta_W$. In some expressions, $\sin^2\theta_W$ is found from the ratio σ_{NC}/σ_{CC}, in which the uncertainties due to the lack of knowledge of the quark and gluon momentum distribution functions cancel each other to a large degree.

The Q^2 evolution and verification of QCD

The dependence of the distribution functions $q(x, Q^2)$ and $F_i(x,Q^2)$ on Q^2 is given by QCD, and it imposes restrictions on the choice of the x dependence of the same functions. Unfortunately, these restrictions are not sufficiently strong to determine unambiguously the x distributions of the quarks and gluons in the nucleon. Nevertheless, a felicitous choice of the x distributions of the quarks and gluons reproduces the Q^2 evolution of both the first and the following moments of the structure functions (see below for the definition of the moments) in a fairly wide interval of Q^2 to within the given accuracy. Thus, we are considering here an approximate choice of the functions $q(x, Q^2)$, $G(x, Q^2)$, and $F_i(x,Q^2)$ that in the intervals $0\leqslant x\leqslant 1$ and $Q_0^2\leqslant Q^2\leqslant Q^2_{\max}$ satisfy with the required accuracy the QCD requirements, i.e., for a certain chosen x distribution ensure correct evolution of the moments with respect to Q^2.

We shall not enter into the theoretical details of the derivation of the evolution of the moments with respect to Q^2, which is determined by the renormalization-group equations. We merely emphasize the difference in the evolution with respect to Q^2 for the singlet and nonsinglet parts of the structure functions determined with respect to the "flavor" $SU(4)$ symmetry. To this end, we introduce some standard definitions.

In the leading logarithmic approximation, as we noted earlier, the connection between the distribution functions and the structure functions is introduced by analogy with the expressions of the QPM. For an isoscalar target and the electromagnetic structure functions [see (86)] the relation has the form

$$F_2^{\mathrm{EM}}(x, Q^2)=\frac{5}{18}x\Sigma(x, Q^2)+\frac{1}{6}x\Delta^{eN}(x, Q^2),$$

where $\Sigma(x,Q^2)=q(x, Q^2)+\bar{q}(x, Q^2)$ and

$$\Delta^{eN}(x, Q^2)=c(x, Q^2)+\bar{c}(x, Q^2)-s(x, Q^2)-\bar{s}(x, Q^2). \tag{99}$$

The combination $\Sigma(x, Q^2)$ is called the singlet combination with respect to the $SU(4)$ flavor symmetry; the combination Δ^{eN} is the nonsinglet part of the function $F_2^{\mathrm{EM}}(x, Q^2)$.

Similar representations can be obtained for the structure functions of deep inelastic neutrino scattering by isoscalar targets. For the charged current

$$\begin{aligned}&F_2^{\nu,\bar{\nu}}=x\Sigma(x, Q^2);\\ &xF_3^{\nu,\bar{\nu}}=xq_v(x, Q^2)\mp x\Delta^{eN}\end{aligned} \tag{100}$$

and for the neutral current

$$\begin{aligned}F_2^{\nu,\bar{\nu}}(x, Q^2)&=x\Sigma(x, Q^2)[\varepsilon_L^2(u)+\varepsilon_L^2(d)+\varepsilon_R^2(u)+\varepsilon_R^2(d)]\\ &\pm x\Delta^{eN}[\varepsilon_L^2(u)+\varepsilon_L^2(d)-\varepsilon_R^2(u)-\varepsilon_R^2(d)];\\ xF_3^{\nu,\bar{\nu}}(x, Q^2)&=xq_v(x, Q^2)[\varepsilon_L^2(u)+\varepsilon_L^2(d)-\varepsilon_R^2(u)-\varepsilon_R^2(d)].\end{aligned} \tag{101}$$

Thus, $F_2^{\nu,\bar{\nu}}$ behaves as a singlet for the charged current and contains a nonsinglet part for the neutral current, while $F_3^{\nu,\bar{\nu}}$ contains singlet and nonsinglet parts for both currents. Thus, any structure function can be expressed in the form

$$F_k(x, Q^2)=F_k^{NS}(x, Q^2)+F_k^{S}(x, Q^2), \tag{102}$$

where $k=2$, 3 or this index can denote the longitudinal function $F_L(x, Q^2)$. The Q^2 evolution of the moments M_n of the nonsingular parts of the structure functions is described by the expressions

$$\left.\begin{aligned}M^{NS}_{n,2}(Q^2)&=\int_0^1 dx x^{n-2}F_2^{NS}(x, Q^2)=\delta_2^{NS}A_n^{NS}\left[\ln\frac{Q^2}{\Lambda^2}\right]^{-\gamma_n^{NS}};\\ M^{NS}_{n,3}(Q^2)&=\int_0^1 dx x^{n-1}F_3^{NS}(x, Q^2)=\delta_3^{NS}A_n^{NS}\left[\ln\frac{Q^2}{\Lambda^2}\right]^{-\gamma_n^{NS}},\end{aligned}\right\} \tag{103}$$

where $\delta_2^{NS}=1/6$ for F_2^{ep} and F_2^{eN}; $\delta_3^{NS}=1$ for $F_3^{\nu,\bar{\nu}}$ (charged currents). For the neutral currents

$$\left.\begin{aligned}\delta_2^{NS}&=\varepsilon_L^2(u)+\varepsilon_R^2(u)-\varepsilon_L^2(u)-\varepsilon_R^2(d) \quad \text{for} \quad F_2^{\nu,\bar{\nu}};\\ \delta_3^{NS}&=\varepsilon_L^2(u)+\varepsilon_L^2(d)-\varepsilon_R^2(u)-\varepsilon_R^2(d) \quad \text{for} \quad F_3^{\nu,\bar{\nu}}.\end{aligned}\right\} \tag{104}$$

The quantities γ_n^{NS} are called anomalous dimensions; they depend on the spins of the quark and gluon fields and can be calculated exactly in QCD perturbation theory. Analytic expressions for γ_n^{NS} and tables of their values can be found in the review of Ref. 84. For different values of n and different numbers of flavors they are different.

For the singlet parts of the structure functions, the expressions for M_n can be written in the leading logarithmic approximation in the form

$$\begin{aligned}M^{S}_{n,2}(Q^2)&=\int_0^1 dx x^{n-2}F_2^{S}(x, Q^2)\\ &=\delta_2^S A_n^-\ln\left[\frac{Q^2}{\Lambda^2}\right]^{-\gamma_N^-}+\delta_2^S A_n^+\ln\left(\frac{Q^2}{\Lambda^2}\right)^{-\gamma_n^+}.\end{aligned} \tag{105}$$

Here $\delta_2^S=5/18$ for F_2^{ep} and F_2^{eN}; $\delta_2^S=1$ for the charged current; and

$$\delta_2^S=\varepsilon_L^2(u)+\varepsilon_L^2(d)+\varepsilon_R^2(u)+\varepsilon_R^2(d) \tag{106}$$

for the neutral current.

It follows from (103) and (105) that all the moments evolve logarithmically with variation of Q^2 and that the singlet moments evolve in a more complicated manner (there are two terms in them). The coefficients A_n^{NS}, A_n^+, and A_n^- are determined by a comparison of the moments with experimental data for some value Q_0^2 and remain constant for all

other values of Q^2. In the leading logarithmic approximation, the coupling constant $\alpha_S(Q^2)$ can be expressed quite simply in terms of $\ln(Q^2/\Lambda^2)$:

$$\alpha_S(Q^2) = \frac{12\pi}{(33-2f)\ln(Q^2/\Lambda^2)}, \quad (107)$$

where f is the number of flavors. Therefore, the expressions for the nonsinglet moments can be put in the form

$$M_n^{NS}(Q^2) = M_n^{NS}(Q_0^2)\left[\frac{\alpha_S(Q_0^2)}{\alpha_S(Q^2)}\right]^{-\gamma_n^{NS}} \quad (108)$$

We have denoted the factor $\delta^{NS}A_n^{NS}$ in (103) by $M_n^{NS}(Q_0^2)\left[\ln(Q_0^2/\Lambda_2)\right]^{\gamma_n^{NS}}$. The expression (103) can also be rewritten as

$$\ln M_n(Q^2) = \ln(\delta_2^{NS}A_n^{NS}) - \gamma_n^{NS}\ln\ln\left(\frac{Q^2}{\Lambda^2}\right), \quad (109)$$

or, differentiating the relation (109) and using (107), we can write

$$\frac{d[\ln M_n(Q^2)]}{d[\ln(Q^2/\Lambda^2)]} = -\gamma_n^{NS}\frac{1}{\ln(Q^2/\Lambda^2)} = -\gamma_n^{NS}\frac{\alpha_S}{12\pi}\frac{33-2f}{3} = \frac{\alpha_S}{2\pi}a_n^{NS}, \quad (110)$$

where

$$a_n^{NS} = -\frac{33-2f}{6}\gamma_n^{NS},$$

or, finally,

$$\frac{d\ln[M_k(Q^2)]}{d\ln[M_n(Q^2)]} = \frac{\gamma_k^{NS}}{\gamma_n^{NS}}. \quad (111)$$

In Fig. 28, the relation (111) expresses the dependence of the ratio of the logarithms of the moments in the form of a straight line whose slope is determined by the anomalous dimensions γ_n, which depend, in addition, on the value of the gluon spin. Thus, the expression (111) permits a transparent verification of the propositions of QCD: a determination of the gluon spin, the evolution with respect to Q^2, the value of Λ, and the form of the structure functions $F_i(x, Q^2)$.

However, such a verification has two serious shortcomings. First, the interval with respect to x within which the structure functions $F_i(x, Q^2)$ are measured does not in the experiments reach the limiting values of x, equal to 0 and 1, as a result of which it is necessary to extrapolate the experimental data to these points in the calculation of the moments [see the expressions (103) and (105)]. This shortcoming is less serious at the energies and momentum transfers Q^2 attainable at the UNK, since the interval of values with respect to x can be significantly extended. Second, unavoidable correlations arise between the moments calculated from one and the same structure function.

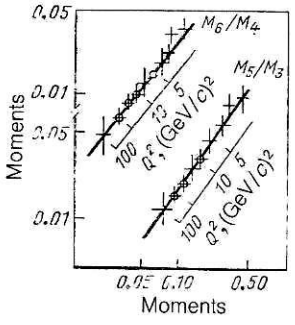

FIG. 28. Relationship between moments of the structure function xF_3.

The most direct verification of the evolution of the functions with respect to Q^2 can be made by means of the QCD evolution equations (the Altarelli–Parisi–Lipatov equations[62]). The solutions of these equations give the functional dependence of the structure functions on Q^2 and x in the complete range of x ($0 \leqslant x \leqslant 1$). Note that to determine the breaking of scaling (i.e., to determine the evolution with respect to Q^2) for the function $xF_3(x, Q^2)$, which occurs in the cross section for neutrino scattering by a nucleon (on an isoscalar target), it is not necessary to know the gluon distribution function. As an example, we write down the evolution equations for the singlet functions:

$$\frac{d\Sigma(x, t)}{dt} = \frac{\alpha_S(t)}{2\pi}\int_x^1 \frac{dy}{y}\left\{\Sigma(y, t)K_{q\to q'}\left(\frac{x}{y}\right) + 2fG(y, t)K_{q\to g}\left(\frac{x}{y}\right)\right\};$$

$$\frac{dG(x, t)}{dt} = \frac{\alpha_S(t)}{2\pi}\int_x^1 \frac{dy}{y}\left\{\Sigma(y, t)K_{g\to q}\frac{x}{y} + G(y, t)K_{g\to q'}\left(\frac{x}{y}\right)\right\}. \quad (112)$$

In these equations, $t = \ln(Q^2/\mu^2)$, μ^2 is a parameter, $K_{q\to q'}(x/y)$ is the kernel of the equation that describes the process of gluon emission by a quark (or $k_{g\to q'}$ is the kernel that describes the transformation of a gluon into a pair of quarks), the kernels of the equations are calculated in accordance with QCD perturbation theory, $\alpha_S(t)$ is the QCD couping constant, Σ is a singlet function, and $G(x, t)$ is the distribution function of the gluons within the target (nucleon, nucleus), and it is also a singlet function.

The evolution equations (112) describe the logarithmic Q^2 dependence of the structure functions. The fundamental constant $\Lambda_{\overline{MS}}$ occurs in these equations as an independent parameter through the coupling constant $\alpha_S(t)$. This parameter $\Lambda_{\overline{MS}}$ determines the behavior of the evolution with respect to Q^2. The determination of its value from experimental is an important task. In Sec. 3, we analyzed the influence of the choice of the x dependence of the structure functions on the determination of $\Lambda_{\overline{MS}}$. Several studies[73,85] have considered the accumulated world data on deep inelastic scattering and have studied the factors that influence the uncertainty in the results of the theoretical analysis.

It was established that at the currently existing energies and momentum transfers Q^2 it is not possible to separate correctly the logarithmic and power-law Q^2 dependences of the structure functions, i.e., it is not possible to separate the twist contributions [the terms with $\tau > 2$ in Eq. (82)]. Therefore, the value of $\Lambda_{\overline{MS}}$ deduced today from the experimental data may also differ appreciably from the true value.

The theoretical analysis of deep inelastic scattering made in 1984 in the study of Ref. 73, in which the twist corrections were calculated in the framework of perturbation theory in the so-called soft-photon approximaiton, led to the following expression for the structure functions with allowance for the twist $\tau = 4$:

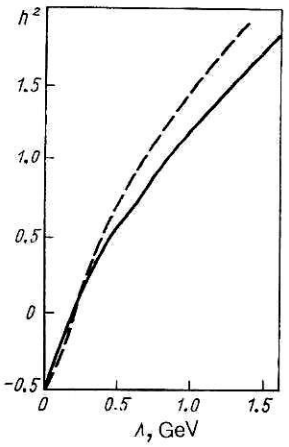

FIG. 29. Correlation between Λ and h. The accuracy of the description of the experimental data hardly changes along the curve (the continuous curve represents the leading logarithmic approximation, and the broken curve is the α_S approximation).

$$F_{2,3}(x,\ Q^2) = F_{2,3}^{\tau=2}(x,\ Q^2) + F_{2,3}^{\tau=4}(x,\ Q^2)$$
$$= \left(1 + \frac{h^2}{Q^2}\, x\, \frac{\partial}{\partial x}\right) F_{2,3}^{\tau=2}(x,\ Q^2), \qquad (113)$$

i.e., the twist correction ($\tau = 4$) was expressed in terms of the x derivative $x(\partial/\partial x)F_i^{\tau=2}(x, Q^2)$. The x dependence of the functions $F_i^{\tau=2}(x, Q^2)$ is known from experiment—in the region $x \lesssim 0.3$ they increase slightly as functions of x, while in the region $x \gtrsim 0.3$ they decrease. Therefore, in the region $x \lesssim 0.3$ the twist corrections are positive, and in the region $x \gtrsim 0.3$ they are negative. Thus, in contrast to the standard approach, in which the twist corrections are taken into account phenomenologically and are taken to be positive from the very beginning, we see that, in general, they may be of variable sign. In this case, the correlation between the parameters $\Lambda_{\overline{MS}}$ and h^2 shown in Fig. 29 indicates that a satisfactory description of the experimental data can be obtained for practically all $\Lambda_{\overline{MS}}$ in the interval $100 \lesssim \Lambda_{\overline{MS}} \lesssim 1000$ MeV (naturally, for a corresponding choice of the value of h^2).

It was also found that $\Lambda_{\overline{MS}}$ depends strongly on the choice of the initial conditions for the QCD evolution equations.

At the UNK the statistics of deep inelastic scattering processes in charged currents can be increased by almost two orders of magnitude compared with present experiments, and the Q^2 region can be extended by an order of magnitude. In such a situation, UNK experiments will be able to answer a number of important questions. Thus, despite the decrease of the contribution of the twist corrections to the structure functions (with increasing Q^2 they decrease in proportion to $1/Q^2$), their influence on the Q^2 evolution is sufficiently pronounced to permit, with allowance for the already available data at $Q^2 \lesssim 200$ (GeV/c)^2, separation of the logarithmic and power-law dependences of the structure functions on Q^2 and determination of the sign of the twist corrections. The extension of the Q^2 region will permit a more detailed investigation of the distribution functions of the heavy quarks, and one will be able to trace the sequence in which they are "switched on," this being important for the investigation of the Q^2 dependence of the running coupling constant $\alpha_S(Q^2)$ of the strong interactions. Separation of the effects of the higher twists will make it possible to obtain information about the quark and gluon correlation functions, which are important characteristics of gluon structure.[73] It will be possible to determine more accurately the values of the fundamental parameters of the standard model and the chiral constants of the neutral currents.

Figure 30 shows the results of the extrapolation[86] of the structure functions determined at the currently accessible Q^2 values to the values $Q^2 \simeq 10^4$(GeV/c)^2, which will be available at future accelerators. Figure 31 gives a comparison with data obtained at the S$p\bar{p}$S collider at $Q^2 = 2000$ (GeV/c)^2, i.e., at the values that will actually be achieved in the UNK neutrino beams. The important part played by the gluon distribution function at $x < 0.4$ can be seen. It should be emphasized that at the currently attainable energies, the measurement of the function $F_2(x, Q^2)$, which can be obtained in deep inelastic electron and muon scattering, is insufficient for accurate determination of the parameter $\Lambda_{\overline{MS}}$ by virtue of the dependence of $\Lambda_{\overline{MS}}$ both on the choice of the gluon distribution function and on the choice of the form of the twist corrections, as we have discussed above. The

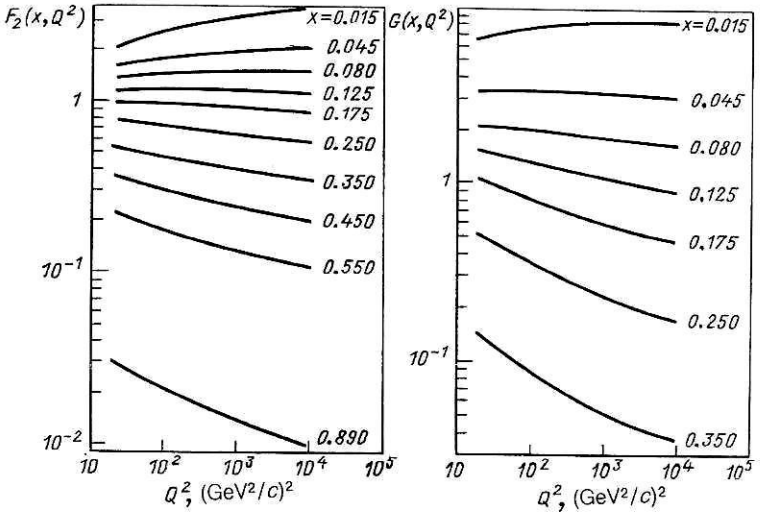

FIG. 30. Extrapolation of the structure functions $F_2(x,Q^2)$ and $G(x,Q^2)$ determined at the currently accessible values of Q^2 up to values $Q^2 \simeq 10^4$ (GeV/c)^2.

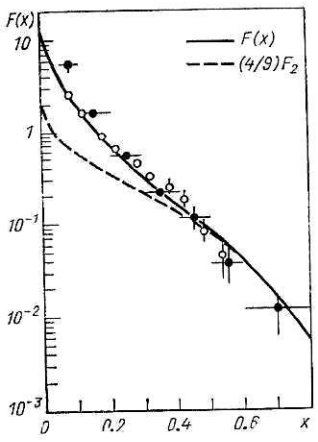

FIG. 31. Comparison of the structure function $F(x)$ found from an experiment at the $p\bar{p}$ collider at $Q^2 = 2000\ (\mathrm{GeV}/c)^2$ with an extrapolation of the structure function determined from deep inelastic scattering of muons.

most direct way to overcome these difficulties is, in particular, to measure with high accuracy the nonsinglet structure function $xF_3(x, Q^2)$ in νN scattering, the evolution of which with respect to Q^2 does not, as we said above, depend on the gluon distribution function.

In contrast to colliders (ep colliders), neutrino investigations permit the use of a wide range of targets and the elimination of the losses of particles emitted at small angles, which are typical for colliders. Of course, a comprehensive detailed analysis must use both neutrino data and the results of investigations of various hard processes at e^1e^-, $p\bar{p}$, and ep colliders.

Spin structure of the nucleon

Hitherto, we have restricted ourselves to discussion of deep inelastic scattering of neutrinos by unpolarized targets. However, it is well known that polarization measurements are an important source of information about the structure and interaction dynamics of particles, a source, moreover, that is sensitive to fine details of the investigated phenomena. The complete picture of the fundamental interactions of hadrons must include a description of the polarization structure of the nucleon. However, hitherto the parton distributions in a polarized nucleon have attracted relatively little attention and have not received a satisfactory description. It is usually assumed that at high energies the parton distributions are concentrated mainly at small x, where the parton polarization is expected to be small, and the correlation between the nucleon spin and the spin of the partons is weak. Experimental information about the spin structure of the nucleon is very sparse, particularly in the region of large Q^2, where the QCD perturbation-theoretical techniques could be used effectively. As regards neutrino experiments with polarized targets, hitherto they have been simply impossible, since the characteristic masses of the targets in neutrino experiments (dictated by the need to accumulate sufficient statistics) must, as a rule, be tens or hundreds of tons, whereas the masses of present-day (cryogenic) polarized targets are tens or hundreds of grams. With the commissioning of the UNK, the situation may be radically changed. The high statistics promised for the neutrino experiments at the UNK will permit fairly high statistics (at the level $\sim 10^3$; see Table I) in targets with a mass of about 1 kg. The creation of cryogenic polarized targets of such mass already appears realistic. Thus, at the UNK there will for the first time be a possibility of investigating the polarization structure of the nucleon in neutrino reactions.[87] This appears to be particularly important in the light of recent experiments on deep inelastic scattering of polarized e and μ by polarized nucleons,[88,89] which yielded interesting and unexpected results that cast doubt on the extent to which the parton structure of the nucleon is understood.[90] It should be emphasized that neutrino polarization experiments can give additional nontrivial information about the part played by different quarks, including sea quarks, and this may be crucial for the understanding of the problem.

We consider first electomagnetic deep inelastic scattering of leptons by polarized nucleons. The cross section of this process is related to the cross section for forward virtual Compton scattering.

Let $T_{\lambda_\gamma\lambda_N,\lambda_\gamma\lambda_N}$ be the amplitude of this process, in which λ_γ and λ_N are the helicity states of the photon and the nucleon. We choose a coordinate system in which the z axis is directed along the momentum of the virtual photon, and the x axis lies in the plane of the scattering of the electron (or muon). The virtual photon has three helicity states, $\lambda_\gamma = 0$, 1, -1, and the nucleon has two, $\lambda_N = \frac{1}{2}$, $-\frac{1}{2}$. The helicity states are conserved in the reaction, and we therefore have four independent amplitudes:

$$\left.\begin{aligned} &T_{1/2} = T(1,\ 1/2;\ 1,\ 1/2);\quad T_L = T(0,\ 1/2;\ 0,\ 1/2);\\ &T_{3/2} = T(1,\ -1/2;\ 1,\ -1/2);\ T_{TL} = T(0,\ -1/2;\ 1,\ 1/2)\end{aligned}\right\} \tag{114}$$

The cross section for scattering of virtual photons by nucleons is related to the imaginary parts of the considered amplitudes,

$$\sigma_{1/2} \sim \mathrm{Im}\,T_{1/2};\ \sigma_{3/2} \sim \mathrm{Im}\,T_{3/2},$$

and to the spin structure functions $G_1(x)$ and $G_2(x)$:

$$\left.\begin{aligned} \sigma_{1/2} - \sigma_{3/2} &= \frac{4\pi^2\alpha}{\nu + Q^2/2M}\,[M\nu G_1(x) - Q^2 G_2(x)];\\ \sigma_{1/2} + \sigma_{3/2} &= \frac{8\pi^2\alpha}{M(\nu + Q^2/2M)}\,F_1(x).\end{aligned}\right\} \tag{115}$$

The functions $G_1(x)$ and $G_2(x)$ occur in the expressions for the cross section for scattering of polarized leptons by polarized nucleons:

$$\begin{aligned}\frac{d^2\sigma}{dE'\,d\Omega} = \frac{\alpha^2\cos^2(\theta/2)}{4E^2\sin^4(\theta/2)}\Big[&W_2(x) + 2\tan^2\frac{\theta}{2}\,(W_1 x)\\ &\pm 2\tan^2\frac{\theta}{2}\,(E + E'\cos(\theta/2))MG_1(x)\\ &\pm 8EE'\tan^2\frac{\theta}{2}\sin^2\frac{\theta}{2}\,G_2(x)\Big].\end{aligned} \tag{116}$$

Here, the $+$ and $-$ signs are taken for antiparallel ($\uparrow\downarrow$) and parallel ($\uparrow\uparrow$) spins of the e and N; θ is the scattering angle of the lepton; E and E' are the energies of the lepton in the initial and final states; and $W_1(x)$ and $W_2(x)$ are structure functions related to the functions $F_1(x)$ and $F_2(x)$ defined above [see (85)]:

$$\nu W_2(x) = F_2(x);\ MW_1(x) = F_1(x).$$

Note that a nonzero asymmetry arises only when the nucleon is polarized in the scattering plane of the leptons. If it is polarized at right angles to this plane, the asymmetry of the scattered leptons is zero; this follows from invariance with respect to time inversion.

By means of the asymmetry coefficient

$$A_{\parallel}=\frac{d^2\sigma(\Downarrow)-d^2\sigma(\uparrow\uparrow)}{d^2\sigma(\Downarrow)+d^2\sigma(\uparrow\uparrow)} \tag{117}$$

we can express (116) in the form

$$A_{\parallel}=\frac{(E+E'\cos\theta)\,MG_1(x)+Q^2G_2(x)}{W_1(x)+\frac{1}{2}\cot^2\frac{\theta}{2}W_2(x)}. \tag{118}$$

In the quark–parton model, the function $G_1(x)$ can be expressed in terms of the functions $g_i^{\uparrow}(x)$ and $g_i^{\downarrow}(x)$, the distributions of quarks of species i with spins parallel and antiparallel to the nucleon spin:

$$G_1(x)=\frac{1}{M^2\nu}g_1(x);\quad g_1(x)=\frac{1}{2}\sum_i e_i^2\left(q_i^{\uparrow}(x)-q_i^{\downarrow}(x)\right),$$

where e_i is the charge of the quark of flavor i.

The Bjorken sum rules[91] relate the integral of $g_1(x)$ to the ratio of the axial and vector coupling constants G_A and G_V measured in nucleon β decay. With allowance for the QCD corrections,[92] we have

$$\int_0^1 dx\,(g_1^p(x)-g_1^n(x))=\frac{1}{6}\left|\frac{G_A}{G_V}\right|\left(1-\frac{\alpha_S}{\pi}\right)$$
$$=0.191\pm0.002\quad(\text{for }\alpha_S=0.27\pm0.02). \tag{119}$$

For the neutron and proton separately Ellis and Jaffe[93] obtained sum rules that use $SU(3)$, current algebra, and the assumption that the sea of strange quarks is unpolarized:

$$\int_0^1 g_1^{p(n)}(x)\,dx=\frac{1}{12}\left|\frac{G_A}{G_V}\right|\left[(\pm1)+\frac{5}{3}\,\frac{3F-D}{F+D}\right]. \tag{120}$$

With allowance for the QCD radiative corrections and the values $F/D=0.632\pm0.024$ and $|G_A/G_V|=1.254\pm0.06$, this gives

$$\int_0^1 g_1^p(x)\,dx\simeq0.189\pm0.005;\quad\int_0^1 g_1^n(x)\,dx\approx-0.002\pm0.005. \tag{121}$$

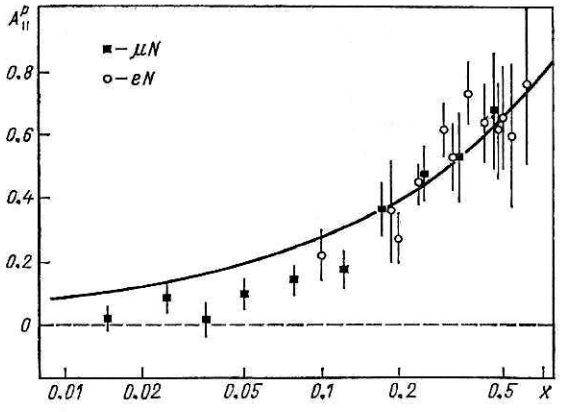

FIG. 32. Asymmetry in eN and μN scattering as a function of x.

The results of the measurements of $A_{\parallel}^p$ made at SLAC and CERN are shown in Fig. 32. In the region in which the experiments overlap the data of the two groups agree. The curve shows the predictions of the Carlitz–Kaur quark model,[94] which describes the data well only for $x>0.2$. A more detailed description of various models is given in Ref. 26. The values of the function $xg_1^p(x)$ extracted from the experiment of Ref. 89 are shown in Fig. 33, in which we also give the values of the integral $\int_{x_m}^1 g_1^p(x)dx$ as a function of x_m; in the limit $x_m\to0$ these give the value

$$\int_0^1 g_1^p(x)\,dx=0.114\pm0.012\,(\text{st})\pm0.026\,(\text{syst}). \tag{122}$$

This result is less than is expected in various theoretical models: 0.189 ± 0.005 (Ellis–Jaffe sum rules[93]); 0.17 ± 0.03 (QCD sum rules[95]); 0.205 (the model of Ref. 94).

Using (121) and (122), we can find

$$\int_0^1 g_1^n(x)\,dx=-0.077\pm0.012\,(\text{st})\pm0.026\,(\text{syst}), \tag{123}$$

a value that is appreciably greater than the one expected on the basis of the Ellis–Jaffe sum rules. By means of (122) and (123) estimates were made in Ref. 89 of the z component of the spin s_z of quarks of various flavors in the proton with $s_z=+\frac{1}{2}$:

$$\left.\begin{aligned}\langle s_z\rangle_u&=\frac{1}{2}\Delta u=0.348\pm0.023\pm0.051;\\ \langle s_z\rangle_d&=\frac{1}{2}\Delta d=-0.280\pm0.023\pm0.051\end{aligned}\right\} \tag{124}$$

and

$$\langle s_z\rangle_{u+d}=+0.068\pm0.047\pm0.103. \tag{125}$$

Thus, the spins of the quarks give only $(14\pm9\pm21)\%$ of the spin of the proton. The remainder must be due to gluons or orbital angular momenta. If it is assumed that the discrepancy from the predictions of the Ellis–Jaffe sum rules is due to polarization of the sea of strange quarks, then we obtain[89]

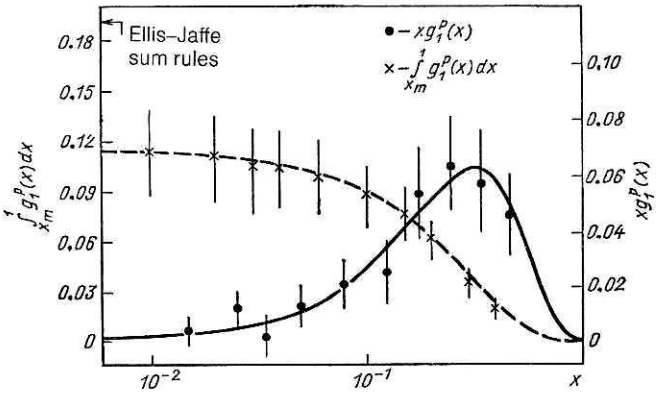

FIG. 33. The quantity $xg_1^p(x)$ (right-hand axis, black circles) as a function of x. The left-hand axis and the crosses show the integral $\int_{x_m}^1 g_1^p(x)dx$ as a function of $x_m=x$.

$$\langle s_z\rangle_u = 0.373 \pm 0.019 \pm 0.39;$$
$$\langle s_z\rangle_d = -0.254 \pm 0.019 \pm 0.039;$$
$$\langle s_z\rangle_s = -0.113 \pm 0.019 \pm 0.039;$$
$$\langle s_z\rangle_{u+d+s} = 0.006 \pm 0.058 \pm 0.117.$$

This last result means that the quarks carry $(1 \pm 12 \pm 24)\%$ of the spin of the proton, and the polarization of the sea of strange quarks may be unexpectedly large.

This situation has been analyzed in the framework of various theoretical models (see, for example, Ref. 96). However, as yet there is no common view with regard to the reasons for the "spin crisis."

As we have already said, experiments on deep inelastic scattering of neutrinos by polarized nucleons at the UNK could play an important part in our understanding of the spin structure of the nucleon and the role played in it by the various constituents. In this connection, the creation of polarized targets of large masses is now urgently necessary. As regards polarization of the neutrinos, it is guaranteed by the very nature of these particles.

3. HADRONIC FINAL STATES

Deep inelastic scattering of neutrinos is an effective way to study the structure of hadronic fragments of partons knocked out of a nucleon by a virtual intermediate boson. The study of hadronic final states gives rise to a great variety of problems, and there are several theoretical QCD models for the description of phenomena that need experimental verification.

The properties of the hadronic final system depend in the general case on the variables x, y, Q^2, and W^2, the square of the total energy of the hadrons in the rest frame of the nucleon (see Fig. 19). The quantity W^2 is given by

$$\left.\begin{aligned} W^2 = M_X^2 = (p+q)^2 = M^2 + 2M\nu + q^2; \\ W^2 = M^2 + 2M\nu - Q^2. \end{aligned}\right\} \qquad (126)$$

The kinematic variables of an individual hadron are defined as follows:

$$x_F = 2p_L^*/W$$

(the asterisk identifies the center-of-mass system of the hadronic state); x_F is the Feynman variable; p_L^* is the longitudinal momentum of the hadron (in the **q** direction; see Fig. 34),

$$y^* = \frac{1}{2}\ln\frac{E^*+p_L^*}{E^*-p_L^*}$$

is the rapidity,

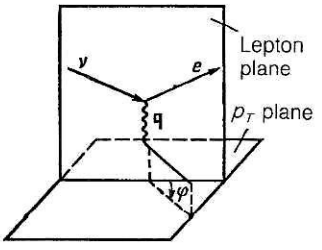

FIG. 34. Kinematic variables that characterize the hadron in the final state. The angle φ is the azimuthal angle of the hadron with respect to the direction **q** of the current; $\varphi = 0$ is the lepton plane.

$$z = E_h/\nu$$

is the fraction of the energy corresponding to an individually considered hadron, p_T is the transverse momentum of the particle with respect to the direction **q** of the total momentum of the hadronic system, and φ is the azimuthal angle of the hadron. Its definition is shown in Fig. 34.

The experimentally observed properties of hadronic systems produced in charged currents are similar to the properties of the hadronic systems produced in hadron–hadron interactions. The most important quantity that characterizes the hadronic system in the final state is the total energy W^2, the value of which determines the properties of the system irrespective of the type of reaction in which the system arose. However, there has recently been discussion of some properties of multiparticle production that also depend on Q^2 and on the azimuthal angle φ.[97]

We shall consider the main problems of the physics of hadronic final states.

Multiplicities and charge distributions

As in hadronic reactions, the mean multiplicity in neutrino processes increases with increasing W, as can be seen from Fig. 35, which shows the results for neutral currents. Outside the resonances, the data agree with a linear dependence[97]:

$$\left.\begin{aligned} \langle n\rangle = a + b\ln W^2, \\ \text{for } \nu p: a = 1.50 \pm 0.16;\ b = 1.01 \pm 0.06 \\ \text{for } \bar\nu p: a = 1.85 \pm 0.29;\ b = 0.84 \pm 0.11 \\ \text{for } h^+ + h^-\ W > 2.7\ \text{GeV} \quad (\text{all } x_F). \end{aligned}\right\} \qquad (127)$$

Note that the slope for the charged currents in νp and $\bar\nu p$ reactions is larger: $b = 1.4$.

The distributions in the forward and backward hemispheres are approximately the same (Fig. 35). These data are in good agreement with the Lund model.

There is found to be a weak dependence of the mean multiplicity of π^+ and π^- production on Q^2 in νp and $\bar\nu p$ reactions. The best fit to the experimental data has the form

$$\langle n_{\pi^\pm}\rangle = a + b\ln W^2 + c\ln Q^2. \qquad (128)$$

Thus, for all x_F, $W > 2.5$ GeV and all Q^2 the values of the coefficients a, b, and c given in Table XIV have been obtained.

It can be seen that the Q^2 and W^2 dependences are characterized by a ratio $c/b \sim 0.1$.

Study of the dependence of $\langle n\rangle$ on W^2 and Q^2 at UNK energies is of great interest.

The mean charge of the current fragments, $\langle Q_F\rangle$, is connected to the charge e_q of the fragmenting quark q by a relation that also includes the probability for production of a $q\bar q$ pair of species i (Ref. 98):

$$\langle Q_F\rangle = e_q - \sum \gamma_i e_i.$$

The absolute value of the quark charge cannot be determined in a study of meson jets alone, but the difference $\langle Q\rangle_j = \langle Q_k\rangle = e_j - e_k$ of the quark charges can be found. Assuming also that $e_u - e_d = e_u - e_s = 1$ and

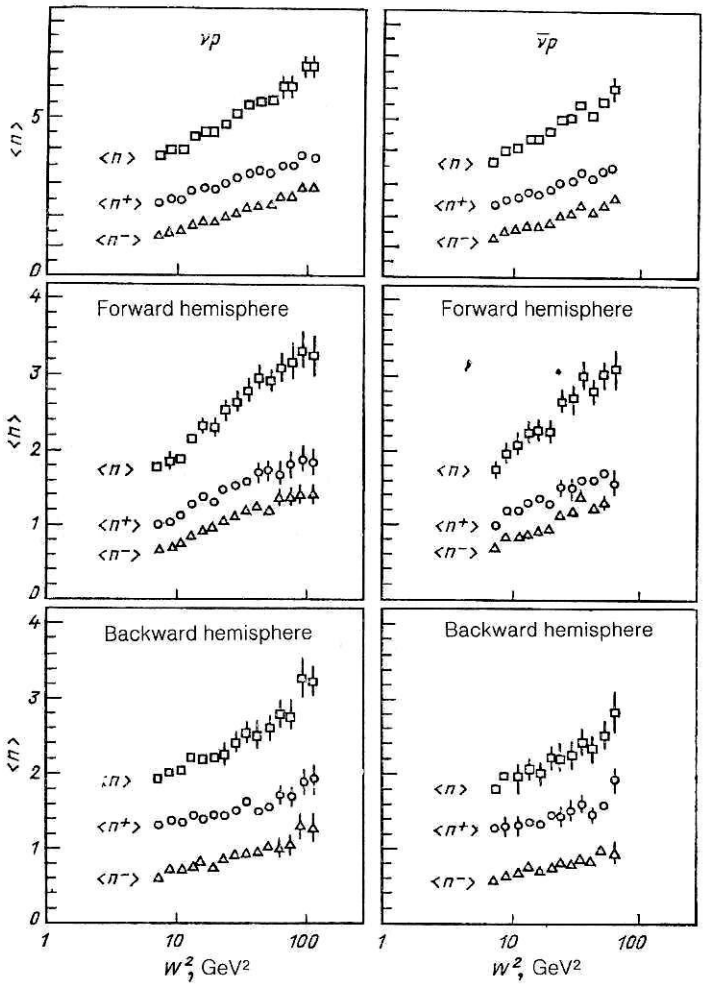

FIG. 35. Mean multiplicities as functions of W^2 in νp and $\bar{\nu}p$ neutral-current reactions. The open squares are for $(\eta^+ + \eta^-)$, the open circles for η^+, and the open triangles for η^- (in the forward and backward hemispheres).

$\gamma_u + \gamma_d + \gamma_s = 1$, we can find for a meson jet initiated by a u or d quark

$$\langle Q\rangle_u = 1 - \gamma_u, \quad \langle Q\rangle_d = -\gamma_u.$$

Thus, the resulting charge is independent of the charge of the quark and is determined by the value of γ.

The situation is changed if there is baryon production. Then

$$\langle Q\rangle_u \approx (1 - P)\,(1 - \gamma_u) + P\,(3e_u - 4/3),$$

where P is the probability of baryon production. For $P = 1/3$, $\langle a\rangle_u = e_u$.

The experiments show that $\langle Q\rangle_F$ depends on W. In experiments at the UNK it will be possible to verify the expected[99] vanishing of this effect as $\sim 1/W$. Asymptotically, the following relation must be satisfied:

$$\Delta Q = \langle Q\rangle_F^{\nu} - \langle Q\rangle_F^{\bar{\nu}} = e_u - e_d.$$

Extrapolation of the existing data ($1/W \to 0$) leads to $\Delta Q = 0.98 \pm 0.15$.[100] A final remark. Gluon emission must increase $\langle n_{\rm ch}\rangle$ with increasing Q^2. In some models, this leads to a relatively rapid growth of the kaon yield if the $g \to s\bar{s}$ channel is important. In addition, gluon fragmentation must increase the soft component. This effect requires further study.

Of great interest are the distributions with respect to x_F and p_T, in which the effect of a "leading" charge (π^+ for ν and π^- for $\bar{\nu}$) is manifested. The p_T^2 dependence so far observed has an exponential nature (Fig. 36), and the mean value of p_T^2 increases with increasing W^2, apparently reaching saturation at $W^2 \gtrsim 200$ GeV^2 (Fig. 37). It will be interesting to investigate the properties of multiparticle produc-

TABLE XIV. Values of the parameters a, b, and c for multiparticle production processes.

Process	a	b	c
νp	0.18±0.02	0.94±0.02	0.10±0.01
$\bar{\nu}p$	0.28±0.02	0.82±0.02	0.10±0.01

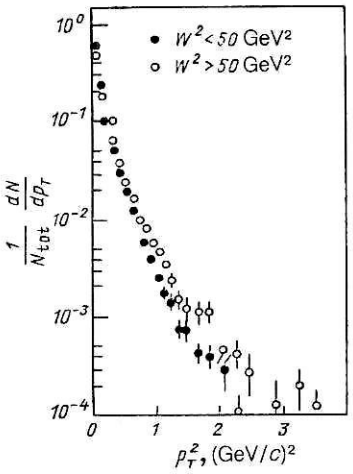

FIG. 36. Distribution with respect to p_T of charged hadrons in two intervals of W^2. The data were obtained in νD and $\bar{\nu} D$ experiments.

tion and some other phenomena, including jet effects, at higher energies and larger momentum transfers at the UNK.

Effects of gluon emission

The study of the transverse momenta p_T of the hadrons is of considerable interest. The various factors that influence p_T are shown in Fig. 38. We see that the transverse momentum of the hadron depends on the transverse momentum of the primary quark, $\langle p_T \rangle_{qu}$, the transverse momentum of the gluon emitted by the quark, $\langle p_T \rangle_{gl}$, and, finally, the transverse momentum $\langle p_T \rangle_{fr}$ of the quark that fragments into hadrons:

$$\langle p_T \rangle^2_{had} = \langle p_T^2 \rangle_{fr} + \langle p_T^2 \rangle_{qu} + \langle p_T^2 \rangle_{gl}.$$

In the framework of the Lund model the quark may emit soft gluons that do not fragment into hadrons because of the smallness of the enery. These soft gluons may make an additional contribution to the transverse momentum of the considered hadron.

The direction $\mathbf{q}$ of the current corresponding to the momentum of the virtual W or Z boson (see Fig. 34) fixes the axis with respect to which the transverse momentum of the hadron is defined. It should be emphasized that in experiments at the UNK with a narrow-spectrum neutrino beam, and, in particular, with tagged neutrinos, knowledge of the energy of the initial neutrino will make it possible to reduce

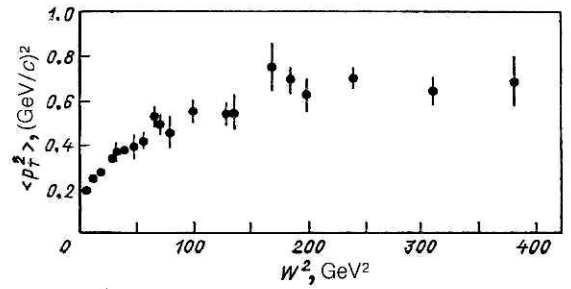

FIG. 37. Mean value of the square of the transverse momentum of charged hadrons as a function of W^2 for $z > 0.4$. The data were obtained in νD, μp, and νNe reactions.

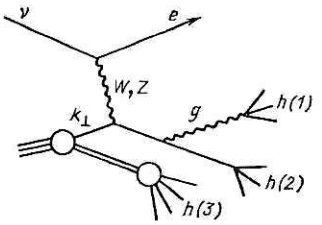

FIG. 38. Production of hadrons in νN deep inelastic scattering; $k_\perp$ is the internal transverse momentum of the quark on which the gauge boson is scattered.

significantly the systematic uncertainties in the determination of $\mathbf{q}$ that are inherent in present-day measurements. The component p_n of the transverse momentum p_T lying outside lepton plane can be determined from the directions of motion of ν and of the final lepton (for example, μ) and, thus, is not subject to the influence of the uncertainties in E_ν.

Gluon emission makes the contribution

$$\langle p_T^2 \rangle_{QCD} \simeq k\alpha_S (Q^2) W^2,$$

where $k \approx 0.03$–0.04, and this opens up a possibility to determine α_S and $\Lambda_{\overline{MS}}$. However, the existing data do not as yet make it possible to distinguish dependences of the type $\langle p_T^2 \rangle \sim W^2$ or W.[100]

If the growth of $\langle p_T^2 \rangle$ with W^2 is entirely due to the emission of one hard gluon, the event must have a structure which reflects the three-particle nature of the final state. For an ideal two-jet event, the "sphericity" S and "aplanarity" A vanish, although in a real situation this result is smeared by the hadronization. Thus, effects of gluon bremsstrahlung can be sought either by studying the W^2 and Q^2 dependences of S and A, or by investigating events with three-jet structure. A sensitive method to test QCD is also to measure the flux of the transverse energy of the hadrons relative to the direction of the momentum transfer.[101] If the parton which is knocked out does not have a momentum component transverse to $\mathbf{q}$ then two jets (in the absence of a gluon jet) are aligned along $\mathbf{q}$, and therefore, $\langle \cos\theta \rangle = \langle \Sigma_i \cos\theta_i (E_i/E) \rangle = 0$. The nonzero transverse momentum of the parton leads to an asymmetry that increases with increasing relative momentum of the neutrino and parton. A kinematic analysis shows[101] that this leads to an excess of events in which the target jets lies between the final lepton and the current jet. At the parton level, when $Q^2 \gg p_T^2$, we have

$$\langle \cos\theta \rangle = -(p_T/Q)(1-y) \pm {}^{1}/_{2},$$

where the + sign is taken for νq and $\bar{\nu} q$ interactions, and the − sign for $\bar{\nu} q$ and $\nu \bar{q}$ interactions.

At $\langle p_T \rangle = 0.3$, this must give $\langle \cos\varphi \rangle \approx -0.1$ at $E_\nu \simeq 100$ GeV. With allowance for the emission of a gluon jet, the contribution to $\langle \cos\varphi \rangle$ has the form

$$\langle \cos\varphi \rangle = -\alpha_S (Q^2) f(x) (1-y)^{\pm 1/2}$$

[where $f(x)$ is a convolution of structure functions] and is approximately -0.1 (Ref. 101). The asymmetry which arises at the parton level is naturally "smeared" by the hadronization and secondary interactions, so that the effect is reduced by about five times. Measurements made at Fermi-

lab[101] revealed a statistically signficant asymmetry: $\langle \cos \varphi \rangle = 0.016 \pm 0.003$. However, the limitation of the range of accessible Q^2 did not permit separation of the effects of the internal momentum p_T and of the QCD gluon emission. Such separation can be achieved in experiments at the UNK.

Fragmentation functions

The cross sections of the single-particle inclusive reactions

$$(\nu, \bar{\nu}) + N \to \mu^{\mp} + h + X$$

can be written in the form[102]

$$\frac{d^2\sigma^h_{\nu p}(\bar{\nu}, \nu)}{dx\, dz\, dQ^2} = \frac{G^2}{2\pi}\left[\left(1 - \frac{x_0}{x}\right)F_1^h + \frac{x_0^2}{2x^2}F_2^h \mp \left(\frac{x_0}{x} - \frac{x_0^2}{2x^2}\right)F_3^h\right], \quad (129)$$

where

$$F_i^h = F_i^h(x, z, Q^2); \quad Q^2 = 2ME_\nu xy; \quad x_0 = Q^2/2ME_\nu;$$

$z = E_h/E$ is the fraction of the parton energy carried away by the hadron.

The functions $F_i^h(x, z, Q^2)$ are products of the density of partons and fragmentation functions, and

$$\sum_h \int_0^1 dz z F_i^h(x, z, Q^2) = F_i(x, Q^2),$$

where $F_i(x, Q^2)$ are the ordinary structure functions of deep inelastic scattering. In the QPM, the functions $F_i^h(x, z, Q^2)$ have a simple factorized form. Thus, for νp scattering, ignoring the contribution of the antiquarks and the Cabibbo angle, we have $F_1^h = F_2^h = -F_3^h$, and the expression (129) can be rewritten as

$$\frac{d^3\sigma^h_{\nu p}}{dx\, dy\, dQ^2} = \frac{G^2}{\pi} d(x) D_q^h(z); \quad D_q^h(z) = \frac{1}{N}\frac{dN}{dZ}. \quad (130)$$

Of course, this primitive model is modified by the contributions associated with gluon emission, which result in a Q^2 dependence of $D(z, Q^2)$, and the factorization is broken. It is convenient to investigate this breaking by means of the double moments with respect x and z of $F_i^h(x, z, Q^2)$. The QCD predictions are particularly simple for the nonsinglet moments (for example, for the difference $D_i^h - D_j^h$).

Effects of higher twists

In Sec. 2 we discussed the influence of the higher twist corrections on the determination of the fundamental parameters of the theory of the electroweak interactions. The influence of the twist corrections is also manifested in the analysis of hadronic final states. The inclusion of twist corrections breaks the factorization in the expression (130). Here, the twist corrections arise from the interaction of quarks due to gluon exchange (Fig. 39). The contribution of the twist corrections for the reactions $\nu N \to \mu^- \pi^+ X$ and $\bar{\nu} N \to \mu^+ \pi^- X$ was calculated in the study of Ref. 103. For example, for the $\bar{\nu} N$ interaction it is taken into account by the final term in the cross section

$$\frac{d^4\sigma(\bar{\nu}N \to \mu^+\pi^- X)}{dx\, dy\, dz\, dQ^2} \sim \frac{(1-z)^2}{z} + \langle k_T^2 \rangle \frac{R(x, y, Q^2)}{z}, \quad (131)$$

where

$$R(x, y, Q^2) = \frac{4}{9}\frac{1-y}{Q^2}\frac{q(x) + \bar{q}(x)}{(1-y)^2 q(x) + \bar{q}(x)}.$$

In (131), $\langle k_T^2 \rangle$ is an independent parameter. Analysis of the Q^2 dependence of the twist corrections showed that it agrees with what is expected in accordance with (131). However, nothing definite can be said about the y dependence.

The simplest exclusive reactions

The processes

$$\nu, \bar{\nu} + p \to \mu^{\mp} p \pi^{\pm}$$

of production of isolated pions are the simplest charged-current exclusive reactions. The data that exist for them refer mainly to the region of small W^2, where the dominant mechanism is resonant excitation of a hadronic system. Because of the difference in the isospins of the final states, the cross sections of the ν and $\bar{\nu}$ reactions differ strongly. There are detailed theoretical predictions for the contributions of the various resonances and the Q^2 and angular dependences of the cross sections in quark models and in the hard-pion model.[104,105] Unfortunately, the existing very sparse statistics do not permit a detailed comparison with these predictions. The values for the cross sections for production of the system $(p\pi)$ at $W < 2$ GeV were found[106] to be $\sigma(\nu p) \sim (68 \pm 7) \times 10^{-40}$ cm^2 and $\sigma(\bar{\nu}p) \sim (30 \pm 40) \times 10^{-40}$ cm^2, in agreement with the theoretical predictions. With increasing W, the angular distribution of the pions becomes more directed along the momentum of the current, and this indicates a transition to a peripheral production mechanism (Fig. 40). As can be seen from Fig. 41, in both reactions the pion carries away almost the entire energy of the current. The mean value of z_π is ~ 0.9, whereas $\langle z_\pi \rangle \simeq 0.6$ at $W < 2$ GeV. Thus, at large W the proton behaves as a spectator.[106]

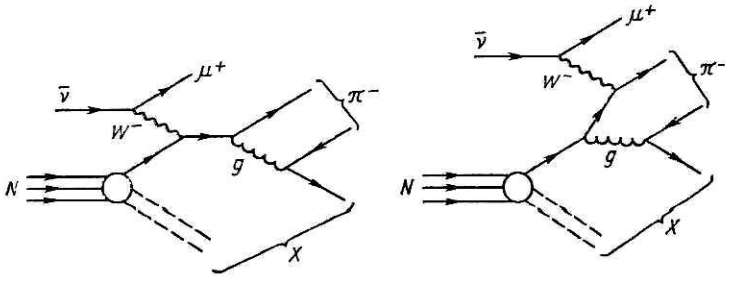

FIG. 39. Gauge-invariant set of diagrams for the $\nu N \to \mu\pi X$ process. The necessary diagram generates twist corrections, since the gluon is emitted by a quark before interaction with a W boson.

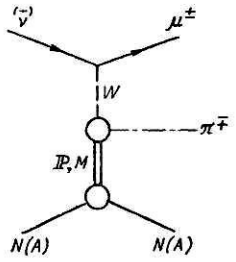

FIG. 40. Diagram of peripheral interaction.

If the exchanged neutral meson M has a definite G parity (and, therefore, there is no V–A interference), the cross sections of the processes initiated by ν and $\bar{\nu}$ must be equal. To within the errors, this is confirmed by the experiments. The cross section can be parametrized in the form

$$\frac{d^3\sigma}{dQ^2\,dW^2\,dt} = \Gamma(E_\nu,\ Q^2,\ W^2)\,\frac{d\sigma}{dt}(Q^2,\ W^2,\ t),$$

where Γ is the flux factor of the virtual boson, and $d\sigma/dt$ is the cross section of the $W^{\pm}\,p \to \pi^{\pm}\,p$ reaction. If M is a Reggeon, then

$$\frac{d\sigma}{dt} \sim \beta(t,\ Q^2)\,s^{2[\alpha(t)-1]}.$$

In Fig. 42 we compare the predicted W^2 dependence for $M = \pi$, V, and $\mathbb{P}$ with experiment. The data clearly rule out exchange of a Pomeron ($\mathbb{P}$) and agree well with π^0 exchange.

The absence of a diffraction contribution is not surprising, since the energies in the experiment of Ref. 106 were fairly low. However, the result does not agree with the prediction of Ref. 105 that f-meson exchange should play the dominant part.

Investigations at the UNK in a wide range of energies will permit more reliable investigation of the reaction mechanism, in particular of the part played by the diffraction contributions.

The prediction of the Regge model with regard to the shrinkage of the peak in the t distribution with increasing W^2

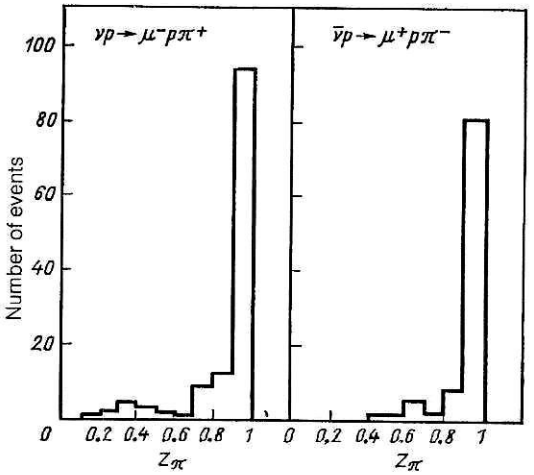

FIG. 41. Distributions with respect to z_π in the processes $\nu p \to \mu^- p\pi^+$ and $\overset{(-)}{\nu} p \to \mu^+ p\pi^-$.

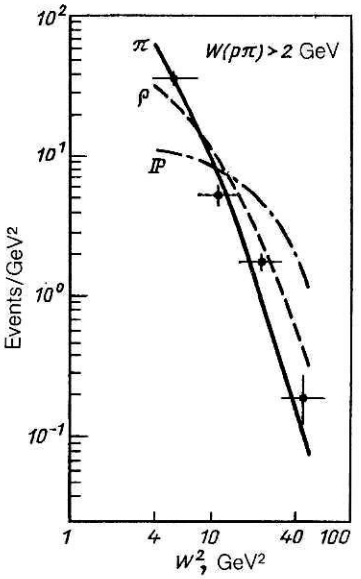

FIG. 42. Distribution with respect to W^2 in the processes $\nu p \to \mu^- p\pi^+$ and $\overset{(-)}{\nu} p \to \mu^+ p\pi^-$.

agrees with experiment—the slope is equal to 1.7 ± 0.2 GeV^2 for $4 \leqslant W^2 \leqslant 8$ GeV^2 and 3.5 ± 0.5 for $W^2 > 8$ GeV^2 (Ref. 106).

The measurement of the correlation between the orientation of the lepton plane and the plane formed by the initial and final protons in the $\mu\pi$ rest frame (the Treiman–Yang criterion) permits deductions about the spin of the system. The experiments agree with $S_M = 0$.

The most general form of the distribution with respect to the azimuthal angle has the form

$$\frac{d\sigma}{d\varphi_\pi} = a + b\cos\varphi_\pi + c\cos 2\varphi_\pi + d\sin\varphi_\pi + e\sin 2\varphi_\pi.$$

Recent measurements[106] have revealed for the first time a nonzero value of $\langle\cos\varphi_\pi\rangle$ (for the definition of φ, see Fig. 34) in exclusive neutrino reactions ($c \simeq d \simeq e \approx 0$), and this indicates interference of the amplitudes with exchange of a W boson having longitudinal and transverse polarizations. A similar effect is observed in some electroproduction reactions, whereas in neutrino deep inelastic scattering F_L is small. It would be interesting to make a more detailed investigation of this phenomenon, since it could give the key to an understanding of the behavior of the function F_L in deep inelastic scattering.

Measurement of the coefficients of $\sin\varphi_\pi$ and $\sin 2\varphi_\pi$ would permit conclusions to be drawn about the T-odd contributions, which could be due to interaction in the final state.

The production of an isolated strange particle in $\overset{(-)}{\nu} p$ interactions, for example,

$$\overset{(-)}{\nu} p \to \mu^{\mp} p K^{\pm}$$

corresponds in quark language to the transitions

$$\bar{\nu}u\ [u] \to \mu^-\bar{s}\ [u];$$
$$\nu s\ [\bar{s}] \to \mu^- u\ [s]$$

and

TABLE XV. Mean multiplicity of ρ^0, ρ^-, and ρ^+ mesons produced in ν and $\bar{\nu}$ beams.

Meson	$\bar{\nu}$Ne, $\langle W\rangle = 4.1$ GeV	νNe, $\langle W\rangle = 5.3$ GeV
ρ^0	0.11 ± 0.02	0.17 ± 0.03
ρ^+	0.05 ± 0.02	0.28 ± 0.04
ρ^-	0.18 ± 0.02	0.04 ± 0.03

$$\bar{\nu}u \to \mu^+ s; \quad \bar{\nu}\bar{s}\,[s] \to \mu^+ \bar{u}\,[s],$$

where the bracket [ ] identifies the sea spectator partner of the quark (or antiquark) that participates in the reaction. All these reactions are Cabibbo-suppressed. Therefore, production of isolated kaons is expected to be at least an order of magnitude weaker than the production of pions. In addition, it must be weaker in νp than in $\bar{\nu}p$.

The experimental separation of these processes is difficult both on account of the problem of separating K from π by kinematic criteria and because of the influence of the background processes $\overset{(-)}{\nu} p \to \mu^{\pm} p \pi^{\mp} \pi^0$, which have a much larger cross section.

Production of resonances

The detected hadrons can be produced either directly in a fragmentation process or as a result of the decay of heavier resonances. For the correct understanding of the fragmentation mechanism and of the details of the final hadronic system, it is important to determine experimentally the role and nature of the resonance production. Analysis of the production of $\pi^+\pi^-$ pairs in ν and $\bar{\nu}$ beams showed that the mean number of ρ^0 particles per event in the charged current is 0.222 ± 0.014 (Ref. 107). The ratios n_{ρ^0}/n_{π^0} and n_ρ/n_π are small at $z \approx 0$ and increase with increasing z, reaching the value 0.6 at $z \sim 0.7$. The Lund model predicts that these ratios must hold for values $\nu/p = 1$, a result that corresponds to the data of the WA-59 experiment.[97] A difference between the dependences on x_F, z, and $p_\perp^2$ for ρ^0 and π^- has been found.[107] The dependences for π^- are concentrated at smaller x_F, z, and $p_\perp^2$ than those for ρ^0. This indicates that the ρ^0 are produced directly, whereas most of the π^- ($> 60\%$) arise from the decay of various resonances, including ρ^0.

In νNe and $\bar{\nu}$Ne reactions the mean multiplicity of the production of ρ^0, ρ^+, and ρ^- mesons in the region $W > 1.5$ GeV has been measured (WA-59 experiment). These data are given in Table XV.

In the framework of the QPM and under the condition of isospin symmetry,

$$(u \to \rho^{\pm}) = (d \to \rho^{\mp}); \; (u \to \rho^0) = (d \to \rho^0)$$

i.e., for production of $\rho^\pm$ on the u quark, etc., the following relations must hold:

$$\langle n_{\rho^\pm}\rangle_\nu = \langle n_{\rho^\mp}\rangle_{\bar{\nu}};$$

$$\langle n_{\rho^0}\rangle_\nu = \langle n_{\rho^0}\rangle_{\bar{\nu}},$$

i.e., the mean number of $\rho^\pm$ mesons produced on an isoscalar target in the neutrino beam must be equal to the mean number of $\rho^\mp$ mesons produced in the $\bar{\nu}$ beam. It can be seen from Table XIV that these relations are well satisfied. From equally simple qualitative arguments it can be asserted that production of ρ^+ mesons occurs more readily on a u quark ($u \to \rho^+ = u\bar{d}$) than $\rho^- = d\bar{u}$. Conversely, the ρ^- meson is more readily produced on the d quark ($\rho^- = d\bar{u}$) than ρ^+. These considerations lead to the inequalities

$$\langle n_{\rho^+}\rangle_\nu > \langle n_{\rho^-}\rangle_\nu;$$
$$\langle n_{\rho^-}\rangle_{\bar{\nu}} > \langle n_{\rho^+}\rangle_{\bar{\nu}},$$

which are also confirmed experimentally (see Table XV).

Figure 43 shows the distribution with respect to $\cos\theta$ for the $\bar{\nu}\text{Ne} \to \rho^0 X$ reaction; θ is the angle of the pion in the ρ^0 rest frame, and $\theta = 0$ corresponds to the direction of the ρ^0 in the WN center-of-mass system.[107] This first measurement of polarization in inclusive deep inelastic neutrino production of ρ^0 indicates a preferred longitudinal ($\lambda = 0$) polarization of the ρ^0 mesons.

The WA-21 experiment[97] has found parity violation in the process of ρ^0 production in the reactions

$$\nu p \to \mu^- \rho^0 X; \; \bar{\nu}p \to \mu^+ \rho^0 X; \; (\rho^0 \to \pi^+\pi^-).$$

The distribution of the ρ^0 mesons is described by the probability

$$\begin{aligned} W(\theta, \varphi) = \frac{1}{4\pi}[1 &- \eta(1 - 3\cos 2\theta) \\ &- 3\sqrt{2}\sin\theta\cos\theta\cos\varphi\,\mathrm{Re}\,(\rho_{10} - \rho_{-10}) \\ &- 3\sin^2\theta\cos 2\varphi\,\mathrm{Re}\,\rho_{1-1} \\ &+ 3\sqrt{2}\sin\theta\cos\theta\sin\varphi\,\mathrm{Im}\,(\rho_{10} - \rho_{-10}) \\ &+ 3\sin^2\theta\sin 2\varphi\,\mathrm{Im}\,\rho_{1-1}]. \end{aligned}$$

Here, θ and φ are the angles of the $\pi^\pm$ meson for decay of ρ^0 in its rest frame, ρ_{mn} are the elements of the spin density matrix of the ρ^0 meson, $\eta = \frac{1}{2}(3\rho_{00} - 1)$, and $\rho_{00} = 0.1$. The

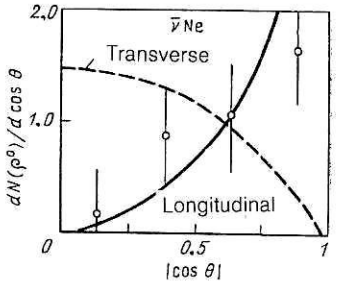

FIG. 43. Distribution with respect to $\cos\theta$ in neutrino-induced production of ρ^0.

last two terms in $W(\theta,\varphi)$ are sensitive to the violation of P parity. In the region $x_F > 0, z > 0.4$, and $W > 3$ GeV the number of ρ^0 mesons for $\sin 2\varphi < 0$ was found to be greater than in the region $\sin 2\varphi > 0$. The imaginary parts of the matrix elements responsible for the violation of P parity were found to be

$$\mathrm{Im}\,(\rho_{10}-\rho_{-10}) = \begin{cases} -0.20 \pm 0.10 & \text{for } \nu p; \\ -0.01 \pm 0.12 & \text{for } \bar{\nu} p; \end{cases}$$

$$\mathrm{Im}\,\rho_{1-1} = \begin{cases} -0.17 \pm 0.08 & \text{for } \nu p; \\ -0.14 \pm 0.09 & \text{for } \bar{\nu} p. \end{cases}$$

In neutrino reactions there has been observed, at the level of a few events, production of $\bar{c}s$ states: $F^{*\prime}$ (2547 ± 60 MeV) and $F^{*\prime\prime}$ (2564 ± 4 MeV), which decay into F^* and $D^*(2010) + K$, respectively (E180 experiment). At the UNK wider perspectives will be opened up for investigation of such reactions. With regard to baryonic resonances, the mechanism of these processes must be more complicated, since a baryon can be produced either from a target diquark or from a $B\bar{B}$ pair.

Azimuthal asymmetry in the angular distribution of π^+ mesons

In the E546 experiment[97] on the reaction $\bar{\nu}\mathrm{Ne} \to$ hadrons a left–right asymmetry was observed with respect to the angle φ (see Fig. 34) for the production of positive π^+ mesons (for $x_F > 0.1$, $\langle \cos\varphi \rangle = -0.029 \pm 0.008$), and no such asymmetry was observed for the negative π^- mesons. This asymmetry does not depend on the variables y, Q^2, and p_T, but is sensitive to the variable x. As yet there is no clear theoretical interpretation of this phenomenon.

Coherent production on nuclei

Coherent production on nuclei is widely used to investigate final states in neutrino reactions. These processes, taking place without disintegration of the nucleus, are characterized by a small momentum transfer, mainly forward emission of the particles, and selection by quantum numbers.

Study of the coherent production of isolated mesons permits investigation of the isotopic and space-time structure of the weak current and verification of the model of vector dominance (Fig. 44) and the hypothesis of partial conservation of the axial current (PCAC).

The PCAC hypothesis is the assumption that at small momentum transfers Q^2 the matrix element of the process $\nu + N \to l + X$ is

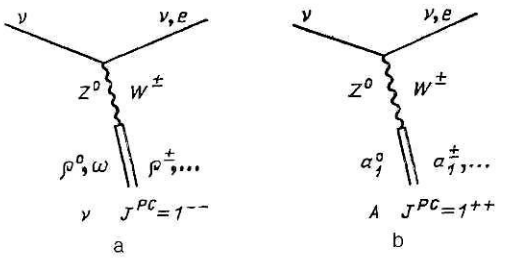

FIG. 44. Diagrams of vector dominance.

$$\nu + N \to l + X \sim \partial_\mu V^\mu + \partial_\mu A^\mu,$$

where V^μ is the vector part of the weak current, and A^μ is its axial part. The law of conservation of the vector current means that $\partial_\mu V^\mu = 0$, and the PCAC hypothesis is that

$$\partial_\mu A^\mu = f_\pi m_\pi^2 \Phi_\pi, \tag{132}$$

where f_π, m_π, and Φ_π are the pion decay constant, mass, and wave function, respectively.

In this case, for example,

$$\frac{d^2\sigma(\nu N \to \mu X)}{dQ^2\,d\nu} = \frac{G_F^2 f_\pi}{4\pi^2}\,\frac{2E_\mu}{\nu E}\,\sigma(\pi N \to X).$$

The coherent production of π^0 mesons in neutral currents is a direct "probe" of the isovector axial-vector part of the electroweak interaction. We note that this process is the main source of the background in experiments on elastic scattering of $\bar{\nu}_\mu$ by electrons. The coherent production of η^0 makes it possible to investigate the isoscalar axial-vector part of the electroweak interaction. In the standard model it is absent, and as yet processes of coherent η^0 production have not been observed experimentally. However, it should be noted that the efficiency of η^0 detection in the experiments[108] was low. In the near future it is proposed to investigate the coherent production of D_S and D_S^* mesons.

The cross section for coherent production of π^0 mesons is proportional to the factor $[\varepsilon_A(u) = \varepsilon_A(d)]^2\rho^2$, and, thus, there is a possibility of experimental determination of the absolute value of the difference of the axial coupling constants of the u and d quarks from measurement of the cross section of this process. The available data,[108]

$$|\varepsilon_A(u) - \varepsilon_A(d)| = 1.10 \pm 0.23$$

are not in conflict with the prediction of the standard model.

In accordance with the model of meson dominance, the overwhelming contribution to the coherent production of an isolated pion is expected from scattering of the longitudinal component A_1. At $Q^2 = 0$, the weak current behaves, in accordance with Adler's hypothesis [see (132)], as a pion, and its coupling to the W meson is determined by the constant f_π. The Q^2 dependence is determined by the propagator of the A_1 meson. These predictions are in reasonably good agreement with experiment.

In the study of Ref. 109 coherent production on nuclei of an isolated hadron h, $\nu A \to \mu h A$, was considered at large Q^2. The authors obtained an extrapolation of Adler's relation to the region $Q^2 \neq 0$ and an expression for the contribution of the cut which appears because of production of a $\rho\pi$ system in the intermediate state (in the region of appreciable momentum transfer Q^2 it would be incorrect to approximate the cut by a pole from the A_1 meson). Verification of the PCAC hypothesis in the region of larger Q^2 is of great interest.

The coherent production of ρ mesons is expected to be analogous to the photoproduction of ρ mesons—the cross section of the process $W^- + A \to \rho^- + A$ can be related to the cross section of elastic ρA scattering through vector dominance. This prediction is also in reasonable agreement with the experimental data.

Inclusive production of strange, charmed, and beauty particles

In the quark–parton model, the production of strange, charmed, and beauty particles is due to processes of associated and isolated production of the corresponding quarks.

The angular distribution of the strange, charmed, and beauty particles, the relative frequencies of their production, their $p_\perp^2$ distributions, the frequency of their appearance in jets, etc.—these are all important characteristics for understanding the structure of the nucleon and the nature of the fragmentation of the quarks of various species.

As an example, we consider some problems associated with the production of strange quarks. The following reactions are possible:

$$\nu + d_v \to \mu^- + u + s + \bar{s};$$
$$\bar{\nu} + u_v \to \mu^+ + d + s + \bar{s};$$
$$\bar{\nu} + \nu_v \to \mu^+ + s.$$

The emitted quark fragments into hadrons in the "forward" direction (current fragmentation), and the remaining diquark—the spectator—fragments into hadrons in the "backward" direction (target fragmentation). This leads to preferred emission of Λ forward and of K^0 forward and backward. An important parameter of the fragmentation models that can be determined experimentally is the ratio s/u of the probabilities of production of $s\bar{s}$ and $u\bar{u}$ pairs in the fragmentation process. It is very convenient to measure s/u in the region of current fragmentation in $\bar{\nu}p$ scattering. Here the dominant process is $\bar{\nu}u \to \mu^+ d$, in which the d quark is emitted in the forward hemisphere. Depending on whether the d quark picks up a $\bar{u}$ quark or an $\bar{s}$ quark from a $u\bar{u}$ pair or an $s\bar{s}$ pair, respectively, π^- or K^0 may be formed. Thus, the K^0/π^- yield ratio at large z directly measures s/u.[110] Unfortunately, there are several experimental difficulties associated with the low statistics at large z, the background from $\bar{\nu}u \to \mu^+ s$, and the contribution of resonances (to the production of π^-). The existing data indicate a strong "suppression of strangeness": $s/u \sim 0.15$–0.20.[110,111] It is interesting that the factor s/u is practically independent of x, W, and Q^2, whereas the production cross sections of K^0, $\bar{K}^0$, and π^-, and the ratio $\langle K^0 \rangle / \langle \pi^- \rangle$ depend on these variables. There is undoubted interest in further and more detailed study of this phenomenon and, in particular, in study of the possible dependence of s/u on the kinematic variables z and p_T and on the energy of the jets.

Mechanisms of the production of charmed particles have been considered in a number of studies.[112,113] The charmed particles can be produced, first, in processes of neutrino scattering by d and s quarks: $\nu d \to \mu c$, $\nu s \to \mu c$; second, they can arise in the process of disintegration of virtual $c\bar{c}$ pairs belonging to the quark sea of the nucleon. It is obvious that this contribution is small because the fraction of $c\bar{c}$ pairs in the sea is small. The transformation of colored quarks into colorless hadrons cannot be understood without allowance for confinement. Since this problem is still unresolved in QCD, the process of quark hadronization is described by phenomenological models that use the distribution functions of the quarks in the hadrons, the quark fragmentation functions $F(z)$, and quark recombination.

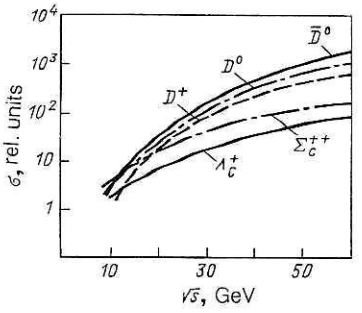

FIG. 45. Energy dependence of the total cross sections for the production of charmed particles.

Inclusive spectra of the charmed D^+, D^-, D^0, $\bar{D}^0$, and F mesons and of Λ_c^+ and Σ_c^{++} baryons produced in νp interactions were calculated in Ref. 113 in the framework of parton ideas. The energy dependence of the total cross sections for production of charmed hadrons is shown in relative units in Fig. 45. The cross sections of the same particles were also obtained as functions of the variable x (Fig. 46). The "hard" nature of the Λ_c^+ and Σ_c^{++} spectra is due to the shape of the three-particle distribution functions. It is clear that the model three-particle distribution functions contain an appreciable amount of theoretical arbitrariness and require serious experimental confirmation.

Cross sections for the production of charmed particles were measured in a recent experiment (the E531 experiment[114]) in a (wide-spectrum) neutrino beam. Data were obtained for a mean neutrino energy of 22 GeV and are given in Table XVI.

The cross section of a quasielastic process was estimated[114]:

$$\sigma(\nu_\mu n \to \mu^- \Lambda_c^+) = 3.7^{+3.7}_{-2.3} \cdot 10^{-40}\ \text{cm}^2.$$

Examples of decay of beauty particles were not observed, and no indications were found of flavor-nonconserving neutral currents.

In the E514 experiment,[115] at mean energy $\langle E_\nu \rangle \sim 60$ GeV of the neutrino beam, the cross-section ratio

$$\frac{\sigma(\nu_\mu N \to \mu^- cX)}{\sigma(\nu_\mu N \to \mu^- X)} = (8.3 \pm 2.3)\ \%$$

was obtained.

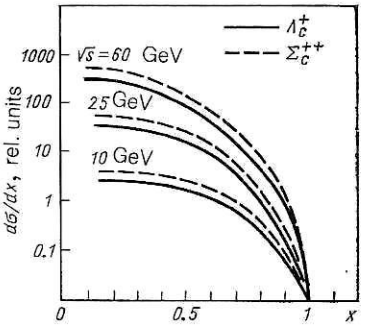

FIG. 46. Dependence of the differential cross sections $d\sigma/dx$ on the variable x (in relative units).

TABLE XVI. Ratios of the cross sections of different processes.

Ratio of cross sections	Fraction, %
$\frac{\sigma(\nu_\mu N \to c\mu^- X)}{\sigma(\nu_\mu N \to \mu^- X)}$	$4.9^{+0.7}_{-0.6}$
$\frac{\sigma(\bar{\nu}_\mu N \to \bar{c}\mu^+ X)}{\sigma(\bar{\nu}_\mu N \to \mu^+ X)}$	$5.8^{+2.9}_{-2.0}$
$\frac{\sigma(\nu_\mu N \to \mu^- \Lambda_c^+)}{\sigma(\nu_\mu N \to \mu^- X)}$	$0.3^{+0.3}_{-0.2}$
$\frac{\sigma(\nu_\mu N \to \nu_\mu c\bar{c}X)}{\sigma(\nu_\mu N \to \nu_\mu X)}$ *	$0.13^{+0.31}_{-0.11}$
$\frac{\sigma(\nu_\mu N \to c\bar{c}X)}{\sigma(\nu_\mu N \to cX)}$*	$0.8^{+1.9}_{-0.7}$

*The data include neutrino and antineutrino interactions.

The relative cross section for the production of charmed particles is shown in Fig. 47.

Thus, as yet we know very little about the processes of production of charmed particles in neutrino interactions. Practically nothing is known about the cross sections for the production of beauty mesons and baryons in neutrino interactions.

Bose–Einstein correlations

The effect of Bose–Einstein correlation consists of an increase in the probability of emission of identical bosons emitted with momenta that are relatively small compared with the uncorrelated case.[116] The origin of the effect is the quantum-mechanical requirement of symmetry of the wave function of identical particles. Thus, the amplitude of a pion that is produced by a source α (β) and arrives at a detector A (B) interferes with the amplitude of the pion produced by the source β (α) and detected by the detector A (B) (Fig. 48):

$$A \sim e^{ikx_1}e^{ikb_1} + e^{ikx_2}e^{ikb_2}$$
$$\begin{pmatrix}\alpha \to A\\ \beta \to B\end{pmatrix} \quad \begin{pmatrix}\beta \to A\\ \alpha \to B\end{pmatrix}.$$

The correlation coefficient

$$C = \frac{\rho(\rho_1, \rho_2)}{\rho(\rho_1)\,\rho(\rho_2)}$$

can be expressed in terms of single- and two-particle densities:

$$\rho(\rho) = \frac{1}{\sigma}\frac{d\sigma}{dp}; \quad \rho(\rho_1, \rho_2) = \frac{1}{\sigma}\frac{d^2\sigma}{dp_1\,dp_2}$$

in the form

$$C = \frac{\sigma\dfrac{d^2\sigma}{dp_1\,dp_2}}{\dfrac{d\sigma}{dp_1}\dfrac{d\sigma}{dp_2}},$$

where σ is the total cross section, $d\sigma/dp_1$ is the single-particle inclusive cross section, and $d^2\sigma/dp_1 dp_2$ is the two-particle cross section.

Study of the Bose–Einstein correlations makes it possible to study the size of the boson source and its lifetime.

It should be noted that not all theoretical models predict the existence of Bose–Einstein correlations. For example, in dual models they are almost completely absent.[117] Bose–Einstein correlations could arise naturally in a string fragmentation model—in the Lund hadronization model.[118] Unfortunately, it is difficult to test this model experimentally. The formalism of the string model is applicable to the case when all particles produced by the "decay" of colored strings are stable. In reality, the collision process results in the production of many resonances with lifetimes and decay lengths that are comparable with the corresponding lifetime and length scale of the string decay. The inclusion of these effects in the string model with a view to separation of the extension and lifetime of the source of the bosons is a very complicated computational problem.

To eliminate kinematic and dynamical correlations that

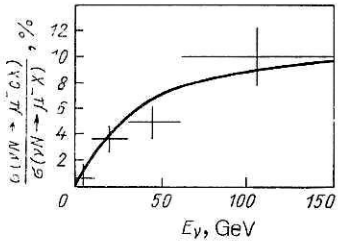

FIG. 47. Relative cross section for production of charmed particles in the charged current [the continuous curve is taken from: R. Brock, Phys. Rev. Lett. **44**, 1027 (1980)].

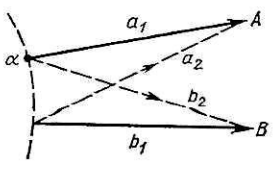

FIG. 48. Illustration of the process of interference of pion amplitudes.

are not associated with the Bose–Einstein effect, it is convenient to use the relationship between the measured probability densities for production of pion (and kaon) pairs of the same sign and of pairs that do not contain correlations:

$$R=\frac{\rho\,(\rho_1\rho_2)}{\rho_0\,(\rho_1\rho_2)}.$$

The quantity $R-1$ is the Fourier transform of the space-time distribution of the flux density of the particles emitted by the source. If $\Delta\mathbf{p}=\mathbf{p}_i-\mathbf{p}_j$ is the difference of the 3-momenta of the two identical particles, then

$$R=|A|^2\simeq 1+\lambda\exp\{-\Delta p^2r^2\},$$

where r^2 is the mean-square radius of the source. The factor λ takes into account the fact that, for a variety of reasons, the interference may not be complete. Sometimes one introduces a factor $[1-(q_0\tau)^2]^{-1}$, where $q_0=|E_1-E_2|$, and τ takes into account the lifetime of the source (in some models) or is related to the depth of the emission layer (in other models). An analysis that uses a description of the source with just one spatial variable r is realistic only in some special situations[119] and for a nonspherical region gives a certain averaged description. To study the dependence of r on the direction, one can use the fact that r actually determines the "length" of the system measured along $\Delta\mathbf{p}$. Therefore, one can investigate the dependence of the correlations on the angle $\theta(\Delta\mathbf{p})$ in the center-of-mass system between the collision axis and the vector $\Delta\mathbf{p}$. In addition, and most importantly, the difference $\Delta\mathbf{p}$, like the "shape" of the source determined from the analysis, depends on the frame of reference in which it is found.

Bose–Einstein correlation is well established in high-energy physics in processes of multiparticle production of pions[119,120] and kaons.[121,122] Data for charged kaons were obtained in $\alpha\alpha$, pp, and $p\bar{p}$ collisions at the AFS facility (CERN, ISP). A measurement was made of the ratio

$$R=\frac{(++)^S+(--)^S}{(++)^D+(--)^D},$$

where $(++)$ and $(--)$ in the numerator with the letter S denote the total numbers of events with K mesons of the same signs in a certain chosen interval $(\Delta p_T, \Delta p_L)$, where Δp_T is the component of $\mathbf{p}_1-\mathbf{p}_2$ transverse to $\mathbf{p}_1+\mathbf{p}_2$ and $\Delta\mathbf{p}_L$ is the component of $\mathbf{p}_1-\mathbf{p}_2$ longitudinal with respect to $\mathbf{p}_1+\mathbf{p}_2$, while $(++)^D$ and $(--)^D$ in the denominator are the corresponding numbers of events with K mesons of the same signs that do not participate in the correlations.

The size of the region of kaon emission is found to be $r\sim 2.4\pm 0.4$ F. Bose–Einstein correlation between identical kaons was established. It was confirmed that the kaons exhibit the same qualitative correlation features that were found for pions—the spatial region $r(KK)$ increases with increasing mean multiplicity of the charged particles, as it does for $r(\pi\pi)$.[122]

The assumption of spherical symmetry of the "source" goes against intuition. Therefore, an attempt was recently made to study Bose–Einstein correlation at a high statistics ($\sim 10^5$) with allowance for the dependence on the angle $\theta(\Delta\mathbf{p})$ for the same $\alpha\alpha$, pp, and $p\bar{p}$ collisions, but for pions. It was found that for pp and $p\bar{p}$ collisions the radial parameter r increases with increasing $|\cos\theta(\Delta\mathbf{p})|$, i.e., the extension of the region of pion emission in the direction of the collision axis is greater than in the transverse direction (the source has a "longitudinal" shape). The maximal difference of the extension parameters reaches the order of 2. At the same time, the growth of the multiplicity was found to be related to the growth of the longitudinal dimension of the source. For the $\alpha\alpha$ collisions the result was found to agree with a spherically symmetric shape.

Measurements for neutrino interactions are much sparser than for hadronic interactions. Figure 49 gives the ratio N_L/N_u of identical and nonidentical pairs of pions in νD and $\bar{\nu}D$ reactions; they agree with standard "dimensions" $r\sim 0.8$ F.

In the light of the foregoing considerations, it is obvious that such measurements give little information. It will be necessary to make a deeper investigation of this phenomenon in the neutrino beams of the UNK with high statistics, improved particle identification, and good momentum resolution on different nuclear targets and in a wide kinematic region in order to investigate the Bose–Einstein correlations in different frames of reference.

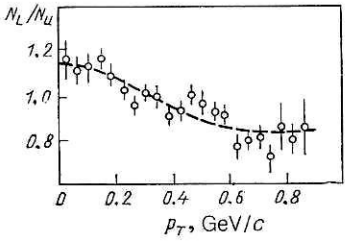

FIG. 49. Ratio of the number N_L of events with the same values of the charges to the number N_U of events with different signs of the charges as a function of p_T.

[1)] The dependence is $\sigma_\nu\sim(Q^2+M_Z^2)^{-2}$, where M_Z is the mass of the Z boson and Q^2 is, as a rule, less than or of the order of M_Z^2; this contrasts with the behavior $\sim 1/Q^4$ of the cross section in electromagnetic processes.

[2)] The numbers in Table I were obtained for a focusing system consisting of three lithium lenses and a detector placed at distance 3.5 km from the shield.[6] They differ by about a factor 3 from the estimates of the study of Ref. 7, in which ideal focusing and a somewhat different geometry were assumed.

[3)] In all that follows, $\sin^2\theta_W$ will be called the "weak mixing angle" instead of the "Weinberg angle."

[4)] The hadronic neutral current can be expressed in terms of ε_L and ε_R in the form

$$J_\mu^H=\sum_i\{[\varepsilon_L(i)\,\bar{q}_i\gamma_\mu(1+\gamma_5)\,q_i]+[\varepsilon_R(i)\,\bar{q}_i\gamma_\mu(1-\gamma_5)\,q_i]\}$$

$$=\sum_i\bar{q}_i\gamma_\mu(g_V^i+g_A^i\gamma_5)\,q_i.$$

Summation over i is made over all quark flavors ($i=u,d,s,c,b,t$). The vector, g_V^i, and axial, g_A^i, coupling constants are expressed in terms of the left (ε_L) and right (ε_R) helicity coupling constants:

$$g_V^i=\varepsilon_L(i)+\varepsilon_R(i);\quad g_A^i=\varepsilon_L(i)-\varepsilon_R(i).$$

[5)] Obtained by conversion of the results for the region 0.4–1 GeV under the assumption $\sigma_D(E)\sim E^{0.85}$.

[6)] For $\sigma_D(E)\sim E^{1/3}$, $\Sigma\nu_\tau\sim 8.8\times 10^4$, and the number of events from all direct neutrinos, i.e., $\Sigma(\nu$, charged current + neutral) is $\sim 9.2\times 10^6$.

[7)] We here ignore the contribution of the heavy b and t quarks.

[1]M. A. Markov, in: *Problems of the History of Natural Science and Technology* [in Russian] (Moscow, 1985), p. 20.

[2]S. L. Glashow, Nucl. Phys. **22**, 579 (1961); S. Weinberg, Phys. Rev. Lett. **19**, 1264 (1967); A. Salam, in *Proc. of the Eighth Nobel Symposium. Aseenäsgarden*, 1968, edited by N. Svartholm (Almqvist and Wiksell, Stockholm, 1968), p. 367.
[3]W. A. Bardeen, H. Fritzsch, and M. Gell-Mann, *Scale and Conformal Symmetry in Hadron Physics*, edited by R. Gatto (Wiley, New York, 1973); D. J. Gross and F. Wilczek, Phys. Rev. D **8**, 3633 (1973); Phys. Rev. Lett. **30**, 1343 (1973); S. Weinberg, Phys. Rev. Lett. **31**, 494 (1973).
[4]Yu. M. Ado, Usp. Fiz. Nauk **145**, 87 (1985) [Sov. Phys. Usp. **28**, 54 (1985)]; A. I. Balbekov, A. A. Vasil'ev, G. L. Vorontsov *et al.*, Fiz. Elem. Chastits At. Yadra **10**, 568 (1979) [Sov. J. Part. Nucl. **10**, 222 (1979)].
[5]K. P. Myznikov, in *Proc. of the Workshop on the Experimental Program at UNK* (Serpukhov, 1988), p. 13.
[6]V. V. Ammosov, V. V. Vasil'ev, V. I. Garkusha, S. P. Denisov *et al.*, ibid., p. 31.
[7]V. A. Tsarev, ibid., p. 118.
[8]S. A. Bunyatov and A. S. Vovenko, ibid., p. 316.
[9]S. P. Denisov *et al.*, in *Proc. of the Working Symposium: Physical Investigations at the IHEP UNK* [in Russian] (Protvino, 1982), p. 167.
[10]V. V. Ammosov *et al.*, in *Proc. of the Working Symposium: Physical Investigations at the IHEP UNK* [in Russian] (Protvino, 1983), p. 69.
[11]V. E. Balakin and A. N. Skrinskiĭ, *Linear Colliding Beams: Prospects for Development* [in Russian] (Publishing House of the Moscow Engineering Physics Institute, Moscow, 1984).
[12]V. A. Tsarev and V. A. Chechin, Fiz. Elem. Chastits At. Yadra **17**, 389 (1986) [Sov. J. Part. Nucl. **17**, 167 (1986)]; V. A. Tsarev and V. A. Chechin, Fiz. Zemli **9**, 81 (1986).
[13]A. De Rújula, S. L. Glashow, R. R. Wilson, and G. Charpak, Phys. Rep. **99**, 341 (1983).
[14]D. Yu. Bardin, "High-precision tests of the standard theory. Lectures for young scientists," Preprint R2-88-189 [in Russian], JINR, Dubna (1988).
[15]R. G. Stuart, Preprint CERN TH 4342/85.
[16]A. A. Akhundov, D. Yu. Bardin, and T. Rieman, Phys. Lett. **166B**, 111 (1986); W. Hollik, Preprint DESY 88-188 (1988).
[17]U. Amaldi, A. Böhm, L. S. Durkin *et al.*, Phys. Rev. D **36**, 1385 (1987).
[18]S. M. Bilen'kiĭ, *Lectures on the Physics of Neutrinos and Lepton–Nucleon Processes* [in Russian] (Énergoatomizdat, Moscow, 1981), p. 215.
[19]J. Panman, "Neutrino interactions," in *Intern. Symposium on Lepton and Photon Interactions at High Energies, Hamburg, 1987*, edited by K. Bartel and R. Rücke (North-Holland, Amsterdam, 1987), p. 553.
[20]A. Sirlin, Phys. Rev. D **22**, 971 (1980); W. J. Marciano and A. Sirlin, Phys. Rev. D **22**, 2695 (1980); S. Sarantakos, A. Sirlin, and W. J. Marciano, Nucl. Phys. **B217**, 84 (1983).
[21]D. Yu. Bardin and V. A. Dokuchaeva, Nucl. Phys. **B246**, 221 (1984).
[22]A. Blondel, *Invited talk at the 22nd Recontres de Moriond: Electroweak Interactions and Unified Theories* (Les Arcs, March 1987); Preprint CERN-EP/87-174 (1987).
[23]D. Yu. Bardin and V. A. Dokuchaeva, Nucl. Phys. **B287**, 839 (1987).
[24]CHARM Collaboration (F. Bergsma, M. Dorenbosch, M. Jonker *et al.*), Phys. Lett. **117B**, 272 (1982); L. A. Ahrens, S. H. Aronson, P. L. Connolly *et al.*, Phys. Rev. Lett. **54**, 18 (1985).
[25]K. S. Lackner, Nucl. Phys. **B153**, 505, 526 (1979).
[26]P. S. Isaev, *Quantum Electrodynamics at High Energies* [in Russian] (Énergoatomizdat, Moscow, 1984), Chap. 2, §2.2, p. 262.
[27]L. B. Okun, Talk at Neutrino-88, Boston (1988).
[28]R. Davis and F. Evans, in *Proc. of the Sixth Leningrad Intern. Seminar on Particle Acceleration and Nuclear Reactions in Outer Space* (Leningrad, 1974), p. 91.
[29]M. B. Voloshin and M. I. Vysotsky, Preprint N1, ITEP (1986); L. B. Okun', M. B. Voloshin, and M. I. Vysotskiĭ, Yad. Fiz. **44**, 677 (1986) [Sov. J. Nucl Phys. **44**, 440 (1986)]; M. J. Dunkan, J. A. Grifols, A. Mendez, and S. Uma Sanakar, Phys. Lett. **191B**, 304 (1987).
[30]D. Yu. Bardin, S. M. Bilenky, and B. Pontecorvo, Phys. Lett. **32B**, 68 (1970).
[31]J. E. Kim, V. S. Mathur, and S. Okubo, Phys. Rev. D **9**, 3050 (1974).
[32]Ya. B. Zel'dovich, Zh. Eksp. Teor. Fiz. **33**, 1531 (1957) [Sov. Phys. JETP **6**, 1184 (1958)]; Ya. B. Zel'dovich and A. M. Perelomov, Zh. Eksp. Teor. Fiz. **39**, 1115 (1960) [Sov. Phys. JETP **12**, 777 (1961)].
[33]J. E. Kim, P. Langacker, M. Levine, and H. H. Williams, Rev. Mod. Phys. **53**, 211 (1981); K. Abe, L. A. Ahrens, K. Amako *et al.*, Phys. Rev. **56**, 1107 (1986).
[34]J. E. Kim, P. Langacker, and S. Sarkar, Phys. Rev. D **18**, 123 (1978).
[35]L. A. Ahrens, S. H. Aronson, P. L. Connolly *et al.*, Phys. Rev. D **35**, 785 (1987).
[36]E. A. Paschos and L. Wolfenstein, Phys. Rev. D **7**, 91 (1973).
[37]C. Geweniger, in *Proc. of the 11th Intern. Conf. on Neutrino Physics and Astrophysics*, edited by K. Kleinknecht and F. Paschos (Nordrichen, 1984), p. 265.
[38]P. D. Gall, Fortschr. Phys. **35**, 115 (1987).
[39]D. Yu. Bardin and V. A. Dokuchaeva, Preprint E2-86-260, JINR, Dubna (1986).
[40]V. A. Bednyakov, I. S. Zlatev, Yu. P. Ivanov *et al.*, Yad. Fiz. **40**, 770 (1984) [Sov. J. Nucl. Phys. **40**, 494 (1984)].
[41]B. Kayser, G. T. Garvey, E. Fischbach, and S. P. Rosen, Phys. Lett. **52B**, 385 (1974).
[42]R. L. Kingsley, F. Wilczek, and A. Zee, Phys. Rev. D **10**, 2216 (1974).
[43]M. Gourdin, in *Proc. of the Intern. Neutrino Conf.* (Aachen, 1976), p. 234 (Vieweg, Braunschweig): K. Kayser, in *Proc. of Neutrino-78* (Purdue, 1978), p. 979.
[44]K. C. Wang, in *Proc. of the 11th Intern. Conf. on Neutrino Physics and Astrophysics* (Nordkirchen, 1984), p. 322.
[45]K. Winter, "Neutral weak current phenomena," in *Report on the 13th Intern. Conf. on Neutrino Physics and Astrophysics* (Boston, Mass., USA, 5–11 June. 1988) (Neutrino-88).
[46]M. A. Kozhushner and E. P. Shabalin, Zh. Eksp. Teor. Fiz. **41**, 949 (1961) [Sov. Phys. JETP **14**, 676 (1962)].
[47]F. Bergsma, J. Dorenbosch, M. Jonker *et al.* (CHARM Collaboration), Phys. Lett. **122B**, 185 (1983).
[48]M. Kobayashi and T. Maskawa, Prog. Theor. Phys. **49**, 652 (1973).
[49]A. Sirlin, Nucl. Phys. **B71**, 29 (1974); Rev. Mod. Phys. **50**, 573 (1978).
[50]L. Maiani, Phys. Lett. **62B**, 183 (1976); L. L. Chan and W. Y. Keung, Phys. Rev. Lett. **53**, 1802 (1984); H. Fritzsch, Phys. Rev. D **32**, 3058 (1985).
[51]K. Kleinknecht, "Weak mixing, *CP* violation and rate decays," in *24th Intern. Conf. on High Energy Physics* (Munich, August 4–10, 1988) (in print).
[52]W. Schmidt-Parcefall, in *International Symposium on Lepton and Photon Interactions at High Energy, Hamburg 27–31 July, 1987*, edited by W. Bartel and R. Rücke (North-Holland, Amsterdam, 1987), p. 257.
[53]C. L. Fogli and D. Haidt, Preprint BA-TH/2-88, January (1988).
[54]M. Jonher, J. Panman, F. Udo *et al.*, Phys. Lett. **102B**, 67 (1981).
[55]L. B. Okun', Yad. Fiz. **41**, 1272 (1985) [Sov. J. Nucl. Phys. **41**, 812 (1985)].
[56]J. C. Auios, J. A. Appel, S. B. Bracher *et al.*, Preprint Fermilab-Conf.-87/143-E.
[57]D. A. Bryman, R. Dubois, T. Numao *et al.*, Phys. Rev. Lett. **50**, 7 (1983).
[58]C. Albajar, M. C. Albrow, O. C. Allkofer *et al.*, Phys. Lett. **185B**, 233 (1987).
[59]D. J. Gross and C. H. Llewellyn-Smith, Nucl. Phys. **B14**, 337 (1969).
[60]S. L. Adler, Phys. Rev. **143**, 1144 (1966).
[61]C. G. Callan and D. J. Gross, Phys. Rev. Lett. **22**, 156 (1969).
[62]L. N. Lipatov, Yad. Fiz. **20**, 181 (1974) [Sov. J. Nucl. Phys. **20**, 94 (1975)]; G. Altarelli and G. Parisi, Nucl. Phys. **B126**, 298 (1977).
[63]L. Baulier and C. Kounnas, Nucl. Phys. **B141**, 423 (1978); J. Kodira and T. Uematsu, Nucl. Phys. **B141**, 497 (1978).
[64]G. Altarelli, R. K. Ellis, and G. Martinelli, Nucl. Phys. **B143**, 521 (1978); **B146**, 544(E) (1979).
[65]J. G. Morfin and J. F. Owens, in *Proc. of Snowman 84* (Colorado, 1984); Fermilab-Conf.-85/15.
[66]Yu. P. Ivanov and P. S. Isaev, Yad. Fiz. **38**, 744 (1983) [Sov. J. Nucl. Phys. **38**, 443 (1983)].
[67]H. Georgi and H. D. Politzer, Phys. Rev. D **14**, 1829 (1976).
[68]D. V. Shirkov, Yad. Fiz. **34**, 541 (1981) [Sov. J. Nucl. Phys. **34**, 300 (1981)]; Teor. Mat. Fiz. **49**, 291 (1981).
[69]M. Aguilar-Benitez, F. C. Porter, J. J. Hernandez *et al.* (Particle Data Group), Phys. Lett. **170B**, 1 (1986).
[70]C. Quigg, H. H. Reno, and T. P. Walker, FNAL-Pub-86-50-AT (1986).
[71]J. J. Aubert, G. Bassompierre, K. H. Becks *et al.*, Nucl. Phys. **B293**, 740 (1987).
[72]L. P. Abbott, W. B. Atwood, and R. M. Barnett, Phys. Rev. D **22**, 582 (1980).
[73]P. S. Isaev and S. G. Kovalenko, Yad. Fiz. **32**, 756 (1980) [Sov. J. Nucl. Phys. **32**, 390 (1980)]; Hadronic J. **3**, 919 (1980); I. S. Zlatev, Yu. P. Ivanov, P. S. Isaev, and S. G. Kovalenko, Yad. Fiz. **35**, 454 (1982) [Sov. J. Nucl. Phys. **35**, 260 (1982)]; V. A. Bednyakov, I. S. Zlatev, P. S. Isaev, and S. G. Kovalenko, Yad. Fiz. **36**, 745 (1982) [Sov. J. Nucl. Phys. **36**, 436 (1982)]; V. A. Bednyakov, I. S. Zlatev, Yu. P. Ivanov *et al.*, Yad. Fiz. **40**, 770 (1984) [Sov. J. Nucl. Phys. **40**, 494 (1984)].
[74]G. Farrar and D. Jackson, Phys. Rev. Lett. **35**, 1416 (1975).
[75]G. Giacomelli, in *Proc. of the CERN-JINR School of Physics* (Urbino, Italy, 1985), p. 266.
[76]D. Allasia, C. Angelini, A. Baldini *et al.*, Phys. Lett. **135B**, 231 (1984).
[77]T. Sloan, in *Proc. of the 17th Intern. Symposium on Multiparticle Dynamics* (Seewinkel, 1986), p. 290.
[78]Yu. P. Ivanov, Yad. Fiz. **44**, 492 (1986) [Sov. J. Nucl. Phys. **44**, 317 (1986)].
[79]J. J. Aubert, G. Bassompierre, K. H. Becks *et al.* (EMC Collaboration),

Phys. Lett. **123B**, 123 (1983).
[80]R. P. Feynman, *Photon–Hadron Interactions* (Addison–Wesley, Reading, Mass., 1972) [Russ. transl., Mir, Moscow, 1975].
[81]E. Reya, Phys. Rep. **69**, 195 (1981).
[82]O. Nachtmann, Nucl. Phys. **B63**, 237 (1973).
[83]S. Dasu, P. de Barbaro, R. C. Walker *et al.*, UR-991, University of Rochester (1987).
[84]A. J. Buras, Rev. Mod. Phys. **52**, 199 (1980).
[85]A. Devoto, D. W. Duke, J. F. Owens, and R. G. Roberts, Phys. Rev. D **27**, 508 (1983); Yu. P. Ivanov and S. G. Kovalenko, Yad. Fiz. **40**, 1277 (1984) [Sov. J. Nucl. Phys. **40**, 812 (1984)].
[86]F. Bergsma, T. Dorenbosh, J. V. Allaby *et al.*, Phys. Lett. **153B**, 111 (1985).
[87]V. A. Tsarev, in *Proc. of the Working Symposium on the Program of Experimental Investigations at the UNK* [in Russian] (Serpukhov, 1988), p. 118.
[88]G. Baum, M. R. Bergström, P. R. Bolton *et al.*, Phys. Rev. Lett. **51**, 1135 (1983).
[89]J. A. Shman, B. Badelek, G. Baum *et al.* (EMC Collaboration), Phys. Lett. **206B**, 364 (1988).
[90]T. Sloan, in *Proc. of the Intern. Europhys. Conf. on High Energy Physics*, Vol. 2 (Uppsala, 1987), p. 857.
[91]J. D. Bjorken, Phys. Rev. **148**, 1467 (1966); D **1**, 1376 (1970).
[92]J. Kodaira, S. Matsuda, T. Muta *et al.*, Phys. Rev. D **20**, 627 (1979); J. Kodaira, S. Matsuda, K. Sasaki, and T. Uematsu, Nucl. Phys. **B159**, 99 (1979).
[93]J. Ellis and R. L. Jaffe, Phys. Rev. D **9**, 1444 (1979); **10**, 1669(E) (1974).
[94]R. Carlitz and J. Kaur, Phys. Rev. Lett. **38**, 673 (1977); J. Kaur, Nucl. Phys. **B128**, 219 (1977).
[95]V. M. Belyaev, B. L. Ioffe, and Y. I. Kogan, Phys. Lett. **151B**, 290 (1985).
[96]R. L. Jaffe, Phys. Lett. **193B**, 101 (1987); F. E. Close and R. G. Roberts, Phys. Rev. Lett. **60**, 1471 (1988); S. J. Brodsky, J. Ellis, and M. Karliner, Phys. Lett. **206B**, 309 (1988); G. Altarelli and G. G. Ross, CERN-TH 5082/88; A. V. Efremov and O. Teryaev, Preprint E2-88-287, Dubna; H. Fritzsch, Preprint MPI-PAE/PYh 45/88, Max Planck Inst.; H. Lipkin, ANL-HEP-RP-88-46; 88-48; M. Anselmino, B. L. Ioffe, and E. Leader, NSF-ITP-88-94.
[97]N. Schmitz, "Hadron production in high energy νN collisions," Neutrino 88.
[98]R. P. Feynman and R. D. Field, Nucl. Phys. **B136**, 1 (1978).
[99]B. Musgrave, in *Intern. Conf. on Neutrinos, Weak Interactions and Cosmology*, Vol. 2 (Bergen, 1979), p. 556.
[100]B. Saitta, in *Intern. Conf. on Neutrino Physics and Astrophysics* (Erice, Sicily, 1980), p. 107.
[101]A. Mukherjee, J. Bofill, W. Busza *et al.*, FNAL-Conf.-86/102-E.
[102]G. Altarelli, R. C. Ellis, G. Martinelli, and S.-Y. Pi, Nucl. Phys. **B160**, 301 (1979).
[103]E. L. Berger and S. J. Brodsky, Phys. Rev. Lett. **42**, 940 (1979); E. L. Berger, Z. Phys. C **4**, 289 (1980); Phys. Lett. **89B**, 241 (1980).
[104]A. A. Bel'kov, Yu. A. Zudin, L. A. Klimenko, and Ya. R. Komachenko, in *Proc. of the Third Working Symposium on the IHEP–JINR Neutrino Detector*, R-1,2-13-83-81 [in Russian] (Dubna, 1983), p. 97.
[105]S. S. Gershteĭn, Ya. Yu. Komachenko, and M. Yu. Khlopov, Yad. Fiz. **32**, 1663 (1980) [Sov. J. Nucl. Phys. **32**, 861 (1980)].
[106]P. Allen, H. Grässler, R. Chulte *et al.*, Nucl. Phys. **B264**, 221 (1986).
[107]P. Allen, H. Grässler, D. Lanske *et al.*, Nucl. Phys. **194B**, 373 (1982).
[108]F. Bergsma, J. Dorenbosch, J. V. Allaby *et al.*, Phys. Lett. **157B**, 469 (1985).
[109]A. A. Bel'kov and B. Z. Kopeliovich, Yad. Fiz. **46**, 874 (1987) [Sov. J. Nucl. Phys. **46**, 499 (1987)].
[110]V. Ammosov, A. H. Amrakhov, A. G. Denisov *et al.*, Phys. Lett. **93B**, 210 (1980).
[111]A. Breakstone, C. D. Buchanan *et al.*, Phys. Lett. **135B**, 510 (1984).
[112]Y. Afek, C. Leroy, B. Margolis, and J. Trischuk, Z. Phys. C **6**, 251 (1980); V. G. Kartvelishvili, A. K. Likhoded, and S. R. Slabospitskiĭ, Yad. Fiz. 28, 1315 (1978); **32**, 236 (1980); **33**, 832 (1981) [Sov. J. Nucl. Phys. **28**, 678 (1978); **32**, 122 (1980); **33**, 434 (1981)]; A. K. Likhoded, S. R. Slabospitskiĭ, and M. V. Suslov, Yad. Fiz. **38**, 727 (1983) [Sov. J. Nucl. Phys. **38**, 433 (1983)].
[113]V. A. Bednyakov, S. A. Bunyatov, and P. S. Isaev, Communication R2-84-820 [in Russian], JINR, Dubna (1984).
[114]N. Ushida, T. Kondo, S. Tasaka *et al.* (E-532 Collaboration), Phys. Lett. **206B**, 375 (1988).
[115]S. A. Bunyatov, Yu. A. Batusov, O. M. Kuznetsov *et al.*, Preprint D-1-88-932 [in Russian], JINR, Dubna (1988).
[116]G. Goldhaber, S. Goldhaber, W. Lee, and A. Pais, Phys. Rev. **120**, 300 (1960); G. I. Kopylev and M. I. Podgoretskiĭ, Yad. Fiz. **15**, 392 (1972); **18**, 656 (1973); **19**, 434 (1974) [Sov. J. Nucl. Phys. **15**, 219 (1972); **18**, 336 (1974); **19**, 215 (1974)].
[117]A. Giovannini and G. Veneziano, Nucl. Phys. **B130**, 61 (1977).
[118]B. Anderson and W. Koffman, Phys. Lett. **169B**, 364 (1986).
[119]M. G. Bowler, Z. Phys. C **29**, 617 (1985).
[120]T. Akesson, M. G. Albrow, S. Almened *et al.*, Phys. Lett. **129B**, 269 (1983); H. Aihara, M.-G. Alston, J. A. Bakken *et al.*, Phys. Rev. D **31**, 996 (1985).
[121]A. M. Cooper, S. N. Ganguli, P. K. Malhotra *et al.*, Nucl. Phys. **B139**, 45 (1978).
[122]T. Akesson, M. G. Albrow, S. Almehed *et al.*, Phys. Lett. **155B**, 128 (1985).

Translated by Julian B. Barbour